REVEALING THE DISTRIBUTION OF ION TRANSPORT PEPTIDE AND FUNCTION OF ITS PROSPECTIVE SECOND MESSENGERS ON THE HINDGUT OF THE ADULT MOSQUITO, *AEDES AEGYPTI*

ANDREEA MATEI

A THESIS SUBMITTED TO
THE FACULTY OF GRADUATE STUDIES
IN PARTIAL FULFILLMENT OF THE REQUIREMENTS
FOR THE DEGREE OF
MASTER OF SCIENCE

GRADUATE PROGRAM IN BIOLOGY

YORK UNIVERSITY

TORONTO, ONTARIO

JUNE 2017

Abstract

The desert locust faces similar dietary and environmental challenges to the adult mosquito in that water must be conserved during unfed states, whereas the expulsion of excess water and ions is necessary in post-fed states. The insect excretory system plays a vital role in maintaining the hydromineral balance of the haemolymph; the haemolymph is analogous to the blood of vertebrates. The excretory system includes the Malpighian tubules and the hindgut, comprised of the anterior ileum and posterior rectum. The endocrine control of the excretory system is accomplished by diuretic and antidiuretic factors that promote fluid excretion and retention, respectively. Unfortunately, ion and water transport mechanisms in the hindgut of insects are not well understood. In the locust, *S. gregaria,* Ion Transport Peptide (ITP) was the first discovered antidiuretic factor acting on the insect hindgut. ITP was later uncovered in other insects including the mosquito, *A. aegypti*, the fruit fly, *D. melanogaster,* the silkworm, *B. mori*, and the tobacco hornworm, *M. sexta.* Amino acid sequence homology was shown to be conserved between insect ITPs and with the Crustacean Hyperglycaemic Hormones (CHHs) peptide family. Several fundamental properties of ITP have been delineated across insect species including its complete amino acid sequence, characteristic features at the protein level, tissue expression profiles, and its suspected intracellular second messengers. A putative model for the mechanism of ITP regulation on ion transport in the locust ileum has been suggested. The only ITP receptors that have been characterized to date belong to the silkworm, *B. mori*. This chapter will review the development of findings linked to the molecular and physiological characteristics of the neuropeptide, ITP.

Acknowledgements

First and foremost, I would like to thank my supervisor Dr. Jean-Paul Paluzzi, for giving me a chance as a research practicum student while in my 3rd year of undergraduate studies, and putting up with me for all of these years. Due to your kindness and endless patience, my time as a research student has easily become the most rewarding experience I have ever taken part of. I would like to thank Dr. Paluzzi for always encouraging me to push myself because who else could pull off an *in situ* the same day their final MSc thesis is due? ONLY one of JP's students. Dr. Paluzzi, you are the greatest supervisor a student could ever hope for, there simply aren't enough ways to thank you. I would also like to thank Dr. Andrew Donini for initially teaching me the SIET technique, but ultimately becoming a mentor for me in all aspects of life – you are truly an inspiration and role model. Thank you to the Donini lab members for their support and guidance throughout the years. I would like to thank my colleagues in the Paluzzi lab including Carmela, Dave, Aryan, Farwa, Fidan, Ali O., Ali U., and our very own Melanie the Explorer.

Thank you to my fellow grad colleagues including Azizia, Dave, Gil, and Lidiya for (emotional) support throughout the years and for providing a collaborative environment that allowed me to expand my thinking, thanks to your creative minds. A special thank you goes out to Azizia whose lab expertise is the reason why I was able to piece together this project. Dave, the most important thing you *tried* to teach me this year was how to make ammonium persulfate, but gosh darn it I just couldn't get it right!

Lastly, my biggest thank you goes to my parents whose love and support have driven me to achieve anything I have set my mind on, say like completing a 1 year MSc. I would like to thank Dr. Dick Nassel for generously providing the DromeITP antiserum.

TABLE OF CONTENTS

LIST OF FIGURES

CHAPTER I: PHYSIOLOGICAL PROPERTIES OF ION TRANSPORT ACROSS THE HINDGUT IN INSECTS

Introduction

Aedes aegypti as a Disease Vectors

Aedes aegypti is an important mosquito species responsible for transmitting many of the world's deadliest diseases. Specifically, *A. aegypti* mosquitoes are of great medical importance as they are the vectors of various arboviruses - viruses transmitted by arthropod vectors (Clemons et al., 2010a). Among these viruses include yellow fever, dengue, chikungunya, and Zika virus. All of these pathogens enter the mosquito through an infectious blood meal, penetrate through the midgut, and spread throughout other parts of the mosquito only to be passed onto their next vertebrate host (Kraemer et al., 2015). Effective and sustainable vector control mechanisms are in urgent need as these mosquitoes continue to transmit arboviruses that can lead to potentially fatal diseases in humans.

The yellow fever virus primarily occurs in tropical regions of Africa, as well as certain parts of South America. The severity of the disease ranges from a febrile illness to severe hepatitis and haemorrhagic fever (Clemons et al., 2010a). Yellow fever infections have been declining due to vector control programs and an effective vaccine developed nearly 80 years ago in 1937 by virologist Max Theiler. Unfortunately, the distribution and delivery of this vaccine is problematic and outbreaks often occur in regions where the vaccinations have not been administered (Clemons et al., 2010a; Kraemer et al., 2015). Extensive vaccination campaigns combined with effective vector-control strategies have significantly reduced the number of yellow fever cases worldwide. However, localized outbreaks continue to occur in parts of Africa and Central and South America, resulting in an estimated 84,000 to 170,000 severe cases and 29,000 to 60,000 related deaths per year, according to the WHO (Paules and Fauci, 2017). In

early 2017, yellow fever virus had broken out in Brazil, with the majority of infections occurring in rural areas; 234 confirmed infections and devastatingly 80 confirmed deaths have been reported as of February 2017 (Paules and Fauci, 2017). This outbreak has been considered out of proportion in comparison to numbers reported in previous years, and has been shown to affect areas in close proximity to major urban areas where the yellow fever vaccine is not routinely administered, which has raised the concern of urban transmission in Brazil. This leads to the fear of travel-related cases of yellow fever occurring in the United States and Canada (Paules and Fauci, 2017).

Threatening over 2.5 billion people worldwide, dengue is the most common arthropod-borne viral infection in the world. It is an epidemic in more than 100 countries located in South-East Asia, the Americas, and the Western Pacific. Shockingly, the dengue febrile illness is the most widespread and significant vector-transmitted disease in the world (Rodenhuis-Zybert et al., 2010). Roughly 400 million infections occur annually, with a mortality rate surpassing 5-20% in some areas (Hasan et al., 2016). Dengue virus infection presents with a diverse clinical picture that ranges from asymptomatic illness to dengue fever to the severe illness of dengue hemorrhagic fever/dengue shock syndrome (DHF/DSS) (World Health Organization, 2009). Dengue has seen a 30-fold upsurge worldwide between 1960 and 2010 due to increased population growth rate, global warming, unplanned urbanization, inefficient mosquito control, frequent air travel, and lack of health care facilities (Hasan et al., 2016). Clinical symptoms most commonly begin within 5-8 days after an infected mosquito has bitten the patient. Moreover, abrupt onset of a high fever, severe headache, pain in muscles and joints, a skin rash, and overall weakness may last several weeks. Upon the manifestation of DHF and DSS, patients normally experience vomiting, shortness of breath, and haemorrhaging from the skin and the

gastrointestinal system, frequently leading to shock followed by death (Slosek, 1986).

Outbreaks of the Chikungunya virus, as with all arboviruses, begin during the rainy season when vector density peaks (Pialoux et al., 2007). The disease was previously limited to Africa and Asia, but has more recently been reported in the Caribbean, South America, and Europe (Kraemer et al., 2015). In 2013, the first local transmission of chikungunya virus in the Western hemisphere was reported in Saint Martin. As of 2014, 576,535 laboratory confirmed chikungunya cases had been reported in the Americas (Staples and Fischer, 2014). The illness manifests itself as an acute illness with fever, skin rashes, and incapacitating arthralgia, or joint pain (Pialoux et al., 2007). There is currently no specific treatment, vaccine, or preventative drug for chikungunya and management includes rest, fluids, analgesics, and antipyretics (Staples and Fischer, 2014).

The Zika virus was initially isolated from the rhesus monkey in the Zika forest of Uganda in 1947. Sporadic human infections were initially reported in Africa and Asia (Musso et al., 2014). The classic infection resembles that of dengue fever and chikungunya manifested by fever, headaches, and skin rashes. Most notably, intrauterine transmission of the Zika virus may lead to fetal abnormalities such as microcephaly: this disease is characterized by abnormal smallness of the head, a congenital condition associated with incomplete brain development (Mlakar et al., 2016). The emergence of the first Zika virus disease cases in the Americas were reported in March 2015, when an outbreak occurred in Bahia, Brazil, thereafter it began to spread northwards at a rapid rate across South and Central America, reaching Mexico by late November 2015 (Gatherer and Kohl, 2017; Petersen et al., 2016). The World Health Organization subsequently issued alerts to the presence of Zika virus in several Latin American countries: Colombia, Surinam, Guatemala, El Salvador, Mexico, Paraguay, Venezuela and

Panama (Gatherer and Kohl, 2017). By March 2016, the virus had spread to at least 33 countries and territories in the Americas (Petersen et al., 2016). On 21 November 2015, the WHO notified the presence of 739 cases of microcephaly in nine states of north-eastern Brazil, the same region as the Zika virus outbreak in that country, by April 2016 these numbers reached an unprecedented total of 1912 noted cases of microcephaly. This lead to the hypothesis that there was a causal association with Zika virus infection during pregnancy (Gatherer and Kohl, 2017). On 1 February 2016, the World Health Organization declared the clusters of microcephaly in babies constituted a Public Health Emergency of International Concern (Heymann et al., 2016).

A temporal and geographic relationship has been observed between Guillain-Barré syndrome and Zika virus outbreaks in the Pacific and the Americas (Oehler et al., 2014). Guillain-Barré syndrome (GBS) is a disorder in which the body's immune system attacks part of the peripheral nervous system. The first symptoms of this disorder include varying degrees of weakness or tingling sensations in the legs; in many instances, the symmetrical weakness and abnormal sensations spread to the arms and upper body. These symptoms can increase in intensity until certain muscles cannot be used at all and, when severe, the person is almost totally paralyzed (Pithadia and Kakadia, 2010; Yuki and Hartung, 2012).

Aedes aegypti Life Cycle and Distribution

It is now established that the ancestor of the domestic form of *A. aegypti* lived in sub-Saharan Africa. The ancestral larval habitat was most likely tree holes, and non-human animals were the main source of blood meals for adult females (Tabachnick, 1991). Female *A. aegypti* mosquitoes lay their eggs just above the water line of natural pools such as tree holes or sitting water in human-generated containers (eg. flower pots, bird baths) (Powell and Tabachnick,

2013). The eggs remain dormant until flooded with water, and can survive desiccation for several months (Clemons et al., 2010a; Clemons et al., 2010b). This oviposition, or egg depositing behaviour, was adapted to natural conditions where rain is unpredictable. If a pool is drying, eggs remain dormant; if rain is plentiful, water rises to flood the eggs, they hatch, and are more likely to have water long enough to undergo development (Powell and Tabachnick, 2013). Upon the eggs hatching, their life cycle consists of four larval stages and one pupal stage, all of which are aquatic. During the larval stages, which last at least four days, larvae are often found at the water surface, as they need to breathe. In addition, larvae swim below the surface to feed on organic particulate matter such as algae and microscopic organisms. Following the fourth instar larval stage, they enter a mobile non-feeding pupal stage that lasts approximately 2 days. The adult lifespan of the *A. aegypti* mosquitoes varies depending on the environmental conditions, but ranges from two weeks to a month (Clements, 1999; Foster and Walker, 2009). *A. aegypti* adults have white scales on the dorsal surface of their thorax and brown to black abdomen also possessing white scales. Their hind legs also have white bands that appear to be stripes (Carpenter and La Casse, 1974) . Adults of both sexes feed on plant nectar, but females possess piercing mouthparts adapted for acquiring vertebrate blood meals that is needed for producing eggs prior to oviposition. Females prefer to blood feed at dusk and dawn, preying primarily on human hosts (Clements, 1999; Clemons et al., 2010b).

Found throughout most tropical to subtropical world regions, *A. aegypti* mosquitoes have a preference for human habitats. This mosquito species is typically concentrated in northern Brazil and Southeast Asia, including all of India. There are relatively few areas of suitability in Europe (only Spain and Greece) and temperate North America (Rodenhuis-Zybert et al., 2010). The distribution of *A. aegypti* mosquitoes in Africa encompasses a much wider range, with

reports of the species in over 30 countries (Kraemer et al., 2015). The species distribution highly depends on the environmental temperature, which is a limiting factor for survival since these mosquitoes need a tropical to temperate environment for optimal survival conditions (Brady et al., 2013). Global expansion of these mosquitoes has been associated with trade and travel. The introduction of the species over long distances and between continents has been associated with international trade routes via shipping, human movement, and transport routes. Thus, the global spread of associated pathogens has undoubtedly been a consequence of increasing globalization (Clemons et al., 2010a; Kraemer et al., 2015; Powell and Tabachnick, 2013; Rodenhuis-Zybert et al., 2010; Tabachnick, 2010).

Ion and Water Balance in *A. aegypti* Mosquitoes

Haemolymph is a fluid that circulates the interior of the arthropod body remaining in direct contact with the animal's tissues, analogous in many ways to the blood of vertebrates. Within the mosquito, haemolymph homeostasis is constantly challenged by feeding strategies and diet, habitat, and the metabolic state of the insect (Phillips et al., 1996). Adult mosquitoes face a similar challenge to other terrestrial insects, that being environmental stressors leading to desiccation; insects have a high surface-to-volume ratio that challenges their ability to conserve water (Coast et al., 2002; O'Donnell, 2011). Larval *A. aegypti* normally reside in fresh water and faces the challenge of gaining water from drinking and through the osmotic flux across the body surface; in sum, the aquatic environment possess stress for the dilution of the haemolymph (Clements, 2000; O'Donnell, 2011). These larvae must also deal with diffusional losses of haemolymph ions to the dilute external medium (Clements, 2000; O'Donnell, 2011; Patrick et al., 2006). Upon pupal eclosion into an adult mosquito, osmoregulatory challenges are sporadic

and dissimilar, varying with the constantly changing external environment and differing gut contents. The mosquito excretory system consists of the Malpighian tubules and the hindgut, including the ileum and rectum, and finally the anus from which the final waste is excreted. In adult mosquitoes, the rectum consists of a thin rectal sac housing six (female) or four (male) rectal pads that protrude into the lumen (O'Donnell, 2011; Patrick et al., 2006). In larvae, the four anal papillae extend from the terminal segment and project into the external medium. Their walls are composed of a one cell thick epithelia, and the lumen is continuous with the haemolymph (Clements, 2000; Donini et al., 2007). The Malpighian tubules arise at the junction between the midgut and hindgut; their apical membrane faces the lumen while the basolateral membrane faces the haemolymph (Clements, 2000). The material eliminated by the anus of insects has been coined "excreta" and it consists of a mixture of undigested foodstuffs and urinary fluid secreted by the Malpighian tubules (Coast, 2007).

Freshwater larvae eliminate an excess water load by producing a bountiful amount of dilute urine through the coordinated activity of the Malpighian tubules and hindgut. The primary urine produced in the Malpighian tubules of larval mosquitoes is a consequence of active potassium and sodium ion secretion from the haemolymph to the tubule lumen, thereafter, water follows down its osmostic gradient (Coast, 2007; Coast, 2009). The primary urine is later modified in specialized segments of the tubules themselves, and finally, in the hindgut (Coast, 2007; Coast, 2009; O'Donnell, 2011). Prior to excretion, ions are actively absorbed from the urine by the rectal papillae back into the haemolymph (Ramsay, 1953).

Non-feeding adult mosquitoes are primarily tasked with conserving body water to avoid the reduction in body volume and to preserve the concentration of haemolymph ions. However, when adult mosquitoes ingest a nectar meal they take on a significant water load and face the

challenge of haemolymph ion dilution. The elimination of this water load is initiated within seconds of feeding and occurs without significant loss of ions (Clements, 2000). The process of achieving ionic homeostasis within the excretory system is initiated at the distal, free-floating, end of the Malpighian tubule. The osmotic pressure of the primary urine secreted by *A. aegypti* Malpighian tubules is similar to that of the haemolymph, and reveals a concentration of Na^+ that is lower, a concentration of K^+ that is higher, and a concentration of Cl^- close to that of the haemolymph (Evans et al., 2009).

The active transport of cations across Malpighian tubule principal cells depends on the activity of an apically located vacuolar-type H^+ ATPase (V-type ATPase) that pumps protons into the lumen (Maddrell and O'Donnell, 1992). Primary active transport of H^+ by the V-type ATPase energizes secondary active transport through alkali cation/H^+ antiporters that drive Na^+ and K^+ export into the lumen. Protons extruded by the V-type ATPase into the lumen are cycled back within the cell through these exchangers driving cellular Na^+/K^+ secretion into the lumen (Pannabecker, 1995; Wieczorek, 1992). Na^+/K^+ transport is a result of secondary active transport; these H^+/alkali cation exchangers are located both basolaterally and apically (Donini et al., 2006; Larsen et al., 2014; Pullikuth et al., 2006). Furthermore, the basolaterally localized $Na^+/K^+/2Cl^-$ co-transporter functions in response to the electrochemical gradient established by the reduction in cellular Na^+; K^+, Cl^-, and these ions are brought into the principal cells from the haemolymph (Ianowski and O'Donnell, 2004; Ianowski et al., 2002; Larsen et al., 2014). Potassium ions can also enter the principle Malpighian tubule cells from the haemolymph through potassium channels, and are secreted into the tubule lumen by a K^+/H^+ antiporter (Wieczorek et al., 2009). At the basolateral membrane of principle cells, a type 3 Na^+/H^+ exchanger (*Ae*NHE3) allows for the uptake of Na^+ from the haemolymph in exchange for intracellular H^+ (Pullikuth et al., 2006).

Finally, water movements during urine production are a passive osmotic consequence of active transepithelial ion secretion; osmotic gradients drive transcellular water transport through aquaporins (O'Donnell, 2009; Pacey and O'Donnell, 2014).

Upon blood feeding, adult female mosquitoes face the extraordinary challenge of avoiding excess fluid and ion uptake from their vertebrate host. Adult females must gorge on a blood meal to harvest the proteins required for production of eggs. Consequently, females must eliminate large quantities of excess water and ions (such as sodium, potassium, and chloride ions) present in the blood plasma, as well as ions that are released from within the red blood cells upon digestion (Clements, 2000; Coast, 2009). Blood feeding insects, such as the well-studied *Rhodnius prolixus*, recover virtually no water during the process of diuresis (Larsen et al., 2014). Excess ions that are absorbed across the midgut are rapidly eliminated by the Malpighian tubules and the hindgut (O'Donnell, 2009; Pullikuth et al., 2006). These excess ions and water from the blood meal are secreted from the haemolymph into the Malpighian tubules, through an active process moving these cations against their electrochemical potentials (Clements, 2000). The plasma composition of a blood meal is high in NaCl, and therefore, the primary urine produced by the Malpighian tubules is highly concentrated in NaCl (Coast, 2009; O'Donnell, 2011). K^+ is released upon the lysis of red blood cells and, if absorbed into the haemolymph must also be eliminated. This may be achieved by expression of the basolateral P-type Na^+/K^+ ATPase (P-type ATPase) within the anterior hindgut that enhances K^+ entry into cells at the expense of Na^+ (Coast, 2009; O'Donnell, 2009; Patrick et al., 2006). However, the P-type ATPase has not been shown to specifically enhance the transcellular transport of K^+ into the lumen of the hindgut, and may therefore play a role in maintaining the ion homeostasis of epithelial cells.

The Mosquito Hindgut

As previously outlined in detail above, the osmo- and ionoregulatory mechanisms in the Malpighian tubules have been very well studied in both larval and adult mosquitoes. Unfortunately, this is not the case for the hindgut, and the exact mechanisms for ion and water transepithelial transport are yet to be determined. The Malpighian tubules will generate a variable load of primary urine that is then delivered to the hindgut to be modified prior to being voided as urine. Thereafter, the bulk of water, ion, and metabolite reabsorption occurs in the rectum. Ultimately, the hindgut will play a dominant role in determining the composition of the excreted matter (Coast, 2009; Larsen et al., 2014). The hindgut is an excretory organ, composed of the anterior ileum and posterior rectum, that completes the excretion process by selectively reabsorbing substances into haemolymph, allowing other substances to pass within the lumen, and actively secreting additional substances into the lumen (O'Donnell, 2011). The rectal cuticle lining has greater permeability than the cuticle lining of the foregut cells, and the epithelial cells of the hindgut are specialized for both active secretion and reabsorption (Nation, 2008). In the locust, the ileum is the major site for isosmotic fluid reabsorption and active Na^+ and Cl^- reabsorption (Phillips et al., 1988; Phillips et al., 1994). Furthermore, passive reabsorption of K^+ can occur by electrical coupling with electrogenic Cl^- transport (Hanrahan and Phillips, 1983). The ileum also plays a major role in acid-base balance by secreting H^+ into the lumen and reabsorbing $HCO3^-$ (Phillips et al., 1994).

The anterior hindgut, or the ileum, possesses an epithelium thicker than that of the rectal sac; nonetheless, both of these areas possess a well-developed basolateral surface rich in mitochondria to aid in the production of ATP necessary to feed ATPases localized on this

membrane. Patrick *et al*., (2006) were the first to examine specific ion transport proteins in the epithelia of the adult mosquito hindgut. The previously mentioned apical V-type ATPase of the Malpighian tubules is also highly expressed on the apical surface of the anterior hindgut epithelia and the rectal pads (Patrick et al., 2006). Unfortunately, there is only scarce literature that explains how the proton gradient facilitates the reabsorption of important ions such as sodium, potassium and chloride in the adult mosquito hindgut. Additionally, a P-type ATPase that is localized on the basolateral surface of the hindgut and rectum of adult mosquito was characterized (Patrick et al., 2006). Intense P-Type ATPase labelling on the basolateral infolding of rectal pads, shown with immunohistochemistry, indicated that the Na^+ pump might be driving absorptive processes following a blood meal. These patterns of basolateral P-type ATPase and apical V-type ATPase localization in the adult hindgut further support the notion that the ileum and rectal pads are sites of ion and water movement (Patrick et al., 2006). As previously mentioned, it is also possible that these ATPases may be playing a role in epithelial cell homeostasis and not in transcellular ion transport, and further research is necessary to elucidate their precise function. Osmoregulation is achieved through the variable expression of aquaporins (AQP), or water channels. For example, it was recently demonstrated that the mosquito prevents reabsorbing water after a blood meal by down regulating the expression of AQPs 1, 2, and 5 in the hindgut (Drake et al., 2015).

The rectum is the most terminally-localized excretory organ, and the major site for final reabsorption of ions, water, and nutrients - it is capable of reabsorbing fluid against strong osmostic gradients. Classical studies elucidated the role of the anal papillae in larval mosquitoes: the uptake of ions from dilute environments against a large concentration gradient (Koch, 1938; Ramsay, 1953). Rectal epithelia revealed a low expression of both ATPases, which helps support

the theory that this is a site solely responsible for reabsorption. Further support for the role of the ileum as absorptive and secretory and the rectum as solely absorptive derives from the epithelial cell structure of these organs. The ileum is composed of simple cuboidal cells, which are characteristic of both absorptive and secretory function. In contrast, the rectal pads are composed of simple columnar cells that function in absorption mechanisms (Clements, 2000; Hanrahan and Phillips, 1983; Piersol, 1897).

The structure and function of the insect neuroendocrine system

The processes in an insect's life that require precisely coordinated control include, but are not limited to, embryonic and postembryonic development, reproductive activity, and changing metabolic and behavioural patterns (Raabe, 1989). Like vertebrates, insects share the use of two integrative control systems, the nervous and endocrine systems. The neuroendocrine system is composed of neurosecretory centers in which active material is synthesized and the neurohaemal structures where the neurosecretory material is stored and released. Many neurons of the central and peripheral nervous system produce hormones that are released locally in the extracellular space, as well as in the circulatory system (i.e. blood or haemolymph) (Hartenstein, 2006). Neurons that produce neurohormones are called neurosecretory cells (NSCs). Neurohaemal organs are responsible for storing and later releasing the products they receive from NSCs (Scharrer, 1987). The neuropeptides released by neurohaemal organs can be released into the bloodstream, or directly into the extracellular space in close proximity to target tissues (Hartenstein, 2006). Ultimately, NSCs and neurohaemal organs form the neuroendocrine system. Prior to exploring the function of the neuroendocrine system, it is important to clearly define the different classes of neuropeptide signalling molecules produced by neuronal tissues:

neurohormones, neurotransmitters, and neuromodulators (Burrows, 2012). Neurohormones are chemical messages released by neurons into the circulatory system, exerting their effects on distant peripheral targets. Neurotransmitters are released from neurons at anatomically specialized junction, diffuse across a narrow cleft, and finally bind appropriate receptors on a postsynaptic neuronal, muscle, or other effector cell. Neuromodulators can affect a group of neurons at various synapses, or effector cells located at further distances (Burrows, 2012).

In insects, the neurosecretory system consists of several sets of NSCs located in the brain and the ventral nerve cord (VNC). The majority of NSCs in the brain are found in the dorso-medial protocerebrum, or the pars intercerebralis (PI) and pars lateralis (PL) (Hartenstein, 2006). Other areas having an abundance of NSCs include the subesophageal ganglion (SEG) and VNC (Fig. 1). These NSCs project their axons to innervate the retrocerebral complex of endocrine glands, the corpora cardiaca (CC) and corpora allata (CA), both of which are located in close proximity to the dorsal vessel (Fig. 1), which is the main pulsatile organ (i.e. heart) that drives haemolymph throughout the open circulatory system of the insect. The NSCs located in the VNC terminate at neurohaemal release sites (Hartenstein, 2006). The axon bundles, or nerves, that innervate the CC include the nervi corpis cardiaci I (nccI) from the PI, nervi corpis cardiaci II (nccII) from the PL and nervi corpis cardiaci III (nccIII) from the SEG (Fig. 1) (Hartenstein, 2006). Notably in *Drosophila melanogaster* (the common fruit fly), the CC, CA, and a third (neuro)endocrine gland, the prothoracic gland (PTG) are fused into a single complex, the ring gland (Hartenstein, 2006). The ring gland surrounds the anterior end of the dorsal vessel, which provides a passageway for neuropeptides to be released directly into the circulatory system allowing efficient delivery to target cells and tissues (Talamillo et al., 2008).

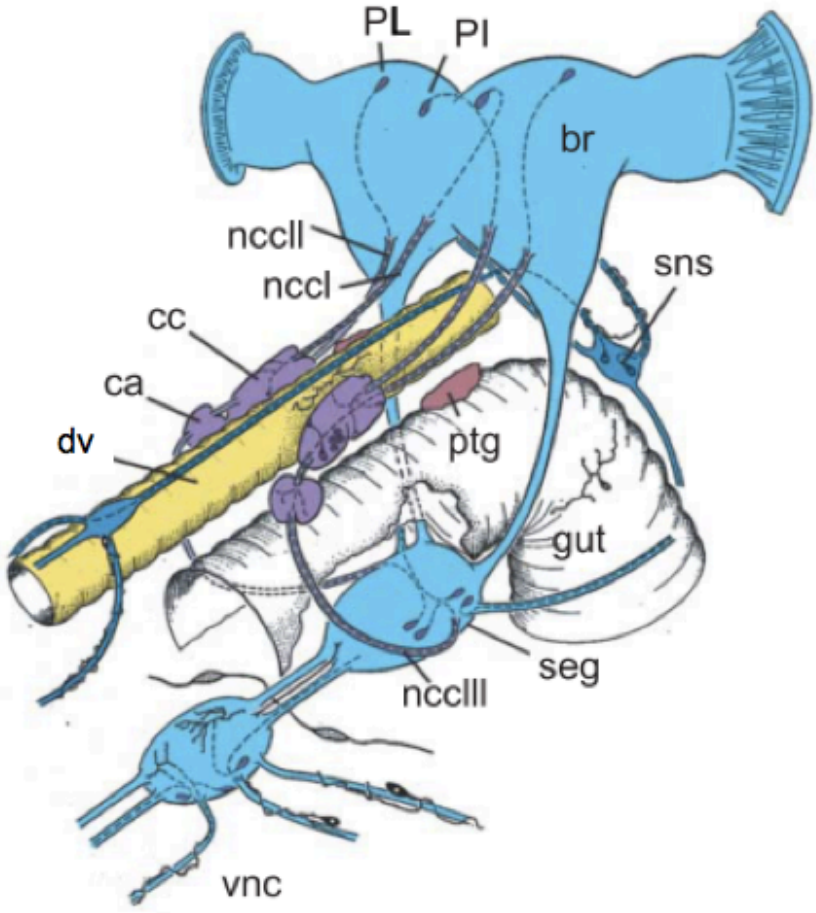

Figure 1: Posterior–dorsal view of insect neuroendocrine system. Central NSCs are located in the pars intercerebralis (PI), pars lateralis (PL), the subesophageal ganglion (seg), and the ventral nerve cord (vnc). The retrocerebral complex of endocrine glands receiving NSC axons consists of the corpora cardiaca (cc) and corpora allata (ca), both of which are located close to the dorsal vessel (dv). NSCs innervate the retrocerebral complex via the nccI nerve (from PI), nccII (from PL), and nccIII (from seg). Secretory axons of NSCs located in the ventral nerve cord terminate at neurohaemal release sites. The prothoracic gland (ptg) is responsible for the synthesis and release of ecdysteroids. The stomatogastric nervous system (sns) contains further NSCs and is functionally closely connected to the ca and cc. Adapted from Hartenstein, 2006.

Peripheral neuroendocrine glands in insects include the CC and the median nerve perivisceral organs (PVOs), while the CA and PTG are defined as peripheral endocrine glands. The CC is divided into two distinct lobes, an unpaired ventral neurohaemal storage lobe, containing the axon terminals of NSCs located in the PI and PL, and a lateral glandular lobe that is formed by its own respective NSCs (Dorn, 1998). However, not all insects possess a storage lobe, therefore the NSC terminal axons would pass through the CC and end in contact with the dorsal vessel (Schooneveld, 1998). PVOs are characterized as neurohemal organs, one of the most prominent sites for release of neurosecretory products into the haemolymph besides the retrocerebral complex (Braunig, 1987). The CA is responsible for the production of juvenile hormone, a fatty acid derivate that has profound effects on larval growth, metamorphosis, egg development, and sexual behaviour (Gilbert et al., 2000). The PL, via its projections to the CA, is the source for positive and negative control over juvenile hormone production. For example, the neuropeptide allatostatin that is produced in the PL inhibits juvenile hormone release (Stay et al., 1996). The PTG is responsible for the production and secretion of ecdysteroids. 20-hydroxyecdysone is well known as the major molting hormone that triggers metamorphosis, which is the transition from one stage of the insect to the next (e.g from larval to pupal stage) (Bollenbacher et al., 1975) .

Endocrine Control of The Hindgut

To ensure their survival, insects (and all animals for that matter) must ensure a precisely timed interplay between hormonal and membrane transport processes to facilitate the rapid removal of excess ions and fluids consumed in a food meal (Pullikuth et al., 2006). During this process known as diuresis, or urine production, diuretic hormones promote fluid formation and rapid secretion by the Malpighian tubules (MTs). The opposite mechanism is known as anti-

diuresis, in which there is a reduction in the net volume of urine produced. Anti-diuretic hormones act upon the hindgut to promote water reabsorption, among other things (Phillips, 1981) and can alternatively directly act upon the Malpighian tubules to inhibit the secretion of primary urine (Coast, 2002; Paluzzi, 2012). Factors that have been characterized to play a diuretic role promoting the secretion of primary urine from the MTs include the biogenic amines tyramine and serotonin, as well as peptides such as corticotropin-releasing factor (CRF)-related peptides, insect kinins, calcitonin-like peptides and the CAPA family of peptides (Paluzzi, 2012). The CAPA family of peptides have also been shown to inhibit fluid secretion in *Rhodnius prolixus* (the kissing bug), suggesting their role in anti-diuresis (Quinlan and O'Donnell, 1998). In *Tenebrio molitor* (the mealworm) native anti-diuretic factor (ADF) has been identified as a potent inhibitor of MT secretion via an increase of intracellular cGMP levels (Eigenheer et al., 2002). *T. molitor* ADFa has also been shown to inhibit the fluid secretion rate of MTs in *A. aegypti* by signaling through intracellular cGMP (Massaro et al., 2004). Unfortunately, the endocrine control of the hindgut is an area that has been relatively unexplored in comparison to the other main excretory organs, namely the Malpighian tubules (Coast, 2009).

The desert locust, *Schistocerca gregaria,* has been extensively studied and faces similar dietary and environmental challenges to the mosquito; water must be conserved during unfed states, whereas the expulsion of water and certain ions is necessary during fed states (Phillips et al., 1996; Robertson et al., 2014). With this rationale, the locust will be used as a model to delineate possible regulatory mechanisms within the hindgut of the adult mosquito, *A. aegypti.* Anti-diuretic hormones of the locust neuroendocrine system play an important role in maintaining the reabsorptive properties of the hindgut - some of which include the neuropeptides chloride transport stimulating hormone (CTSH) and ion transport peptide (ITP) (Phillips and

Audsley, 1995). CTSH mediates its actions on the rectal epithelia through a cyclic adenosine monophosphate (cAMP)-mediated pathway, and has been shown to promote the active reabsorption of chloride ions by stimulating an electrogenic Cl^- pump (Hanrahan and Phillips, 1983). In addition, the energy for potassium ion reabsorption through channels on the apical membrane of the rectal epithelia is driven by the action of the Cl^- pump. Finally, CTSH inhibits the active secretion of protons (Phillips and Audsley, 1995; Phillips et al., 1988) (Figure 2). ITP is also suggested to act through the second messenger cAMP to increase chloride, sodium, and potassium ion reabsorption across the hindgut of *S. gregaria* (Audsley et al., 2013). The driving mechanism for ion and water absorption is the electrogenic Cl^- pump that establishes the electrical coupling necessary for K^+ ion passive reabsorption (Phillips et al., 1986; Phillips et al., 1988) (Figure 3). In the context of the hindgut, water reabsorption is achieved by following the osmotic gradient created by ion reabsorption (Clements, 2000; Nation, 2008). Both neuropeptide hormones act through cAMP-mediated pathways to recycle ions and water in the locust, ultimately regulating haemolymph homeostasis. Taken together, this provides insight on the action of neuropeptide hormones that have been less characterized in *A. aegypti,* which may control reabsorptive processes over the adult mosquito hindgut in a similar manner.

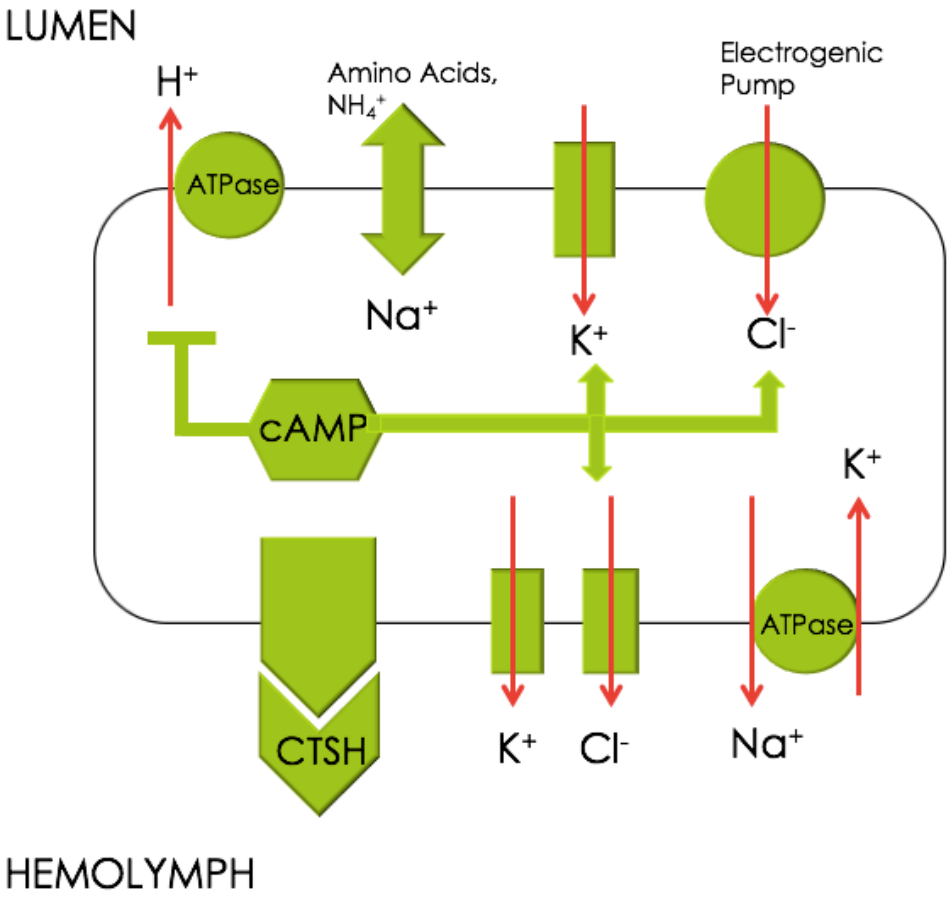

Figure 2: A model illustrating membrane ion transport mechanisms in locust rectal pad epithelial cells. The active entry of Cl^- is enhanced by low luminal K^+ concentration and by high intracellular cAMP, which is elevated by the neuropeptide Chloride transport-stimulating hormone (CTSH). cAMP has also been proposed to stimulate passive transport of K^+ across the apical membrane (lumen-facing), and passive Cl^- exit across the basal membrane (haemolymph-facing). A basolateral Na^+/K^+-ATPase transports potassium into the cell and sodium to the haemolymph. Ultimately, there is active fluid transport to the haemolymph side. Circles represent major ion pumps, rectangles represent ion channels, and two-sided arrows represent countertransport**.** Adapted from Hanrahan and Phillips, 1983 and Phillips et al., 1988.

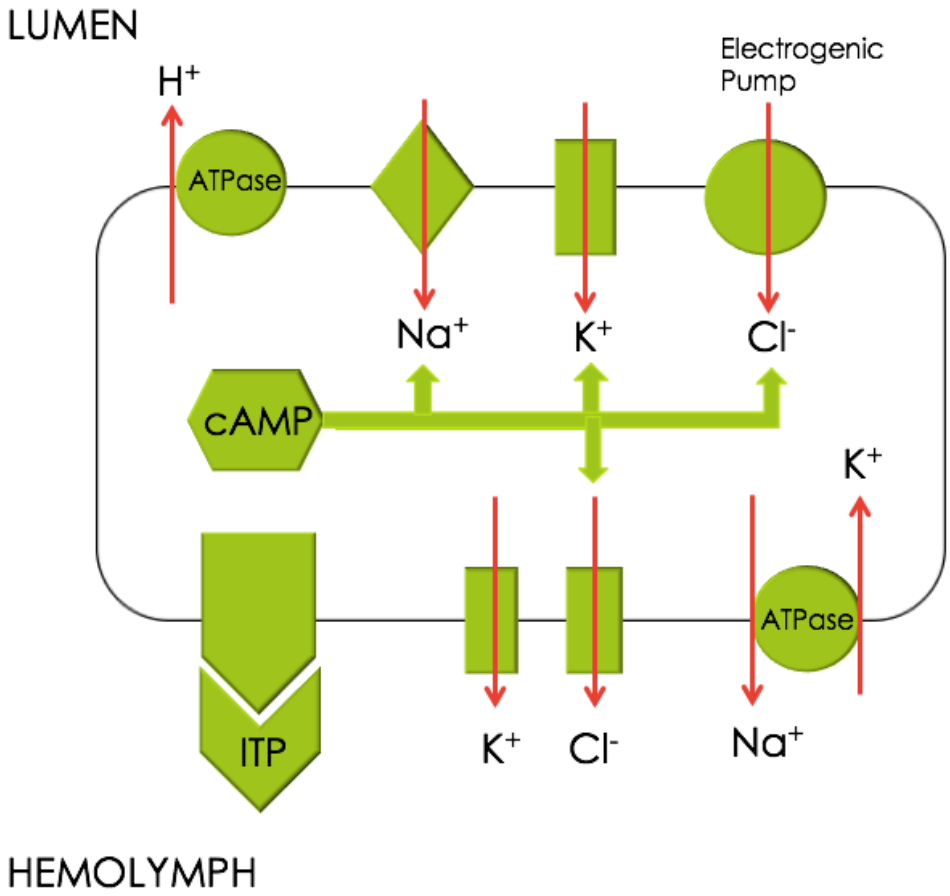

Figure 3: A model for the control of ion transport across the locust ileum via intracellular cAMP. *Schistocerca gregaria* ion transport peptide (SchgrITP) binds to its receptor (a proposed GPCR) resulting in the elevation of intracellular cyclic AMP, stimulating Cl^- (electrogenic pump), Na^+ (unknown mechanism) and K^+(ion channel) entry at the apical (lumen-facing) membrane. cAMP also stimulates the basolateral (haemolymph-facing) exit of Cl^- (ion channels). Circles represent major ion pumps, rectangles represent ion channels, and diamonds represent unknown transporters. Adapted from Audsley *et al*., 2013.

The relatively novel-discovered heterodimeric glycoprotein hormone GPA2/GPB5 has been proposed to regulate ionic and osmostic balance in insects such as the fruit fly, *D. melanogaster* and mosquito, *A. aegypti* (Paluzzi, 2012; Paluzzi et al., 2014; Sellami et al., 2011). The transcript expression of its receptor, *A. aegypti* leucine-rich containing GPCR 1 (AedaeLGR1), showed expression in tissues of the alimentary canal such as the midgut, Malpighian tubules, as well as the hindgut and expression was enriched in adult stage insects (Paluzzi et al., 2014). Similarly, the LGR1 receptor in the *D. melanogaster* was shown to localize to hindgut epithelia by *in situ* hybridization (Sellami et al., 2011). Like CTSH and ITP in the locust, GPA2/GPB5 has been suggested to play an anti-diuretic role in both adult *D. melanogaster* and adult *A. aegypti* (Paluzzi et al., 2014; Sellami et al., 2011; Vandersmissen et al., 2014). Considering the adult hindgut tissue localization of the apical V-type H+-ATPase and basolateral P-type Na+/K+-ATPase (Patrick et al., 2006), it has been suggested that GPA2/GPB5 may regulate the activity of these two transporters to enable the retention of Na^+ ions towards the haemolymph and eliminate excess K^+ in the urine. This theory was supported by Paluzzi *et al*., (2014) where the Scanning Ion-Electrode Technique (SIET) was used to determine the effect of treating the hindgut with a recombinant form of GPA2/GPB5. The outcome of this study revealed that recombinant *A. aegypti* GPA2/GPB5 lead to a decrease in net secretion of Na^+ by the ileum, measured as decreased lumen-directed sodium flux, and caused increased Na^+ absorption in the rectum. There was a decrease in K^+ absorption across all areas of the hindgut examined along the hindgut (Paluzzi et al., 2014). These findings revealed that GPA2/GPB inhibited natriuresis, or sodium excretion, and promoted kaliuresis, or potassium excretion, and provided insight on the first presumed anti-diuretic factor acting on the hindgut of the mosquito, *A. aegypti* (Paluzzi et al., 2014).

Discovery of Ion Transport Peptide in *S. gregaria*

Prior to the purification and identification of Ion Transport Peptide, the entire central nervous system of *S. gregaria* was surveyed for stimulatory activity. Tissue extracts were prepared by harvesting brain, corpora cardiaca, corpora allata, subesophageal ganglia and all eight ventral ganglia from adult male locusts, 2-6 weeks past their final molt. Glands were immediately frozen on dry ice and protein extracts were prepared by mechanically homogenizing tissues in saline. Bioassays were conducted by measuring changes in transepithelial potential, or short-circuit current (I_{SC}), upon voltage clamping of ileal tissue (Audsley and Phillips, 1990). Proteinaceous factors detected in the brain, corpus cardiacum (CC), and the 4th and 7th ventral ganglia (VG) stimulated ileal I_{SC} in a dose-dependent manner (Audsley and Phillips, 1990).These findings prompted Audsley *et al*., (1992) to purify the predominant ileal stimulant derived from the CC. Using reverse-phase high performance liquid chromatography, they isolated and purified this protein factor from CC extracts and named it Ion Transport Peptide (ITP) (Audsley et al., 1992a). They used an ileal I_{SC} bioassay, an indicator of Cl^- transport, to show that purified ITP from CC extracts indeed stimulated Cl^--dependent short circuit current across the locust ileum. Short-circuit current (I_{SC}) is a direct continuous measure of electrogenic ion transport. The locust ilea I_{SC} were previously reported to be Cl^--dependent and a measure of electrogenic active transport of this anion (Irvine et al., 1988). The purified *S. gregaria* ITP (SchgrITP) was shown to have an unblocked amino-terminus (N-terminus), a molecular mass of approximately 8652 Da, and the first 33 amino acid residues were discovered (Audsley et al., 1992a; Meredith et al., 1996). Further studies were conducted to compare the effects of purified ITP and crude CC extracts on ileal I_{SC}, where both were found to increase Cl^-, K^+, and Na^+ reabsorption. In addition, H^+ secretion in the ileum (J_H), was abolished by high concentrations of ITP (Audsley et

al., 1992b).

In 1996, Meredith *et al*. sought to elucidate the entire amino acid sequence of SchgrITP. They utilized degenerate primers, and screened a locust brain complementary DNA (cDNA) library, to clone the cDNA that encoded the known partial 33 amino acid N-terminal sequence identified earlier (Audsley et al., 1992a). This group went on to identify the complete cDNA that contained 517 base pairs, and encoded the complete open reading frame for the ITP prepropeptide of 130 amino acid residues (Meredith et al., 1996). They further illustrated a 55-residue leader sequence, within which lies the signal peptide, and the complete 72-residue sequence of the mature peptide. Six cysteine residues, proposed to participate in intramolecular disulphide bridge formation, were localized to positions 7, 23, 26, 39, 43, and 52 of ITP (Meredith et al., 1996). The three disulphide bridges are necessary for determining the distance between essential motifs and the N- or C-terminus. Thus, they were thought to be fundamental for the biological activity of ITP (King et al., 1999). When the disulphide bonds formed between cysteine groups were reduced by carboxymethylation, SynITP lost its biological activity, demonstrated by its inability to stimulate ileal I_{SC}. Even if only one of the cysteine residues involved in disulphide bridge formation was mutated to an alanine, biological activity of SynITP was compromised as I_{SC} was significantly reduced. Specifically, mutating a single cysteine to an alanine was shown to abolish up to 90% of SynITP's biological activity (King et al., 1999).

Meredith *et al*., (1996) also discovered ITP-Long form (ITPL), which contained a 121 base pair insert at amino acid position 40 of ITP. The mature ITPL peptide was only 4 amino acids longer than ITP, and contained a unique carboxy-terminus (C-terminus) with only 36% sequence identity with ITP (Phillips et al., 1998). The six cysteine groups of locust ITP were found to be conserved in locust ITPL as well (Meredith et al., 1996). The Meredith group also

characterized the tissue localization of both ITP and ITPL; ITP mRNA was detected in the brain and CC, while ITPL mRNA was detected in flight muscle tissue, hindgut, and MTs. Notably, an ileal bioassay showed that ITPL had no stimulatory effect on ileal I_{SC} in the locust, however, it inhibited the stimulatory effect of synthetic ITP on ileal I_{SC} (Ring et al., 1998).

Characterizing the ITP peptide domains

In a review by Phillips *et al*., (1998) it was proposed that the shared N-terminus of ITP and ITPL is what permits the neuropeptide to bind to its receptor. The absence of both the C-terminal alpha-helix and C-terminal amidation in ITPL was suggested to block receptor activation; ITPL may be functioning as an ITP receptor antagonist (Phillips et al., 1998). Coast *et al*., (2002) proposed that the function of the terminal 20 amino acids in ITPL are to disrupt the specific activation structure of the ITP C-terminus (Coast, 2002). A domain swap mutation replacing the SchgrITP N-terminus with that of shrimp CHH resulted in a complete loss in stimulatory activity of ileal short-circuit current (Zhao et al., 2005), solidifying the importance of the N-terminus in the biological activity of ITP. Increasing truncation of the C-terminus was used to investigate the role of the C-terminus in receptor binding and ileal activation (Wang et al., 2000). Simply removing the amidation and dibasic cleavage recognition site, -GKK, of the C-terminus reduced the biological activity of ITP by two orders of magnitude, shown through its inability to stimulate ileal I_{SC}. Further truncation of one (-LGKK), two (-ILGKK), or five amino acids (-MVEILGKK) at the C-terminus all completely abolished the biological activity of ITP. Interestingly, *in vitro* amidation of ITP increased the specific biological activity, hence indicating that amidation of the C-terminus is required for full biological activity. Particularly, removal of the C-terminal leucine residue at position 72 not only abolished stimulatory activity, but also

reduced ITP-receptor binding (Wang et al., 2000). This lead to the proposal that binding and signal transduction sites in ITP overlap, and they are not exclusively located within either the N- or C-terminus (Wang et al., 2000).

Characteristic features of all ITPs

All insect ITPs and ITPLs share five conserved characteristics. (1) Six cysteine residues are located in the same position to allow for the formation of three intramolecular disulphide bonds. (2) The mature peptides are 72 amino acids in length, except for dipteran species that have one extra N-terminal amino acid. (3) The presence of aromatic amino acids (Phe or Tyr) in position 3 (or positions 2, 4 or 3 in dipteran ITPs) of the N-terminal alpha-helix are a conserved feature that has been proposed to be important for biological activity. (4) The highest conservation of amino acids lies within the core structure of the first 40 or 41 amino acids. (5) In regards to ITP only, C-terminal amidation confers protection against carboxypeptidase degradation (Dircksen, 2009).

Markedly, four major groups of neurons produce ITP or ITPL: (1) pars lateralis NSCs in the protocerebrum that possess axonal projections with release sites in CC/CA (retrocerebral complex); (2) interneurons of the brain and ventral nerve cord (subesophageal ganglia, thoracic and abdominal ganglia) which may connect NSCs to other neurons; (3) efferent neurons such as those found in the abdominal ganglia of *D. melanogaster,* which innervate the hindgut directly; and (4) NSCs associated with neurohemal organs of the peripheral nervous system that likely only produce ITPL (Dircksen, 2009).

Tissue expression profile of ITPs

Although the tissue expression profile of SchgrITP mRNA had been previously outlined in 1996, the peptide had not yet been detected in the locust tissue (Meredith et al., 1996). Macins *et al*., (1999) performed a western blot analysis using antibodies for SchgrITP and SchgrITPL to identify the tissue expression profile of the peptide. This study was the first to immunologically detect SchgrITP in the CC of other orthopteran insects, pertaining to the same order as the desert locust (Macins et al., 1999). Among these insects included *Schistocerca gregaria* (desert locust), *Locusta migratoria* (migratory locust), and *Acheta domesticus* (house cricket). *S. gregaria* brain and CC tissue contained immunopositive material that co-migrated with SynITP at around 8700 Da. The immunopositive material was presumed to be SchgrITP. *S. gregaria* brain, ileal, or rectal tissue did not react with a SchgrITPL specific antibody, suggesting the absence of the longer peptide isoform in these tissues. CC tissue from other orthopteroids, including *L. migratoria* and *A. domesticus*, probed with antibodies raised to SchgrITP, all contained immunopositive bands that co-migrated with *S. gregaria* CC extracts or SynITP (Macins et al., 1999). This was interpreted as evidence for ITP in the CC of these insects. The immunoreactivity of SchgrITP present in both the brain and CC implied that it is synthesized by neurosecretory cells in the brain, and stored in the CC. It would be later released from the CC into the haemolymph, where it would elicit its effects by binding to its specific receptor (Macins et al., 1999).

In 2007, Dai *et al*. set out to uncover the expression of ITP gene products in the central and peripheral neurons of insects. Initially, RT-PCR was used with total RNA derived from either the brain or VNC to test for the presence of *Manduca sexta* ITP and ITPL (MasITP/MasITPL). Their results showed that both peptides were found in the brain, however

MasITP was absent from RNA extracts of the ventral nerve cord. With these preliminary findings, they performed fluorescence *in situ* hybridization (FISH) to observe the tissue specific expression of peptide transcripts in *M. sexta, B. mori,* and *S. americana.* In *M. sexta,* they found evidence for expression of ITPL, but not ITP in the neurons of the ventral ganglia and the peripheral nervous system. Additionally, neither ITP nor ITPL gene transcripts were observed in the cells of the subesophageal ganglion. Notably in larvae, a group of five dorsolateral neurosecretory cells in each hemisphere of the brain exhibited increased expression of MasITP/ITPL. Furthermore, their axons showed strong MasITP immunoreactivity, however neither CC nor CA stained for MasITP/ITPL transcripts. Immunohistochemistry was used to survey the presence of ITP/ITPL in the brain of *B. mori* and *S. americana* larvae. Very similar results were obtained in *B. mori* brain tissue where six pairs of dorsolateral cells showed ITP/ITPL immunoreactivity with their axon projections to the CC/CA complex having strong ITP but lacking any ITPL immunoreactivity. Unfortunately, they were unable to show specific staining in the CNS of *S. americana* as they used a primary antibody specific for the C-terminus of MasITP, which possesses considerable sequence differences to that of *S. americana* (Dai et al., 2007).

Later in 2008, Dircksen *et al*. investigated the localization of ITP in the central and peripheral nervous system of *D. melanogaster* throughout postembryogenesis. Western blots of larval CNS tissue and adult heads were used to confirm the existence of a single ITP-immunoreactive band at approximately 8.2 kDa (expected 8.9 kDa). Using both immunohistochemistry and FISH, they uncovered two groups of ITP-immunoreactive neurons in the brain and abdominal ganglia that persisted throughout metamorphosis from the first larval stage into the adult stage. In larval brain, the most prominent and strongly staining group of ITP-

immunoreactive cells was comprised of four bilateral pairs of neurons (ipc-1 neurons). In adult *D. melanogaster,* the four pairs of ipc-1 neurons always occur in posteriodorsal and mediolateral positions. Additionally, there are three more groups of ITP-immunoreactive neurons in the brain of adults: ipc-2 through ipc-4. All larval and prepupal stages contained a prominent pair of ITP-immunoreactive subesophageal neurons located in a ventromedial position. In regards to abdominal neurons, one pair of strongly labelled dorsolateral and two or three pairs of faintly stained ventrolateral to ventromedial pairs of ITP neurons were found in the eighth abdominal neuromeres of larvae, pupae, and adults; it is important to note that their staining intensity varied considerably, and they were often not visible in larvae (Dircksen et al., 2008; Omoto et al., 2016). Neuromeres are strictly defined regions of the central nervous system belonging to one body segment. Each neuromere contains the neural circuitry responsible for processing sensory signals and controlling the movements of the body segment they belong to (Niven et al., 2008).

Conserved Ion Transport Peptide gene among insects

Dai *et al*. (2007) were the first to identify conserved ITP genes, which by alternative splicing, can produce two different peptides (ITP and ITPL) in *M. sexta* (tobacco hornworm), *Bombyx mori*, and *A. aegypti*. A smaller transcript variant produces a peptide containing an amidated C-terminus (ITP), while the other longer transcript variant yields a peptide possessing an unblocked C-terminus (ITPL). In every insect that ITP/ITPL has been studied, it was uncovered that both peptides shared a common N-terminal sequences but had diverging C-termini (Dai et al., 2007). Specifically, in two mosquito species, *A. gambiae* and *A. aegypti*, a relatively longer exon 2 containing an additional 3' untranslated region differs from the equivalent exon sequence observed in *M. sexta* and *B. mori*. Furthermore, Dai and colleagues

found that one transcript arising from exons 1 and 3 encodes *A. aegypti* ITP (AedaeITP). Moreover, two possible transcript variants, encoding identical protein sequences, are involved in *A. aegypti* ITPL (AedaeITPL): exons 1 and 2, or exons 1, 2, and 3. Analysis of both cDNA and genomic DNA sequences of AedaeITP/ITPL indicated that exon 1 encodes a putative signal peptide of 23 amino acids, a propeptide of 7 amino acids, wherein lies a dibasic processing site (KR), and the N-terminal region of the mature peptide (amino acids 1-40). Exon 2 includes the remaining open reading frame (ORF) encoding the C-terminal mature peptide of AedaeITPL (amino acids 41-78) and finally the 3'UTR. Exon 3 includes the remaining ORF encoding the C-terminus of AedaeITP (amino acids 41-73), followed by a GKK amidation and dibasic cleavage recognition sites, and the 3'UTR. To date, no studies have been conducted to localize AedaeITP and AedaeITPL within the central and peripheral neurons of larval and adult *A. aegypti* (Dai et al., 2007).

Physiological actions of Ion Transport Peptide in *S. gregaria*

To determine the physiological action of SchgrITP and SchgrITPL, Audsley *et al*., (2006) measured the concentration of both peptides in the CC and haemolymph of fed vs. starved locusts. Both peptides were found in similar amounts in the CC, however, it was noted that ITP was degraded faster and overall measurements were less reliable. There was a four-fold increase in haemolymph ITPL in recently fed locusts compared to starved animals, suggesting a role for ITPL in post-feeding osmoregulation (Audsley et al., 2006). The presence of ITPL in the haemolymph provided further evidence that ITPL may be released to antagonize the activity of ITP. An eighty-fold increase in haemolymph ITP was observed in fed locusts, however, less than 3% of the total immunoreactivity was attributed to native ITP. Audsley *et al.* (2006) proposed

that this more hydrophobic immunoreactivity is neither native ITP nor a metabolic breakdown product; using high-performance liquid chromatography it was shown that over 95% of the immunoreactivity eluted later than synthetic ITP, implying that ITP binds something in the haemolymph that makes it appear more hydrophobic (Audsley et al., 2006). This study was the first to show immunoreactivity of ITP and ITPL in the haemolymph, further supporting that these peptides are released from the CC into the haemolymph (Audsley et al., 2006; Dai et al., 2007; Dircksen et al., 2008; Drexler et al., 2007).

The first model for the control of transepithelial ion transport in the ileum was proposed in the desert locust (Audsley et al., 2013). SynITP was shown to elevate intracellular levels of both cyclic adenosine monophosphate (cAMP) and cyclic guanosine monophosphate (cGMP) in a dose-dependent manner, measured over a 15-minute period. Additionally, 5 mM of cGMP was shown to increase the fluid reabsorption of the ileum, presumably through the stimulation of Cl^- transport (Audsley et al., 2013). These findings lead Audsley *et al*., (2013) to propose that ITP may act on separate receptors in the ileum, to elicit the elevation of different intracellular signalling molecules. It was hypothesized that the receptors are most likely GPCRs with a membrane bound adenylyl or guanylyl cyclase causing an increase in intracellular cAMP and cGMP, respectively. When ITP binds to a GPCR on the basolateral, haemolymph-facing membrane, intracellular cAMP is increased. cAMP stimulates the apical, lumen-facing, Cl^- electrogenic pump and increases the uptake of Cl^- ions from the lumen into the cell. These Cl^- ions are then released into the haemolymph through Cl^- channels on the basolateral membrane, which are also stimulated by cAMP. Passive transport of K^+ at the apical membranes is enhanced by cAMP, and K^+ ions are electrically coupled to the flow of Cl^-. Finally, Na^+ reabsorption is increased as cAMP stimulates Na^+ conductance at the apical membrane. The result of increased

intracellular cAMP ultimately leads to the reabsorption of Cl^-, K^+, and Na^+ into the haemolymph. Further, flowing down its osmostic gradient, water is reabsorbed as well (Audsley et al., 2013).

It has been reported that ITP may bind to a second distinct receptor, activating a membrane-bound guanylyl cyclase, leading to increased intracellular levels of cGMP. cGMP likely directly stimulates an apical Cl^- electrogenic pump and activates the opening of channels in the basolateral membrane to increase the reabsorption of Cl^- (Audsley et al., 2013) (Figure 4). This is supported by the observation that the addition of cGMP has been shown to stimulate Cl^- dependent short circuit current across locust ilea (Audsley and Phillips, 1990). By an unknown mechanism, it has been proposed that cGMP stimulates lumen-directed H^+ transport at the apical membrane (Audsley et al., 2013). These models proposed by Audsley *et al.,* (2013) are preliminary and should be interpreted with caution, as no receptor for SchgrITP has been discovered in the locust to date. In 2014, the first presumed receptors for ITP and ITPL were elucidated in *B. mori* (Nagai et al., 2014). Nagai *et al*., (2014) identified three *B. mori* orphan neuropeptide G-protein coupled receptors (GPCRs), BNGR-A4, -A24, and -A34, as receptors for ITP and ITPL. All receptors were shown to respond to recombinant ITPs. Interestingly, recombinant ITP was shown to elevate intracellular levels of cGMP upon receptor binding (Nagai et al., 2014). The finding that the receptors for ITP in *B. mori* are GPCRs that elevate intracellular cGMP lends support to the model of ITP action on ileal ion transport in *S. gregaria*, postulated earlier by Audsley *et al.,* in 2013 (Audsley et al., 2013; Nagai et al., 2014). More recently, this same group identified that the orphan *B. mori* GPCR BNGR-A24 is an ITPL receptor that also acts as a receptor for all five *B. mori* tachykinin-related peptides (TRPs); ITPL and TRPs are endogenous orthosteric, or primary, ligands of BNGR-A24 that may activate discrete intracellular signalling pathways (Nagai-okatani et al., 2016).

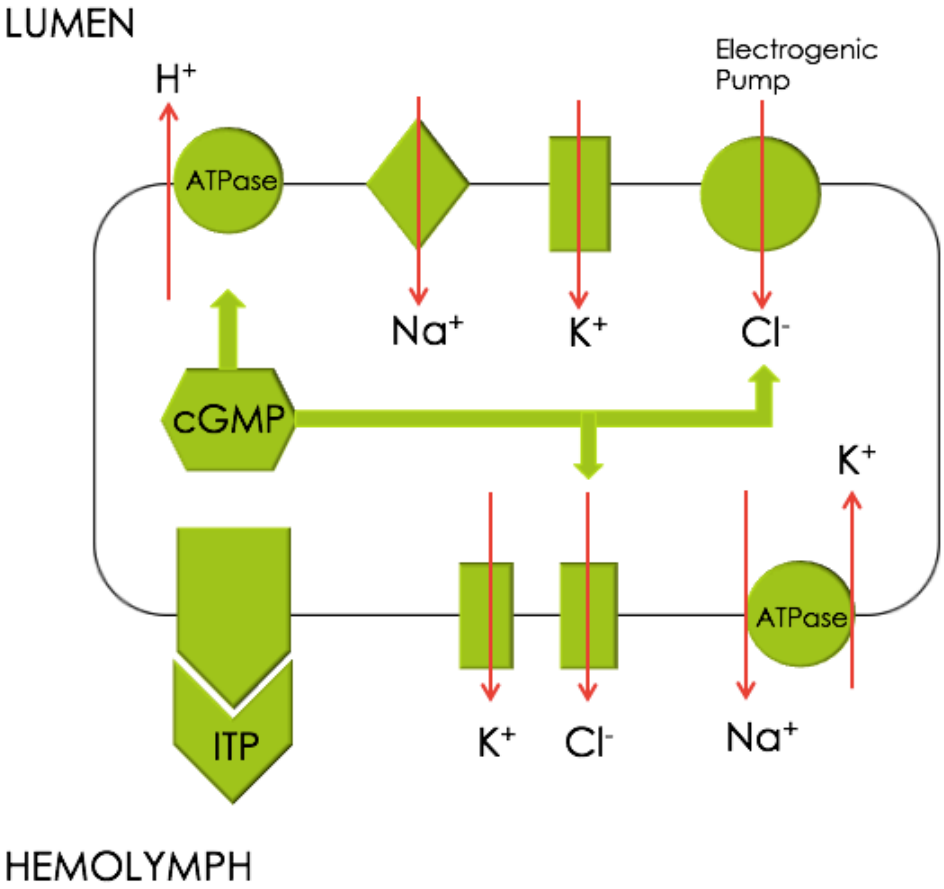

Figure 4: A model for the control of ion transport across the locust ileum via intracellular cGMP. Activation of a potential membrane-bound guanylyl cyclase causes increased cGMP stimulating Cl^- (electrogenic pump) entry at the apical (lumen-facing) membrane, and basolateral (haemolymph-facing) exit of Cl^- (ion channels). cGMP stimulates apical lumen-directed transport of H^+ (unknown mechanism), which is responsible for expelling H^+ into the excreta. Circles represent major ion pumps, rectangles represent ion channels, and diamonds represent unknown transporters. Adapted from Audsley *et al*., (2013).

Research objectives and Hypotheses

It has been well characterized that the adult mosquito *A. aegypti* is a renowned primary vector for many harmful diseases (Clemons et al., 2010a). Since these diseases inflict serious harm on millions of people worldwide annually, it is imperative that their physiology is meticulously explored to provide new avenues geared towards disease-vector control. Unfortunately, most research to date has been centered on the larval life stage. In addition, most research on the excretory system has been focused on the midgut and Malpighian tubules. Nevertheless, the hindgut plays a key role in maintaining osmotic and ionic homeostasis. Iono- and osmoregulation are necessary processes for the mosquito to maintain haemolymph composition within narrow limits, further retaining constant internal conditions, or homeostasis. Moreover, the neuropeptides mediating control of the mosquito ileum are yet to be identified. As mentioned above, ITP was the first characterized major stimulant of ileal reabsorption and was described in the desert locust, *S. gregaria* (Audsley et al., 1992a; Audsley et al., 1992b). The desert locust faces similar dietary and environmental challenges to the adult mosquito; water and ions must be conserved during unfed states, whereas the expulsion of excess water and ions is necessary in post-fed states (Phillips et al., 1996). With this rationale, research conducted in the locust was used to model possible regulatory mechanisms within the hindgut of the adult mosquito, *A. aegypti.*

The primary goal of my research was to investigate the localization and physiological role of ITP in the adult mosquito, *A. aegypti.* My first objective included (i) generating a functional ITP recombinant peptide, utilizing an endocrine-derived cell culture system involving mouse anterior pituitary (AtT-20) cells to express either *A. aegypti* ITP (AedaeITP) or *D. melanogaster* ITP (DromeITP). The AtT-20 cell line is a mouse pituitary tumour cell line that

secretes adrenocorticotropic hormone (ACTH), therefore, it has been used widely to study peptide secretion. In particular, AtT20 anterior pituitary cells were shown to secrete ACTH into the media bathing the cells (Buonassisi et al., 1962). *I hypothesized that using an endocrine-derived cell culture model, AtT20, would allow for the optimal production of recombinant AedaeITP or DromeITP in comparison to a non-endocrine-derived cell line, specifically HEK293T.* This prediction was reinforced by previous studies that used the endocrine AtT-20 cell culture system to study secreted peptides; results showed peptides were secreted into the culture medium post-transfection (Gamby et al., 1996; Macdonalds et al., 1989).

The distribution and localization of AedaeITP has not been examined in *A. aegypti,* therefore (ii) using immunohistochemistry, I investigated the localization of AedaeITP within the nervous system of *A. aegypti*, particularly in the brain, thoracic, and abdominal ganglia. *I hypothesized that AedaeITP peptide would be distributed throughout neurosecretory cells of the nervous system. In particular, I predicted to find significant staining in neurons of the central nervous system (site of production), and the CC (site of storage and release).* This hypothesis was formulated on the basis of past research conducted on the localization of DromeITP in adult *D. melanogaster*, where it was shown that ITP-immunoreactive neurons were found in the brain, CC, and in the terminal abdominal ganglia (Dircksen et al., 2008).

Finally, to determine the physiological role of AedaeITP, (iii) the Scanning Ion-selective Electrode Technique (SIET) was utilized to investigate whether AedaeITP and its putative second messengers, cAMP and cGMP, influenced ion transport across the adult *A. aegypti* hindgut epithelium. Using SIET allowed for measurement of epithelial transport of potassium and sodium using their respective ion-selective ionophores. In the desert locust, synthetic ITP was shown to elevate intracellular levels of both cAMP and cGMP. Additionally, cGMP was

shown to increase the fluid reabsorption of the ileum, presumably through the stimulation of Cl^- transport (Audsley et al., 2013). With respect to the physiological action of ITP, this neuropeptide has been well characterized as an anti-diuretic factor acting on the locust ileum (Phillips et al., 1998). As a result, *I hypothesized that ITP would play a role in promoting haemolymph-directed ion transport (i.e absorption) of K^+ and Na^+ in the adult mosquito, A. aegypti. Furthermore, it was expected that ITP's putative second messengers, cAMP and cGMP, would have similar actions on increasing ion reabsorption*.

References

Audsley, N. and Phillips, J. E. (1990). Stimulants of ileal salt transport in neuroendocrine system of the desert locust. *Gen. Comp. Endocrinol.* **80**, 127–137.

Audsley, N., McIntosh, C. and Phillips, J. E. (1992a). Isolation of a neuropeptide from locust corpus cardiacum which influences ileal transport. *J. Exp. Biol.* **173**, 261–74.

Audsley, N., McIntosh, C. and Phillips, J. E. (1992b). Actions of Ion-Transport Peptide from Locust Corpus Cardiacum on Several Hindgut Transport Processes. *J. Exp. Biol.* **173**, 275–288.

Audsley, N., Meredith, J. and Phillips, J. E. (2006). Haemolymph levels of Schistocerca gregaria ion transport peptide and ion transport-like peptide. *Physiol. Entomol.* **31**, 154–163.

Audsley, N., Jensen, D. and Schooley, D. A. (2013). Signal transduction for Schistocerca gregaria ion transport peptide is mediated via both cyclic AMP and cyclic GMP. *Peptides* **41**, 74–80.

Bollenbacher, W. E., Vedeckis, W. V. and Gilbert, L. I. (1975). Ecdysone titers and prothoracic gland activity during the larval–pupal development of Manduca sexta. *Dev. Biol.* **44**, 46–53.

Brady, O. J., Johansson, M. A., Guerra, C. A., Bhatt, S., Golding, N., Pigott, D. M., Delatte, H., Grech, M. G., Leisnham, P. T., Maciel-de-Freitas, R., et al. (2013). Modelling adult Aedes aegypti and Aedes albopictus survival at different temperatures in laboratory and field settings. *Parasites {&} Vectors* **6**, 351.

Braunig, P. (1987). The satellite nervous system - an extensive neurohemal network in the locust head. *J. Comp. Physiol.* **160**, 69–77.

Buonassisi, V., Sato, G. and Cohen, A. (1962). Hormone-producing cultures of adrenal and pituitary tumor origin. *Proc. Natl. Acad. Sci.* **48**, 1184–1190.

Burrows, M. (2012). *The neurobiology of an insect brain*. Oxford Scholarships.

Carpenter, S. J. and La Casse, W. J. (1974). *Mosquitoes of North America (north of Mexico)*. University of California.

Clements, A. (1999). *The Biology of Mosquitoes: Volume 1: Development, Nutrition and Reproduction*. New York, NY: Chapman and Hall.

Clements, A. (2000). *The Biology of Mosquitoes: Development, Nutrition and Reproduction*. London: Chapman & Hall.

Clemons, A., Haugen, M., Flannery, E., Tomchaney, M., Kast, K., Jacowski, C., Le, C., Mori, A., Holland, W. S., Sarro, J., et al. (2010a). Aedes aegypti: An emerging model for vector mosquito development. *Cold Spring Harb. Protoc.* **5**,.

Clemons, A., Mori, A., Haugen, M., Severson, D. W. and Duman-Scheel, M. (2010b). Culturing and egg collection of Aedes aegypti. *Cold Spring Harb. Protoc.* **5**,.

Coast, G. et al. (2002). Insect Diuretic and Antidiuretic Hormones. *Handb. Biol. Act. Pept.* **29**, 279–409.

Coast, G. (2007). The endocrine control of salt balance in insects. *Gen. Comp. Endocrinol.* **152**, 332–338.

Coast, G. M. (2009). Neuroendocrine control of ionic homeostasis in blood-sucking insects. *J. Exp. Biol.* **212**, 378–86.

Coast, G. M., Orchard, I., Phillips, J. E. and Schooley, D. A. (2002). Insect diuretic and antidiuretic hormones. *Adv Insect Physiol* **29**, 279–409.

Dai, L., Zitnan, D. and Adams, M. (2007). Strategic expression of Ion Transport Peptide Gene

Products in Central and Peripheral Neurons of Insects. *J. Comp. Neurol.* **500**, 353–367.
Dircksen, H. (2009). Insect ion transport peptides are derived from alternatively spliced genes and differentially expressed in the central and peripheral nervous system. *J. Exp. Biol.* **212**, 401–12.
Dircksen, H., Tesfai, L. K., Albus, C. and Nässel, D. R. (2008). Ion transport peptide splice forms in central and peripheral neurons throughout postembryogenesis of Drosophila melanogaster. *J. Comp. Neurol.* **509**, 23–41.
Donini, A., Patrick, M. L., Bijelic, G., Christensen, R. J., Ianowski, J. P., Rheault, M. R. and Donnell, M. J. O. (2006). Secretion of Water and Ions by Malpighian Tubules of Larval Mosquitoes : Effects of Diuretic Factors , Second Messengers , and Salinity. **79**,.
Donini, A., Gaidhu, M. P., Strasberg, D. R. and O'Donnell M, J. (2007). Changing salinity induces alterations in haemolymph ion concentrations and Na+ and Cl- transport kinetics of the anal papillae in the larval mosquito, Aedes aegypti. *J Exp Biol* **210**, 983–992.
Dorn, A. (1998). Comparative structural aspects of development in neuroendocrine systems. *Microsc. Anat. Invertebr.* **11**, 1059–1092.
Drake, L. L., Rodriguez, S. D. and Hansen, I. A. (2015). Functional characterization of aquaporins and aquaglyceroporins of the yellow fever mosquito, Aedes aegypti. *Sci. Rep.* **5**, 7795.
Drexler, A. L., Harris, C. C., Dela Pena, M. G., Asuncion-Uchi, M., Chung, S., Webster, S. and Fuse, M. (2007). Molecular characterization and cell-specific expression of an ion transport peptide in the tobacco hornworm, Manduca sexta. *Cell Tissue Res.* **329**, 391–408.
Eigenheer, R., Nicholson, S., Schegg, K., Hull, J. and Schooley, D. (2002). Identification of a potent antidiuretic factor acting on beetle Malpighian tubules. *Proc Natl Acad Sci USA* **99**, 84–89.
Evans, A. M., Aimanova, K. G. and Gill, S. S. (2009). Characterization of a blood-meal-responsive proton-dependent amino acid transporter in the disease vector, Aedes aegypti. *J. Exp. Biol.* **212**, 3263–3271.
Foster, W. A. and Walker, E. D. (2009). Mosquitoes (Culicidae). In *Medical and veterinary entomology* (ed. Mullen, G. R. (Gary R.) and Durden, L. A.), pp. 207–260. Elsevier.
Gamby, C., Waage, M. C., Allen, R. G. and Baizer, L. (1996). Growth-associated Protein-43 (GAP-43) Facilitates Peptide Hormone Secretion in Mouse Anterior Pituitary AtT-20 Cells *. **271**, 10023–10028.
Gatherer, D. and Kohl, A. (2017). Zika virus : a previously slow pandemic spreads rapidly through the Americas. **1**, 269–273.
Gilbert, L. I., Granger, N. A. and Roe, R. M. (2000). The juvenile hormones: historical facts and speculations on future research directions. *Insect Biochem. Mol. Biol.* **30**, 617–644.
Hanrahan, J. W. and Phillips, J. E. (1983). Cellular mechanisms and control of KCl absorption in insect hindgut. *J. Exp. Biol.* **106**, 71–89.
Hartenstein, V. (2006). The neuroendocrine system of invertebrates : a developmental and evolutionary perspective. *J. Endocrinol.* **190**, 555–570.
Hasan, S., Jamdar, S. F. and Alalowi, M. (2016). Dengue virus : A global human threat : Review of literature. 1–6.
Heymann, D., Hodgson, A., Sall, A., Freedman, D., Staples, J., Althabe, F. and Al, E. (2016). Zika virus and microcephaly: why is this situation a PHEIC? *Lancet* **387**, 719–21.
Ianowski, J. P. and O'Donnell, M. J. (2004). Basolateral ion transport mechanisms during fluid secretion by Drosophila Malpighian tubules: Na+ recycling, Na+:K+:2Cl- cotransport and

Cl- conductance. *J Exp Biol* **207**, 2599–2609.
Ianowski, J. P., Christensen, R. J. and O'Donnell, M. J. (2002). Intracellular ion activities in Malpighian tubule cells of Rhodnius prolixus: evaluation of Na+-K+-2Cl- cotransport across the basolateral membrane. *J. Exp. Biol.* **205**, 1645–1655.
Irvine, B., Audsley, N., Lechleitner, R., Meredith, J., Thomson, B. and Phillips, J. E. (1988). Transport properties of locust ileum in vitro: Effects of cy- clic AMP. *J. Exp. Biol.* **137**, 361–385.
King, D. S., Meredith, J., Wang, Y. J. and Phillips, J. E. (1999). Biological actions of synthetic locust ion transport peptide (ITP). *Insect Biochem. Mol. Biol.* **29**, 11–18.
Koch, H. J. (1938). The absorption of chloride ions by the anal papillae of Diptera larvae. *J Exp Biol* **15**, 152–160.
Kraemer, M. U. G., Sinka, M. E., Duda, K. A., Mylne, A., Shearer, F. M., Barker, C. M., Moore, C. G., Carvalho, R. G., Coelho, G. E., Van Bortel, W., et al. (2015). The global distribution of the arbovirus vectors *Aedes aegypti* and *Ae. albopictus*. *Elife* **4**, e08347.
Larsen, E. H., Deaton, L. E., Onken, H., O'Donnell, M., Grosell, M., Dantzler, W. H. and Weihrauch, D. (2014). Osmoregulation and excretion. *Compr. Physiol.* **4**, 405–573.
Macdonalds, M. R., Takedas, J., Ricejll, C. M. and Krauses, E. (1989). Multiple Tachykinins Are Produced and Secreted upon Post-translational Processing of the Three Substance P precursor proteins. *J. Biol. Chem.* **264**, 15578–15592.
Macins, A., Meredith, J., Zhao, Y., Brock, H. W. and Phillips, J. E. (1999). Occurrence of ion transport peptide (ITP) and ion transport-like peptide (ITP-L) in orthopteroids. *Arch Insect Biochem Physiol* **40**, 107–118.
Maddrell, S. and O'Donnell, M. (1992). Insect malpighian tubules: V-ATPase action in ion and fluid transport. *J. Exp. Biol.* **172**, 417–429.
Massaro, R., Lee, L., Patel, A., Wu, D., Yu, M., Scott, B., Schooley, D., Schegg, K. and Beyenbach, K. (2004). The mechanism of action of the antidiuretic peptide Tenmo ADFa in Malpighian tubules of Aedes aegypti. *J. Exp. Biol.* **207**, 2877–2888.
Meredith, J., Ring, M., Macins, a, Marschall, J., Cheng, N. N., Theilmann, D., Brock, H. W. and Phillips, J. E. (1996). Locust ion transport peptide (ITP): primary structure, cDNA and expression in a baculovirus system. *J. Exp. Biol.* **199**, 1053–1061.
Mlakar, J., Korva, M., Tul, N., Popović, M., Poljšak-Prijatelj, M., Mraz, J., Kolenc, M., Resman Rus, K., Vesnaver Vipotnik, T., Fabjan Vodušek, V., et al. (2016). Zika Virus Associated with Microcephaly. *N. Engl. J. Med.* 160210140106006.
Musso, D., Nilles, E. J. and Cao-Lormeau, V. M. (2014). Rapid spread of emerging Zika virus in the Pacific area. *Clin. Microbiol. Infect.* **20**, O595–O596.
Nagai, C., Mabashi-Asazuma, H., Nagasawa, H. and Nagata, S. (2014). Identification and characterization of receptors for ion transport peptide (ITP) and ITP-like (ITPL) in the silkworm Bombyx mori. *J. Biol. Chem.* **289**, 32166–32177.
Nagai-okatani, C., Nagasawa, H. and Nagata, S. (2016). Tachykinin-Related Peptides Share a G Protein-Coupled Receptor with Ion Transport Peptide-Like in the Silkworm Bombyx mori. 1–14.
Nation, J. (2008). *Insect Physiology and Biochemistry, Second Edition*. CRC Press.
Niven, J. E., Graham, C. M. and Burrows, M. (2008). Diversity and Evolution of the Insect Ventral Nerve Cord. *Annu. Rev. Entomol.* **53**, 253–271.
O'Donnell, M. J. (2009). Too much of a good thing: how insects cope with excess ions or toxins in the diet. *J. Exp. Biol.* **212**, 363–372.

O'Donnell, M. J. (2011). Mechanisms of excretion and ion transport in invertebrates. *Compr. Physiol.* 1207–1289.

Oehler, E., Watrin, L., Larre, P. and Al, E. (2014). Zika virus infection complicated by Guillain- Barre syndrome — case report, French Polynesia. *Euro Surveill* **19**,.

Omoto, J. J., Lovick, J. K. and Hartenstein, V. (2016). ScienceDirect Origins of glial cell populations in the insect nervous system. *Curr. Opin. Insect Sci.* **18**, 96–104.

Pacey, E. K. and O'Donnell, M. J. (2014). Transport of H+, Na+ and K+ across the postePacey, E. K., & O'Donnell, M. J. (2014). Transport of H+, Na+ and K+ across the posterior midgut of blood-fed mosquitoes (Aedes aegypti). Journal of Insect Physiology, 61(1), 42–50. http://doi.org/10.1016/j.jins. *J. Insect Physiol.* **61**, 42–50.

Paluzzi, J. P. V (2012). Anti-diuretic factors in insects: The role of CAPA peptides. *Gen. Comp. Endocrinol.* **176**, 300–308.

Paluzzi, J. P. V, Vanderveken, M. and O'Donnell, M. J. (2014). The heterodimeric glycoprotein hormone, GPA2/GPB5, regulates ion transport across the hindgut of the adult mosquito, Aedes aegypti. *PLoS One* **9**, e86386.

Pannabecker, T. (1995). Physiology of the Malpighian tubule. **40**, 493–510.

Patrick, M. L., Aimanova, K., Sanders, H. R. and Gill, S. S. (2006). P-type Na+/K+-ATPase and V-type H+-ATPase expression patterns in the osmoregulatory organs of larval and adult mosquito Aedes aegypti. *J. Exp. Biol.* **209**, 4638–51.

Paules, C. and Fauci, A. (2017). Yellow Fever- once again on the radar screen in the Americas. *N. Engl. J. Med.* **376**, 1397–1399.

Petersen, L., Jamieson, D., Powers, A. and Honein, M. (2016). Zika Virus.

Phillips, J. (1981). Comparative Physiology of Insect Renal-Function. *Am. J. Physiol.* **241**, R241-257.

Phillips, J. E. and Audsley, N. (1995). Neuropeptide control of ion and fluid transport across locust hindgut. *Integr. Comp. Biol.* **35**, 503–514.

Phillips, J., Hanrahan, J., Chamberlin, M. and Thomson, B. (1986). Mechanisms and control of reabsorption in insect hind- gut. *Adv. In Insect Phys.* **19**, 330–422.

Phillips, J. E., Audsley, N., Lechleitner, R., Thomson, B., Meredith, J. and Chamberlin, M. (1988). Some Major Transport Insect Absorptive Mechanisms of. **90**, 643–650.

Phillips, J. E., Thomson, R. B., Audsley, N., Peach, J. L. and Stagg, A. P. (1994). Mechanisms of Acid-Base Transport and Control in Locust Excretory System. *Physiol. Zool.* **67**, 95–119.

Phillips, J. E., Wiens, C., Audsley, N., Jeffs, L., Bilgen, T. and Meredith, J. (1996). Nature and control of chloride transport in insect absorptive epithelia. *J. Exp. Zool.* **275**, 292–299.

Phillips, J. E., Meredith, J., Audsley, N., Richardson, N., Macins, A. and Ring, M. (1998). Locust Ion Transport Peptide (ITP): A Putative Hormone Controlling Water and Ionic Balance in Terrestrial Insects. *Integr. Comp. Biol.* **38**, 461–470.

Pialoux, G., Gaüzère, B. A., Jauréguiberry, S. and Strobel, M. (2007). Chikungunya, an epidemic arbovirosis. *Lancet Infect. Dis.* **7**, 319–327.

Piersol, G. (1897). *Normal Histology*. JB Lippincott Company.

Pithadia, A. B. and Kakadia, N. (2010). Guillain-Barré syndrome (GBS). *Pharmacol. Reports* **62**, 220–232.

Powell, J. and Tabachnick, W. J. (2013). History of domestication and spread of Aedes aegypti--a review. *Mem Inst Oswaldo Cruz* **108**, 11–17.

Pullikuth, A. K., Aimanova, K., Kang'ethe, W., Sanders, H. R. and Gill, S. S. (2006).

Molecular characterization of sodium/proton exchanger 3 (NHE3) from the yellow fever vector, Aedes aegypti. *J. Exp. Biol.* **209**, 3529–3544.

Quinlan, M. and O'Donnell, M. (1998). Anti-diuresis in the blood-feeding insect Rhodnius prolixus Stal: antagonistic actions of cAMP and cGMP and the role of organic acid transport. *J. Insect Physiol.* 561–568.

Raabe, M. (1989). *Recent developments in insect neurohormones*. Plenum Press.

Ramsay, J. a (1953). Exchange of sodium and potassium in mosquito larvae. *J Exp Biol* **30**, 79–89.

Ring, M., Meredith, J., Wiens, C., MacIns, A., Brock, H. W., Phillips, J. E. and Theilmann, D. A. (1998). Expression of Schistocerca gregaria ion transport peptide (ITP) and its homologue (ITP-L) in a baculovirus/insect cell system. *Insect Biochem. Mol. Biol.* **28**, 51–58.

Robertson, L., Donini, A. and Lange, A. B. (2014). K+ absorption by locust gut and inhibition of ileal K+ and water transport by FGLamide allatostatins. *J. Exp. Biol.* 3377–3385.

Rodenhuis-Zybert, I. A., Wilschut, J. and Smit, J. M. (2010). Dengue virus life cycle: Viral and host factors modulating infectivity. *Cell. Mol. Life Sci.* **67**, 2773–2786.

Scharrer, B. (1987). INSECTS AS MODELS IN. 1–16.

Schooneveld, H. (1998). Neurosecretion. *Microsc. Anat. Invertebr.* **11**, 467–486.

Sellami, A., Agricola, H. J. and Veenstra, J. A. (2011). Neuroendocrine cells in Drosophila melanogaster producing GPA2/GPB5, a hormone with homology to LH, FSH and TSH. *Gen. Comp. Endocrinol.* **170**, 582–588.

Slosek, J. (1986). Aedes aegypti mosquitoes in the Americas: A review of their interactions with the human population. *Soc. Sci. Med.* **23**, 249–257.

Staples, E. and Fischer, M. (2014). Chikungunya Virus in the Americas — What a Vectorborne. *N. Engl. J. Med.* **371**, 887–889.

Stay, B., Fairbairn, S. and Yu, C. G. (1996). Role of allatostatins in the regulation of juvenile hormone synthesis. *Arch Insect Biochem Physiol* **32**, 287–297.

Tabachnick, W. J. (1991). Evolutionary genetics and arthropod-borne disease: the yellow fever mosquito. *Am. Entomol.* **37**, 12–26.

Tabachnick, W. J. (2010). Challenges in predicting climate and environmental effects on vector-borne disease episystems in a changing world. *J Exp Biol* **213**, 946–954.

Talamillo, A., Sánchez, J., Cantera, R., Pérez, C., Martín, D., Caminero, E. and Barrio, R. (2008). Smt3 is required for Drosophila melanogaster metamorphosis. *Development* **135**, 1659 LP-1668.

Vandersmissen, H. P., Van Hiel, M. B., Van Loy, T., Vleugels, R. and Vanden Broeck, J. (2014). Silencing D. melanogaster lgr1 impairs transition from larval to pupal stage. *Gen. Comp. Endocrinol.* **209**, 135–147.

Wang, Y.-J., Zhao, Y., Meredith, J., Phillips, J. E., Theilmann, D. A. and Brock, H. W. (2000). Mutational analysis of the C-terminus in ion transport peptide (ITP) expressed in Drosophila Kc1 cells. *Arch. Insect Biochem. Physiol.* **45**, 129–138.

Wieczorek, H. (1992). The insect V-ATPase, a plasma membrane proton pump energizing secondary active transport: molecular analysis of electrogenic potassium transport in the tobacco hornworm midgut. *J. Exp. Biol.* **172**, 335–343.

Wieczorek, H., Beyenbach, K. W., Huss, M. and Vitavska, O. (2009). Vacuolar-type proton pumps in insect epithelia. *J. Exp. Biol.* **212**, 1611–1619.

World Health Organization (2009). *Dengue: guidelines for diagnosis, treatment, prevention*

and control. World Health Organization.

Yuki, N. and Hartung, H.-P. (2012). Guillain–Barré Syndrome. *N. Engl. J. Med.* **366**, 2294–2304.

Zhao, Y., Meredith, J., Brock, H. W. and Phillips, J. E. (2005). Mutational analysis of the N-terminus in Schistocerca gregaria ion-transport peptide expressed in Drosophila Kc1 cells. *Arch. Insect Biochem. Physiol.* **58**, 27–38.

CHAPTER II: REVEALING THE DISTRIBUTION OF ION TRANSPORT PEPTIDE AND FUNCTION OF ITS PROSPECTIVE SECOND MESSENGERS, CYCLIC AMP AND CYCLIC GMP, ON THE HINDGUT OF THE ADULT MOSQUITO, *AEDES AEGYPTI*

Abstract

In the locust, Ion Transport Peptide (ITP) was the first characterized antidiuretic factor shown to act on the hindgut, which was later discovered in other insects including the mosquito, *Aedes aegypti*. The present study aimed to delineate the function of ITP within the hindgut of the mosquito, *A. aegypti* – the vector responsible for spreading a range of diseases, such as dengue and yellow fever. In order to generate a functional ITP recombinant peptide, an endocrine-derived cell culture system involving mouse anterior pituitary (AtT-20) cells was used to express both *Drosophila melanogaster* ITP (DromeITP) and *A. aegypti* ITP (AedaeITP). Protein extracts were isolated from AtT-20 cells transiently expressing either AedaeITP or DromeITP, and samples were processed through western blot analysis using a primary antiserum against the C-terminal region of DromeITP (42% homology to the AedaeITP C-terminus). A band size of approximately 9 kDa was detected in protein samples from both ITP-transfected cells, however a higher molecular weight band at approximately 13 kDa was detected in protein samples from DromeITP-transfected cells. This higher molecular weight band was suggested to be a glycosylated variant of ITP, as shown by its loss upon PNGase F treatment. Using wholemount immunohistochemistry surveying the central nervous system of adult *A. aegypti*, ITP-like immunoreactivity was revealed in cells located in the brain, thoracic ganglia, and posteriorly within each of the abdominal ganglia. Using SIET to measure ion transport across the hindgut, the influence of recombinant AedaeITP and its suspected second messengers, cAMP and cGMP, were investigated. Results indicate that application of cAMP generally promoted haemolymph directed Na^+ flux (i.e absorption), while it generally inhibited K^+ absorption.

Conversely, cGMP generally promoted lumen-directed Na^+ flux (i.e secretion). Recombinant AedaeITP did not have a significant effect on Na^+ flux across the hindgut of either sex.

Introduction

Insects are constantly faced with fluctuating environmental conditions, which are particularly detrimental considering their high surface-to-volume ratio, challenging their ability to maintain internal homeostasis of ions and water (O'Donnell, 2011). For example, unfed terrestrial insects must avoid desiccation by conserving internal water and ion levels. Conversely, fed insects are challenged with the potential dilution of their haemolymph, requiring them to expel excess water and ions (O'Donnell, 2011). The excretory system of mosquitoes plays a pivotal role in maintaining hydromineral balance of the haemolymph, which is analogous to the blood of vertebrates. Haemolymph is a fluid that circulates the interior of the arthropod body, remaining in direct contact with the animal's tissues (Phillips et al., 1996). Haemolymph homeostasis is maintained by the mosquito excretory system consisting of the Malpighian tubules and the hindgut, the latter of which is subdivided into the anteriorly located ileum and posteriorly positioned rectum, and lastly the anus from which the final waste product is excreted (O'Donnell, 2011). MTs arise at the junction between the midgut and the hindgut (Coast, 2002). The process of achieving ionic homeostasis within the excretory system is initiated at the distal, free-floating, end of the MTs. MTs secrete a primary urine at the midgut-hindgut junction, that is isosmotic to the haemolymph, and is directed posteriorly towards the ileum (O'Donnell, 2009). Primary urine production is driven by active cation (K^+/Na^+) transport into the lumen, establishing a transepithelial voltage favoring passive entry of the counter ion Cl^-. Osmotically obliged water enters the lumen down the transepithelial osmotic gradient created by the net secretion of KCl and NaCl (Coast, 2007). Tubules of blood feeders produce a final urine rich in

NaCl, however with time, Na^+ excretion falls and K^+ excretion rises. Additionally, in the desert locust, *Schistocera gregaria,* the MTs secrete a KCl-rich primary urine (Phillips and Audsley, 1995). The normal action of the unstimulated cell will return Na^+ to the haemolymph, which exits through the Na^+/K^+-ATPase, and only K^+ and Cl^- will be transported from cell to lumen. This explains why unstimulated tubules secrete fluid composed largely of KCl (Beyenbach, 2003; O'Donnell, 2011). After a blood meal, MTs of the mosquito *A. aegypti* secrete primary urine high in Na^+ to rid the insect of excess Na^+ from the plasma portion of a blood meal. K^+ secretion may be stimulated later, as K^+ enters the haemolymph only after red blood cells are digested (Williams and Beyenbach, 1983).

The most extensively studied insect hindgut is that of the desert locust, *S. gregaria* (Phillips et al., 1986). Upon entry to the hindgut, the primary urine undergoes selective reabsorption of water, ion, and metabolites (Coast, 2002). The main driving force of ion reabsorption within the hindgut is the apical (lumen-facing) electrogenic Cl^--pump. K^+ is the major counter cation absorbed, which follows Cl^- passively by electrical coupling (Phillips and Audsley, 1995). Transport of Na^+ is driven by the basolateral Na^+/K^+-ATPase, and movement of Na^+ from the lumen to the cell is coupled to the excretion of ammonium (O'Donnell, 2011). The activity of the organs comprising the insect excretory system is controlled by diuretic and antidiuretic hormones. Generally, diuretic hormones stimulate primary urine secretion by MTs, whereas antidiuretic hormones increase fluid reabsorption from the hindgut (Coast, 2002). However, CAPA peptides were found to inhibit fluid secretion from the MTs of larval *A. aegypti*, and *Rhodnius prolixus* (a vector of Chagas' disease), suggesting their role as antidiuretic factors acting on MTs (Ionescu and Donini, 2012; Orchard and Paluzzi, 2009). More recently, GPA2/ GPB5 has been the first suggested antidiuretic hormone acting on the hindgut of both

adult *Drosophila melanogaster* (fruit fly) and adult *A. aegypti* (Paluzzi et al., 2014; Sellami et al., 2011; Vandersmissen et al., 2014). In *A. aegypti*, the Scanning Ion-Electrode Technique (SIET) was used to determine that treating the hindgut with a recombinant form of GPA2/GPB5 caused a decrease in net secretion of Na^+ by the ileum, measured as decreased lumen-directed sodium flux, and caused increased net Na^+ absorption in the rectum. There was a decrease in K^+ absorption across all areas of the hindgut examined along the hindgut (Paluzzi et al., 2014).

Unfortunately, the endocrine control of the insect hindgut has been relatively unexplored in comparison to the MTs (Coast, 2009). Hindgut epithelial mechanisms, including its endocrine control responsible for reabsorption, have been well characterized only in the desert locust, *S. gregaria* (Phillips and Audsley, 1995). The desert locust faces similar dietary and environmental challenges to the adult mosquito; water must be conserved during unfed states, whereas the expulsion of excess water and ions is necessary in post-fed states (Phillips et al., 1996). With this rationale, the locust will be used to model possible regulatory mechanisms within the hindgut of the adult mosquito, *A. aegypti.* Early bioassay work measuring the Cl^--dependent short circuit current (I_{SC}) of locust ilea showed that extracts of the CNS, particularly the brain and retrocerebral complex, increased ion and fluid reabsorption; electrogenic Cl^- transport was stimulated which results in the net absorption of NaCl, KCl, and osmotically obliged water (Audsley et al., 1992b; Phillips et al., 1986). In 1992, Ion Transport Peptide (ITP) was the first identified antidiuretic hormone mediating its effects on the ileum of *S. gregaria.* Audlsey *et al.* isolated ITP from crude CC extracts, and it was found to be closely related to crustacean hyperglycaemic hormones (CHHs) (Audsley et al., 1992a; Audsley et al., 1992b). The purified *S. gregaria* ITP (SchgrITP) was shown to have an unblocked amino-terminus (N-terminus), a molecular mass of approximately 8652 Da, and the first 33 N-terminal amino acid residues were

determined (Audsley et al., 1992a). Further studies were conducted to compare the effects of purified ITP and crude CC extracts on ileal I_{SC}, where both were found to increase Cl^-, K^+, and Na^+ reabsorption. In addition, H^+ secretion in the ileum (JH), was abolished by high concentrations of ITP (Audsley et al., 1992b).

Using a molecular biology approach, Meredith *et al*. identified the complete amino acid sequence of SchgrITP that is encoded by the cloned cDNA containing the complete open reading frame for the ITP prepropeptide of 130 amino acid residues (Meredith et al., 1996). They further illustrated a 55-residue leader sequence, within which lies the signal peptide, and the complete 72-residue sequence of the mature peptide. Six cysteine residues, proposed to participate in disulphide bridge formation, were localized in positions 7, 23, 26, 39, 43, and 52 of SchgrITP (Meredith et al., 1996). The three disulphide bridges are necessary for determining the distance between essential motifs and the N- or C-terminus, therefore, they were thought to be fundamental for the biological activity of ITP (King et al., 1999). Meredith *et al*., (1996) also discovered an ITP-Long form (ITPL), which contained a 121 base pair insert at amino acid position 40 of ITP. The mature ITPL peptide was only 4 amino acids longer than ITP, and contained a unique carboxy-terminus (C-terminus) with only 36% sequence identity with ITP; the C-terminus of ITP but not ITPL is amidated (Dircksen, 2009; Phillips et al., 1998). The six cysteine groups of locust ITP were found to be conserved in locust ITPL as well (Meredith et al., 1996). In a review by Phillips *et al*., (1998) it was proposed that the shared N-terminus of ITP and ITPL is what permits the neuropeptide to bind to its receptor. The absence of both the C-terminal alpha-helix and C-terminal amidation in ITPL was suggested to block receptor activation (Phillips et al., 1998). ITPL, not being hindgut bioactive alone is considered a competitive inhibitor of ITP action on putative hindgut ITP receptors (Phillips et al., 2001).

Upon stimulation of the locust hindgut with either crude CC extracts or cAMP, electrogenic Cl^- transport is stimulated approximately 10-fold. It was proposed that cAMP likely directly stimulates the apical Cl^- pump and opens K^+ and Cl^- channels in both apical and basolateral membranes to cause increased ion and water reabsorption (Phillips et al., 1998). Preliminary observations by Audsley *et al.* (1992b) reported that ileal tissue levels of intracellular cyclic AMP were increased one hour after treatment with purified native ITP (Audsley et al., 1992b). Taken together, these findings suggested that cAMP is the principal second messenger for ITP acting on locust ileum (Phillips et al., 1998). Interestingly, ITP was shown to inhibit H^+ secretion, a process not mimicked by cAMP, which lead to the suggestion that ITP may also act through a different second messenger (Audsley et al., 2013). Upon incubating whole locust ilea with variable amounts of SchgrITP, cyclic AMP and cyclic GMP competitive ELISA assays were used to measure levels of cyclic nucleotides. It was discovered that intracellular levels of both cGMP and cAMP were elevated in locust ilea incubated with crude CC extracts or SchgrITP, suggesting that both these cyclic nucleotides are involved in the signal transduction pathway initiated SchgrITP (Audsley et al., 2013).

Evidence for differential tissue expression of ITP and ITPL was provided by Dai *et al.* (2007), in the moths *Manduca sexta and Bombyx mori.* It was shown than ITP is expressed in bilaterally-paired lateral brain neurosecretory cells in the brain, with projections to the retrocerebral complex (CC/CA). ITPL is expressed in peripheral neurosecretory cells and neurons of the ventral ganglia (Dai et al., 2007). Dircksen *et al*. investigated the localization of *D. melanogaster* ITP (DromeITP) in the central and peripheral nervous system of *D. melanogaster* throughout postembryogenesis. In all postembryonic stages, immunohistochemistry and FISH techniques revealed the presence of four NSCs in the lateral

protocerebrum that project to the CC and partly to the CA (Dircksen et al., 2008).
In the adult brain, these NSCs come to lie in a posterior dorsal–lateral positions, from where they innervate the retrocerebral complex (CC and CA). In larvae and pupa only, a strongly staining ITP-immunoreactive interneuron occurs in the subesophageal ganglia. In regards to abdominal neurons, one pair of strongly labelled dorsolateral and two or three pairs of faintly stained ventrolateral to ventromedial pairs of ITP neurons were found in the eighth abdominal neuromeres. The axons of the strongly stained abdominal neurons leave the ventral nerve cord through the eighth abdominal nerve (Dircksen et al., 2008).

Dai *et al*. (2007) were the first to identify conserved processing of ITP genes in insects, which by alternative splicing, can produce two different peptides (ITP and ITPL) in *A. aegypti.* A smaller transcript variant produces a peptide containing an amidated C-terminus *A. aegypti* ITP (AedaeITP), while the other longer transcript variant yields a peptide possessing an unblocked C-terminus *A. aegypti* ITPL (AedaeITPL). In every insect that ITP/ITPL has been studied, it was uncovered that both peptides share a common N-terminal sequence but had diverging C-termini (Dai et al., 2007). However, nothing is known on the expression pattern, tissue distribution, or putative physiological function of ITP in *A. aegypti*. The objective of the present investigation was to confirm the existence, delineate the localization, and explore the potential physiological function of ITP in adult *A. aegypti* mosquitoes. Thus, we sought to characterize the sex- and nervous tissue-specific distribution patterns of ITP at the protein level for the first time in adult *A. aegpti.* The current study sought to develop a cell culture system to produce recombinant AedaeITP as conventional peptide synthesis for ITP is not feasible due to its length and significant cost. Furthermore, to determine the physiological role of ITP on putative target tissues, the Scanning Ion-selective Electrode Technique (SIET) was utilized to investigate

whether ITP and its proposed second messengers, cAMP and cGMP, influence ion transport across the adult *A. aegypti* hindgut epithelium. The results show that the endocrine derived cell culture system serve as an appropriate model for the production of native recombinant ITP. For the first time, DromeITP has been suggested to undergo a posttranslational modification involving *N*-glycosylation. Immunohistochemistry has revealed the distribution of AedaeITP in the central nervous system of adult *A. aegypti* mosquitoes in the brain, thoracic and abdominal ganglia.

Materials and Methods

Dissection and Preparation of Hindgut Tissues

Adult mosquitoes, between 1-4 days old, were anesthetised on ice for 5 minutes, after which they were pinned in the thorax into a Sylgard-lined petri dish. Mosquitoes being tested for K^+ transport by SIET were dissected under Ca^{2+}-free *Aedes* saline consisting of 153.4 mM NaCl, 3.4 mM KCl, 1.8 mM $NaHCO_3$, 1 mM $MgSO_4$, 25 mM HEPES, and 5 mM glucose adjusted to pH 7.1. Ca^{2+}-free saline was used to reduce spontaneous contractions of the hindgut while ion flux measurements were recorded (Paluzzi et al., 2014). For measurements of Na^+ transport by SIET, mosquitoes were dissected under Ca^{2+}-free *Aedes* saline containing 153.4 mM NaCl, 3.4 mM KCl, 1.8 mM NaHCO3, 1 mM $MgSO_4$–$7H_2O$, 25 mM HEPES, and 5 mM glucose. Saline pH was adjusted to 7.1, and Na^+ concentration was reduced to 20 mM with equimolar substitution of 130 mM N-methyl-D-glucamine to improve the signal to noise ratio during Na^+ SIET recordings (Pacey and O'Donnell, 2014). Forceps were used to grip the most posterior abdominal segment, peel away the cuticle, and excise the hindgut from the mosquito. The dissected hindgut was then transferred from the dissection dish to a 35mm Petri dish (BD

Biosciences Canada, Missisauga, ON) filled with either of the saline solutions described above for measurements of each respective ion. The 35 mm Petri dishes were pre-coated with 100 µl droplets of 0.01% poly-L-lysine (150-300 kDa, Sigma-Aldrich, Oakville, ON), and then air-dried to promote adhesion of the gut to the bottom of the dish. Furthermore, hot melt glue arenas surrounded the poly-L-lysine coated area to facilitate the use of small saline volumes in the range of 200-300µL.

Ion-selective Microelectrodes

To measure ion flux across the basolateral surface of the hindgut, ion-selective microelectrodes were constructed with glass capillary tubes (TW-150-4, World Precision Instruments, Sarasota, FL, USA). The glass capillaries were pulled into micropipettes on a Sutter P-97 Flaming Brown pipette puller (Sutter Instruments, San Rafael, CA, USA). Thereafter, the micropipettes were silanized with N,N-dimethyltrimethylsilylamine (Fluka, Buchs, Switzerland) applied to the interior of a glass petri dish which was inverted over the group of micropipettes (1:2 ratio of number of probes to µL of silanizing solution; for 15 probes, 30 µl of dimethyltrimethylsilylamine was used). Silanization was performed at 350°C for one hour, upon which the micropipettes were cooled before use. For potassium ion measurements, the micropipette was backfilled with 150 mM KCl and frontloaded with K^+ ionophore (potassium ionophore I cocktail B; Fluka, Bachs, Switzerland). The microelectrode was calibrated before each preparation using 150 mM KCl and 15 mM KCl with 135 mM NaCl. For sodium ion measurements, the micropipette was backfilled 150 mM NaCl and frontloaded with Na^+ ionophore (sodium ionophore II cocktail A; Fluka, Buchs, Switzerland). The microelectrode was calibrated before each preparation using 150 mM NaCl and 15 mM NaCl with 135 mM KCl.

Reference electrodes were prepared by filling a capillary tube with 3M KCl containing 3% agar (thanks to Dr. Donini for the preparation of reference electrodes). The reference electrode was connected to the headstage with an electrode holder containing a silver pellet and filled with 3M KCl; it was allowed to rest within the saline bath surrounding the hindgut preparation.

Scanning Ion-selective Electrode Technique (SIET)

The ion-selective microelectrode was fitted onto an Ag/AgCl wire electrode holder that was connected to a headstage. The headstage was connected to an amplifier (Applicable Electronics, Forestdale, MA, USA) whose motion was controlled by three computerized stepper motors, which allowed the electrode to move along the X, Y, and Z-axes. Automated Scanning Electrode Technique (ASET) software version 2.0 was used to make SIET measurements and to control the motion of the motors. Measurements of voltage gradients were achieved by placing an ion-selective microelectrode within 5 μm of the hindgut tissue, and moving the microelectrode tip perpendicularly to the tissue surface between two points separated by 100 μm. The sampling protocol used a wait time of 4 seconds after microelectrode movement and a recording time of 1 seconds following the wait period. Upon sampling within 5 μm of the tissue surface, the microelectrode was then moved to a position 100 μm perpendicular to the tissue, where another wait and sample period was completed. This sampling protocol was repeated three times at each measurement site along the hindgut, and the voltage difference between the two sites was used to calculate a voltage gradient by the Automated Scanning Electrode Technique software (ASET; Science Wares, East Falmouth, MA, USA). Three independent measurements (each consisting of three move, wait, and sample cycles) were made consecutively at each site.

SIET Measurements

Recordings were taken beginning at the rectum-ileum junction, which served as an anatomical landmark, and then moving anteriorly towards the ileum, and posteriorly towards the rectum in 50 μm intervals for measurements with cAMP and cGMP (see Figure 5). Measurements with recombinant AedaeITP were taken in 200 μm intervals across the ileum and 100 μm intervals across the rectum. The number of measurement sites varied between hindgut preparations due to their varying lengths; however, measurements were taken over the majority of the hindgut's total length.

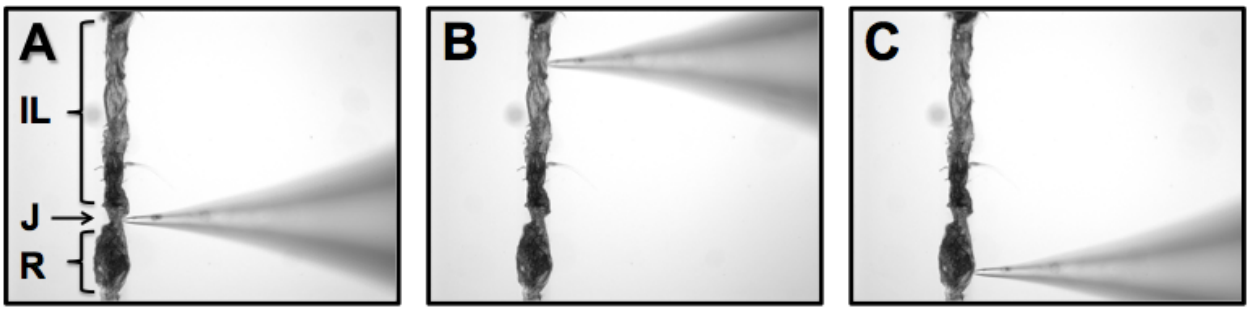

Figure 5: Still images of the dissected mosquito hindgut adhered to the bottom of a poly-L-lysine coated Petri dish. The images show the position of the ion-selective microelectrode relative to the tissue during a typical SIET experiment. As shown in (A), measurements were initiated at the ileum-rectum junction (J) and proceeded with measurements (B) anteriorly over the ileum (IL) and subsequently in the (C) posterior direction over the rectum (R).

For potassium and sodium measurements with either cAMP or cGMP, control measurements were taken by adding 300 µL of the appropriate saline to the hot melt glue arenas surrounding the tissue preparation. Measurements with 8-bromo cAMP (8-bromoadenosine 3', 5'-cyclic monophosphate; Sigma-Aldrich, Oakville, ON, CA), a membrane permeable analog of cAMP, were made by adding 3µL of 100 mM 8-bromo cAMP to 297µL of saline to achieve a 1 mM final concentration. Similarly, a final concentration of 1 mM of 8-bromo cGMP (8-bromoguanosine 3', 5'-cyclic monophosphate; Sigma-Aldrich, Oakville, ON, CA), a membrane permeable analog of cGMP, was made by adding 3µL of 100 mM 8-bromo cGMP to 297µL of saline.

Measurements containing the recombinant *A. aegypti* ITP were taken with sodium only. All cell transfections to prepare the desired recombinant *A. aegypti* ITP are outlined below. Based on a previous study utilizing SIET that used a concentration of 1 nM of FGLamide allatostatins to determine their effects on K^+ transport in the locust gut (Robertson et al., 2014), a concentration of 1 nM of recombinant *A. aegypti* ITP was used with SIET for sodium ion flux recordings. Control trials were prepared by adding an equivalent volume of concentrated untransfected AtT-20 cell media with saline into a 300 µL total volume. Recombinant ITP trials were prepared by adding an appropriate volume of *A. aegypti* ITP-transfected concentrated AtT-20 cell media with saline into a 300 µL total volume to achieve a 1 nM final concentration. Control and experimental trials with cAMP, cGMP or ITP, were compared between male and female adults.

To obtain background voltage readings, the microelectrode tip was positioned at a reference site located several hundred micrometers away from the tissue, and the same sampling protocol described above was followed; this was performed for all tissue preparations. SIET

measurements of the ileum and rectum were initiated immediately after the completion of reference scans. Measurements along the hindgut with cAMP and cGMP treatments were made in 50 μm intervals; a maximum of 16 site recordings (equating to 800 μm anterior to the rectum/ileum junction) were taken of the ileum, and a maximum of 8 site recordings (equating to 400 μm posterior to the rectum/ileum junction) were taken of the rectum. Due to the homogeneity of ion flux recordings across the length of either the ileum or rectum observed with cAMP/cGMP, the intervals sampled across the hindgut were increased. For recombinant *A. aegypti* ITP preparations, recording in 200 μm intervals, a maximum of 4 site recordings (equating to 800 μm anterior to the rectum/ileum junction) were taken of the ileum. Recording in 100 μm intervals, a maximum of 4 site recordings (equating to 400 μm posterior to the rectum/ileum junction) were taken of the rectum for recombinant ITP preparations. Up to 100 minutes were required to complete SIET measurements on each tissue sample for cAMP/cGMP and up to 30 minutes were required for AedaeITP preparations.

Calculation of Ion Flux

Calculation of ion flux used in this study has been described previously (Paluzzi et al., 2014; Robertson et al., 2014). The measured voltage gradients obtained from the ASET software program were converted into a concentration gradient for Na^+ or K^+ using the equation:

$$\Delta C = C_B 10^{(\Delta V/S)} - C_B$$

ΔC represents the concentration gradient between the two points measured at the hindgut tissue in μmol cm^{-3}, C_B represents the background ion concentration (the average of the concentrations at all points) in μmol cm^{-3}, ΔV represents the voltage gradient measured at the tissue surface less the voltage gradient at the reference site in μV, and S is the Nernst slope of the electrode in μV.

Fick's first law of diffusion was used to calculate the Na^+ or K^+ flux based on the concentration gradient through the equation:

$$J = D\Delta C/\Delta X$$

J represents the net flux of the ion in pmol cm^{-2} s^{-1}, D is the diffusion coefficient of the ion ($1.92x10^{-5}$ cm^2 s^{-1} for K^+; $1.55x10^{-5}$ cm^2 s^{-1} for Na^+) (Lide, 2002), ΔC represents the concentration gradient in µmol cm^{-3}, and ΔX represents the excursion distance, expressed in centimeters, separating the points where voltage was recorded by the microelectrode.

PCR, Gel Separation, and Preparation of expression vectors

PCR reactions were used to test AedaeITP primers previously outlined by Dai *et al*., (2007) (Table 1) as well as DromeITP primers (Table 2). Amplification was performed using Q5 High Fidelity DNA Polymerase, following manufacturer guidelines (New England Biolabs, Whitby, ON, CA), and whole adult 3-day-old male and female *A. aegypti* cDNA as template. RNA was extracted from whole adult 7-day-old male and female *D. melanogaster* using the DNAaway RNA mini-prep kit (Bio Basic Canada Inc., Markham, ON, CA) following the manufacturers protocol. Total RNA (~100ng) was used for cDNA synthesis using iScript™ Reverse Transcription Supermix (Bio-Rad Laboratories, Mississauga, ON, CA) following recommended guidelines including primer annealing at 25 °C for 5 min and reverse transcription at 42 °C for 20 min. The resultant PCR product specificity was confirmed through gel electrophoresis and remaining sample was purified using a PureLink PCR purification kit (Life Technologies, Burlington, ON, CA), and A-tailed using Taq polymerase. Products were then cloned into the pGEM-T Easy Vector (Promega, Madison, WI, USA) and transformed into competent survival strain *E. coli* cells, and subsequently the bacterial cells were diluted into SOC media. This

solution then applied onto agar plates containing ampicillin and X-gal, at different plating volumes (e.g.100 µL and 200µL) and colonies were grown overnight in a 37°C incubator. Inserts were excised from pGEM T-Easy by NotI digestion and subcloned into the mammalian expression vector, pcDNA $3.1^{(+)}$ (Life Technologies, Burlington, ON, CA) that was previously digested with *Not*I and dephosphorylated to reduce non-recombinants, after which expression constructs were screened for directionality by colony PCR using gene-specific forward primers and the BGH vector-specific reverse primer. Overnight cultures were grown to increase the copy number of the expression vector, which was subsequently purified (PureLink-midiprep kit; Invitrogen, Burlington, ON, CA). Expression constructs were sequenced to determine base accuracy (Center for Applied Genomics, Hospital for Sick Children, Toronto, ON, CA) prior to use for cell culture transfection.

Table 1: PCR primers for AedaeITP/ITPL

Primer Name	**Primer Sequence (5'-3')**	**Expected Product Size (BP)**
AedaeITP/AedaeITPL1	Forward: CAACGAGAGTTTTCATTTCTGG Reverse: TTACTTCTTCCCCAACATTTCG	1069 384
AedaeITPL1	Forward: CAACGAGAGTTTTCATTTCTGG Reverse: TGTGAAGTTCAACGCGATAG	1091
AedaeITPL2	Forward: CAACGAGAGTTTTCATTTCTGG Reverse: GGCTGCTTATAACGTGTTTGGA	405

Table 2: PCR primers for DromeITP

Primer Name	**Primer Sequence (5'-3')**	**Expected Product Size (BP)**
DromeITP-kozak2 & DromeITP-rev	Forward: GCCACCATGTGTTCCCGCAACATAAAG Reverse: GCACTTTACTTGCGACCCA	332

Wholemount Immunohistochemistry

To visualize the spatial distribution of AedaeITP in the central nervous system of adult mosquitoes, four-day-old adult male and female *A. aegypti* were used. Mosquitoes were anesthetized with brief exposure to carbon dioxide, punctured in the thorax with forceps, and then incubated in 4% paraformaldehyde fixative overnight at RT. Tissue dissections of the central nervous system, keeping the brain, thoracic ganglia, and the ventral nerve cord (including the abdominal ganglia) intact, were performed in 1x PBS. Samples were then incubated on a rocker for 1h at RT in 4% Triton X-100, 10% normal sheep serum (NSS) (v/v) and 2% BSA (w/v) prepared in PBS. Three subsequent washes were performed in PBS, incubating for 15 minutes each in between washes, after which the dissected nervous tissue was incubated on a rocker for 48 h at 4°C in a 1:500 dilution of primary antiserum solution (0.4% Triton X-100, 2% NSS (v/v) and 2% BSA (w/v) in PBS), which was prepared one day before use to reduce non-specific binding. Anti-DromeITP rabbit primary antiserum was used, prepared against an antigen sequence from the C-terminal region of DromeITP, which shares 41.7% sequence identity and 75% sequence similarity to the homologous C-terminal region of AedaeITP (Figure 6). Following the incubation in primary antiserum, tissues were washed three times with 1x PBS, incubating for 15 minutes in between washes. The samples were then incubated on a rocker overnight at 4°C with Cy3-labelled goat anti-rabbit secondary antibody (1:200 dilution; Sigma-Aldrich, Oakville, ON, CA) in 10% NSS made up in PBS and protected from light. Nervous tissues were mounted on cover slips with mounting media containing a 1:500 dilution of 4′,6-Diamidino-2-phenylindole dihydrochloride (DAPI) made up in a 1:1 solution of PBS and glycerol. DAPI was used to allow for the visualization of cell nuclei and tissue preparations were analyzed using a Lumen Dynamics X-Cite™ 120Q Nikon fluorescence microscope (Nikon,

Mississauga, ON, CA). Image stitches of the entire CNS were obtained using an EVOS FL Auto live-cell imaging system (Life Technologies, Burlington, ON, CA).

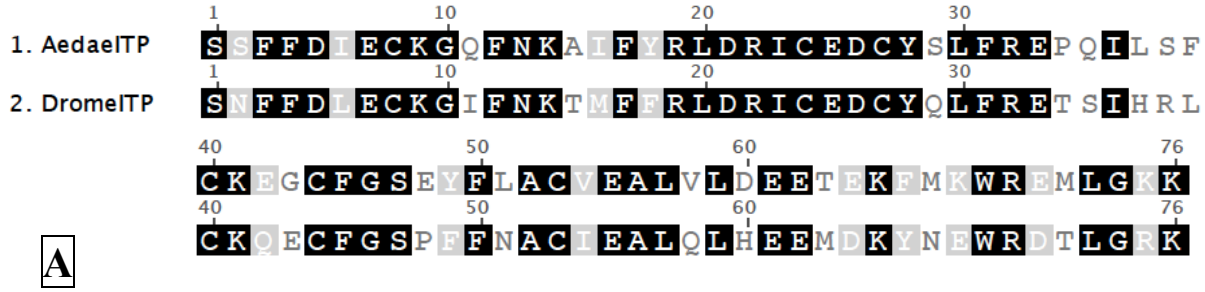

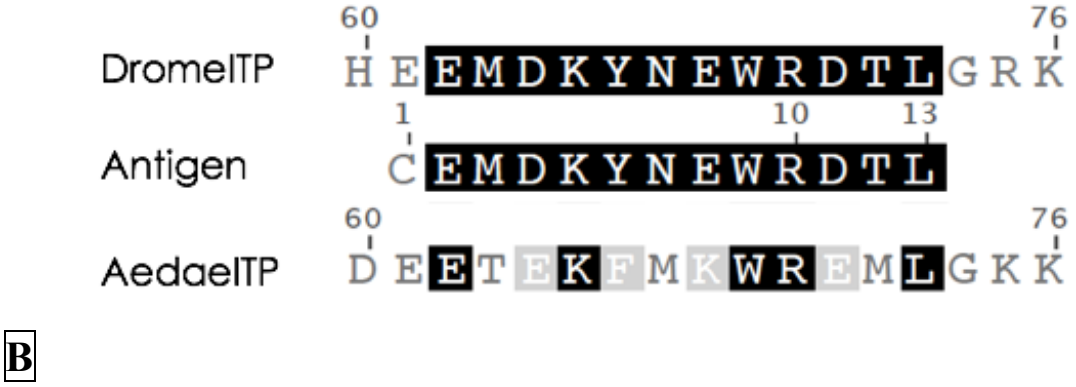

Figure 6: Amino acid sequence alignment of AedaeITP and DromeITP. Complete amino acid sequence alignment of AedaeITP and DromeITP (A), and amino acid sequence alignment of the antigen, and the antigen region of DromeITP and AedaeITP (B). Given the antigen is 12 residues, there is only 5/12 identity (41.7%) and 9/12 (75%) similarity between the *Drosophila* antibody antigen and the homologous region in the *Aedes* ITP.

Transient expression of ITP in AtT-20 and HEK293T cell lines

Mouse pituitary AtT-20 cell lines (AtT-20/D16vF2) and human embryonic kidney cells (HEK293T) (ATCC, Manassas, VA, USA) were grown and maintained in a water-jacketed incubator at 37 °C, 5% CO_2. AtT-20 cells were cultured in complete media containing 90% Dulbecco's Modified Eagle's Medium (DMEM), 10% fetal bovine serum, 1X antimycotic-antibiotic. DMEM used to make complete media for HEK293T cells contained nutrient mixture F-12 (DMEM/F12; 1:1) (Thermo Fisher, Rockford, IL, USA). Cells were grown to approximately 90% confluency and were transiently transfected using Lipofectamine LTX transfection reagent (Life Technologies, Burlington, ON, CA) following a 3:1 transfection reagent (μL) to plasmid DNA (μg) ratio. The pcDNA $3.1^{(+)}$ expression vector possessing either AedaeITP or DromeITP were used. Protein for western blot analyses was purified and concentrated from the media the cells grew in 24 and 48 h post-transfection using Amicon Ultra-0.5 Centrifugal Filter Unit with Ultracel-3K; filters had a 3 kDa molecular weight cut off (Merck Millipore Ltd., Cork, IRL).

Recombinant ITP peptide quantification using Enyzme-Linked Immunosorbent Assay (ELISA)

Final protein concentrations were calculated using an enzyme-linked immunosorbent assay (ELISA). 96-well plates were coated with 100 μL/well of a 1:1000 dilution of anti-DromeITP rabbit primary antiserum made up in carbonate buffer (15 mM Na_2CO_3-H_2O and 35 mM $NaHCO_3$ in water; pH 9.4) and incubated overnight at 4 °C. Plate contents were discarded, blotted, and washed two times with 250 μL/well of carbonate wash (0.05% TWEEN 20 (v/v), 350 mM NaCl, 2.7 mM KCl, 1.5 mM KH_2PO_4, 5.15 mM Na_2HPO_4-H_2O in water). Thereafter, wells were blocked for 1.5h at RT with 250 μL/well of carbonate block comprised of 0.5% skim

milk powder (w/v) and 0.5% BSA (w/v) in PBS. The carbonate block was discarded and wells were incubated on a rocker for 1h at RT with 100 µL/well standard Drome-ITP amidated antigen or the homologous Aedae ITP amidated sequence or unknown samples secreted from AtT-20 cells (all made up in carbonate block). Afterwards, 100 µL/well of $0.5x10^{-9}$M biotinylated-DromeITP amidated antigen (in carbonate block) was added and incubated overnight at 4°C. The following day, plate contents were discarded, blotted, and washed four times with 250 µL/well carbonate wash, and incubated at 4ºC for 1.5 h with 100 µL/well Avidin-HRP (1:2000; Bio-Rad, Mississauga, ON, CA). Finally plate contents were discarded, blotted and washed three times with 250µL/well of carbonate wash. 100µL/well of 3,3',5,5'-tetramethylbenzidine (TMB) substrate (Sigma-Aldrich, Oakville, ON) were added and incubated for 5-15 minutes at RT and monitored for color development. Reactions were stopped with 100µL/well 2N HCl and absorbance was measured at 450 nm using a Synergy 2 Modular Multi-Mode Plate Reader (BioTek, Winooski, VT, USA). Due to the poor binding of AedaeITP, the concentration determined for DromeITP was used to estimate the concentration of AedaeITP in the unknown protein samples.

Western blot analyses

Protein electrophoresis was performed using a 15% SDS-PAGE gel under reducing conditions. Protein samples were loaded with a 1:1 ratio of 2X Laemmli buffer (beta-mercaptoethanol 1:100). Gels were migrated at 120 V for 90 min before being transferred to methanol-activated polyvinylidene difluoride (PVDF) membranes (Thermo Fisher, Rockford, IL, USA) using a wet transfer system at 100 V for 75 min. Following transfer, PVDF membranes were blocked for 1h at RT in PBS containing 0.1% Tween-20 (BioShop, Burlington, ON,

Canada) and 5% skim milk powder (PBSTB). Blots were incubated on a rocking platform overnight at 4 °C with either a 1:500 and 1:1000 dilution of anti-DromeITP rabbit primary antiserum made up in PBSTB for AedaeITP and DromeITP blots, respectively. The next day, membranes were washed three times, incubating for 15 minutes between washes, in PBS containing 0.1% Tween-20 (PBST). Blots were then incubated with PBSTB containing a 1:100 dilution of goat anti-rabbit HRP conjugated secondary antibody (Life Technologies, Burlington, ON, CA) for 1h at RT. Blots were subsequently washed three times, changing the wash every 5 minutes, with PBST. Finally, blots were incubated with Clarity Western ECL Blotting Substrate, and images were acquired using a ChemiDoc MP Imaging System (Bio-Rad Laboratories, Mississauga, ON).

Initial blots unveiled an additional unpredicted higher molecular weight band at approximately 13 kDa for DromeITP protein samples. *In silico* analysis using the NetNglyc server, which predicts N-Glycosylation sites, revealed that DromeITP but not AedaeITP contains a predicted glycosylation site (http://www.cbs.dtu.dk/services/NetNGlyc/) (Figure 7). To validate whether ITP undergoes glycosylation, samples were treated with N-glycosidase F (PNGase F) (New England Biolabs, Whitby, ON, CA), following manufacturer guidelines, to validate if the peptide contained asparagine-linked (N-linked) carbohydrate side chains indicative of glycosylation during post-translational modification. A modification made to the manufacturer guideline being that samples were not heated at 100 °C prior to PNGase F treatment. Control reactions were treated similarly, but did not include PNGase F enzyme.

```
Name:  AedesITP         Length:  73
SSFFDIECKGQFNKAIFYRLDRICEDCYSLFREPQILSFCKEGCFGSEYFLACVEALVLDEETEKFMKWREML
.............................................................................  80

(Threshold=0.5)

No sites predicted in this sequence.
```

A

```
Name:  DromeITP         Length:  73
SNFFDLECKGIFNKTMFFRLDRICEDCYQLFRETSIHRLCKQECFGSPFFNACIEALQLHEEMDKYNEWRDTL
............N................................................................  80

(Threshold=0.5)
------------------------------------------------------------------------
SeqName      Position  Potential    Jury    N-Glyc
                                  agreement result
------------------------------------------------------------------------
DromeITP       13 NKTM   0.7622     (9/9)   +++
------------------------------------------------------------------------
```

B

Figure 7: *In silico* analysis of predicted *N*-glycosylation sites for AedaeITP (A) and DromeITP (B) using the NetNglyc server.

Results

Western blot analyses

Protein extracts were isolated from either AtT-20 or HEK293T cells transiently expressing *A. aegypti* ITP (AedaeITP) and incubated with a primary antibody against the C-terminal region of *D. melanogaster* ITP (DromeITP), which shares 41.7% similarity to the AedaeITP C-terminal region. A band size of approximately 9 kDa was detected in protein samples isolated 24 h post ITP-transfection from AtT-20 cells (Figure 8a), however, this band was absent when the media was collected 48 h post AedaeITP-transfection from AtT-20 cells (Figure 8b). Interestingly, there was no band detected in protein samples isolated 24 or 48 h post ITP-transfection from HEK293T cells (Figure 8a, b). In untransfected negative control samples of either cell type, no bands were detected (Figure 8a, b).

A similar band size of approximately 9 kDa was recognized in protein isolations purified 24 or 48 h post DromeITP-transfection from AtT20 cells (Figure 9a, b). Additionally, a higher molecular weight band at approximately 13 kDa was detected in protein samples from DromeITP-transfected cells (Figure 9a, b). Based on *in silico* predictions, this higher molecular weight band was believed to be a glycosylated variant of DromeITP (Figure 7). Indeed, this was confirmed to be the case as shown by the loss of the higher molecular weight band (13 kDa) upon PNGase treatment with only the 9 kDa band remaining (Figure 10). When both AedaeITP and DromeITP protein isolations were loaded on the same blot, there was a loss of the previously observed band at approximated 9 kDa in protein isolated from AedaeITP-transfected cells (Figure 9a, b).

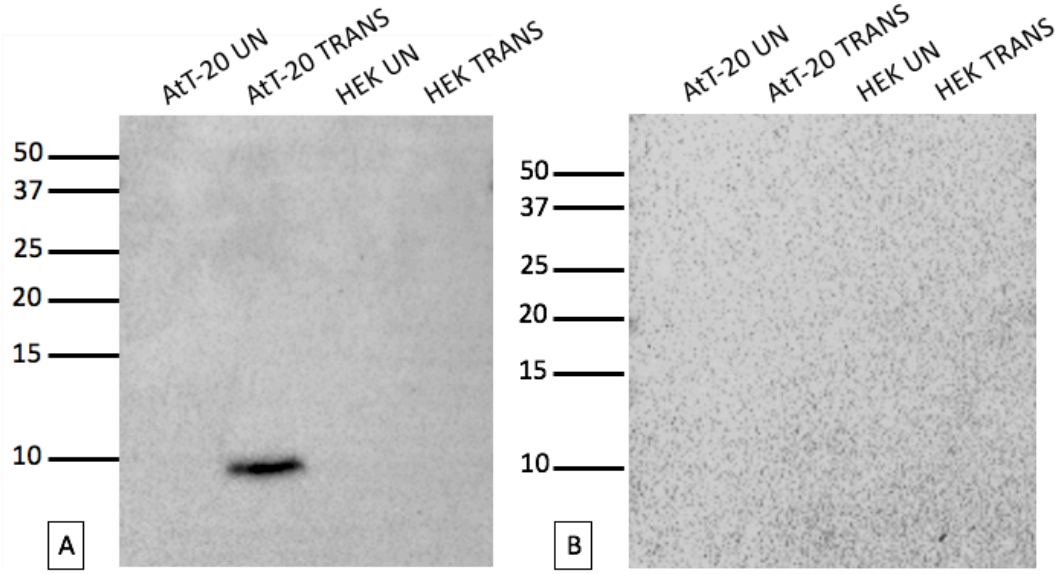

Figure 8: Western blot analysis of protein isolated from AtT-20 and HEK cells. Protein was isolated after 24 h (A) and 48 h (B) from media bathing AtT-20 and HEK AedaeITP-transfected (TRANS) and untransfected (UN) cells. An expected sized band at ~9 kDa was only observed in lanes containing protein isolations from AedaeITP-transfected AtT20 cells 24 h post-transfection (A).

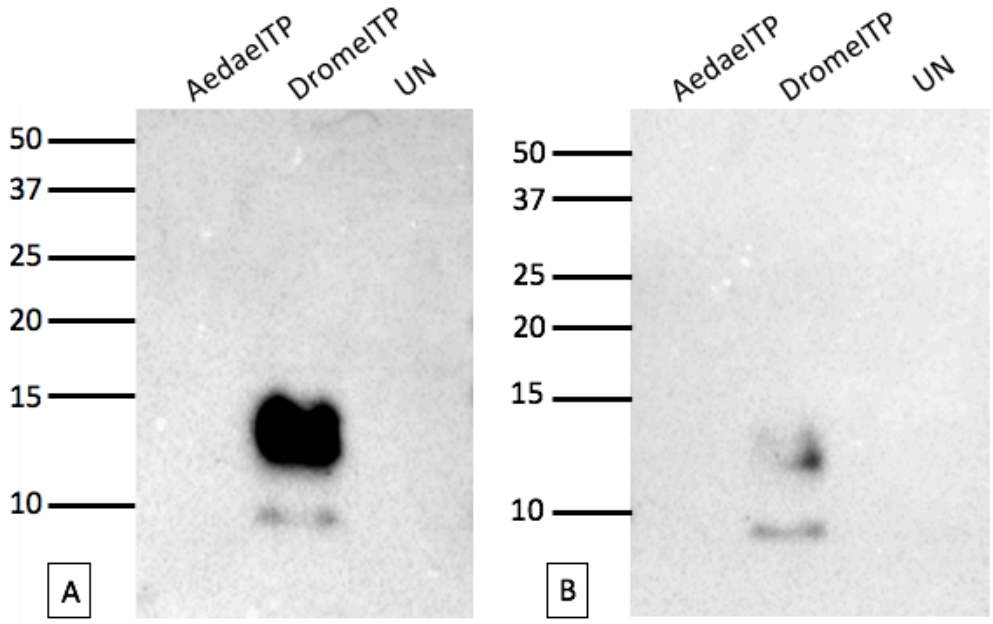

Figure 9: Western blot analysis of protein isolated from AtT-20 cells transfected with AedaeITP or DromeITP. (A) Protein isolated from AtT-20 cells transfected with AedaeITP or DromeITP and untransfected cells (UN) harvested after 48 h and (B) protein isolated from AtT-20 cells transfected with AedaeITP or DromeITP and untransfected cells (UN) collected after 24 h. An expected band size at ~9 kDa was only observed in lanes containing protein isolations from DromeITP-transfected AtT20 cells 24 and 48 h post-transfection (A, B). Additionally, a band was observed in protein fractions from DromeITP-transfected cells 24 and 48 h post-transfection at ~13kDa (A, B).

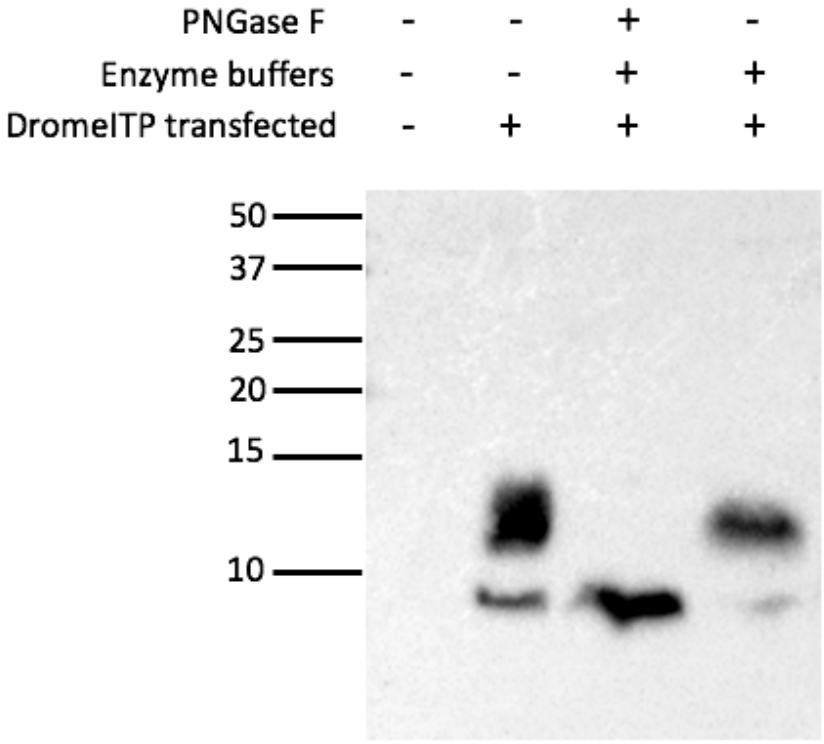

Figure 10: Western blot analysis of DromeITP glycosylation. Protein samples isolated 48 h post DromeITP-transfection from AtT20 cells were treated with PNGase F (N-glycosidase F). DromeITP undergoes N-linked glycosylation as treatment with PNGase F eliminates the 13 kDa band and intensifies the band present at 9 kDa.

AedaeITP-immunoreactivity in the central nervous system of adult *A. aegypti*

Using whole mount immunohistochemistry, the central nervous system (CNS) of four-day-old adult *A. aegypti* was surveyed for ITP-immunoreactivity. Areas of the CNS explored for ITP-immunoreactivity included the brain, thoracic ganglia, and the ventral nerve cord (housing the six abdominal ganglia). Similar staining was observed in the CNS of both adult males and females. In the adult brain, ITP-immunoreactivity of cells located laterally in the posterior region of each brain hemisphere was observed (Figure 11, 12a, 18). Findings indicate ITP-immunoreactive cells located medioposteriorly and ventrally on each of the six abdominal ganglia of the ventral nerve cord (Figure 11-17). ITP may exit the proposed neurosecretory cells of the abdominal ganglia through processes; visualizing the same abdominal ganglia through different focal planes revealed ITP-immunoreactivity migrating anteriorly on the ganglia and emanating laterally through projections to putative neurohaemal sites (Figure 13, 14). It is difficult to determine how many ITP-immunoreactive neurosecretory cells are present within each of the abdominal ganglia, therefore, counting how many DAPI-stained neurosecretory cell nuclei that resided closely with the ITP-immunoreactivity was used to predict the number of cells. ITP-immunoreactivity was seen to co-localize with both one and two nuclei, suggesting the presence of either one (Figure 15a, 16a) or two neurosecretory cells (Figure 15b, 16b). Findings in the terminal abdominal ganglion (i.e. the sixth abdominal ganglion) suggests that there are two (Figure 17a) to three ITP-immunoreactive neurosecretory cells (Figure 17b) present in females and males, respectively. Finally, the presence of one ITP-immunoreactive cell located medioposteriorly in the thoracic ganglia was reported in both sexes (Figure 12a, b). Whole mounts of central nervous system tissue (including the brain, thoracic ganglia, and ventral nerve cord) from 4th instar larvae showed no immunoreactive staining (data not shown).

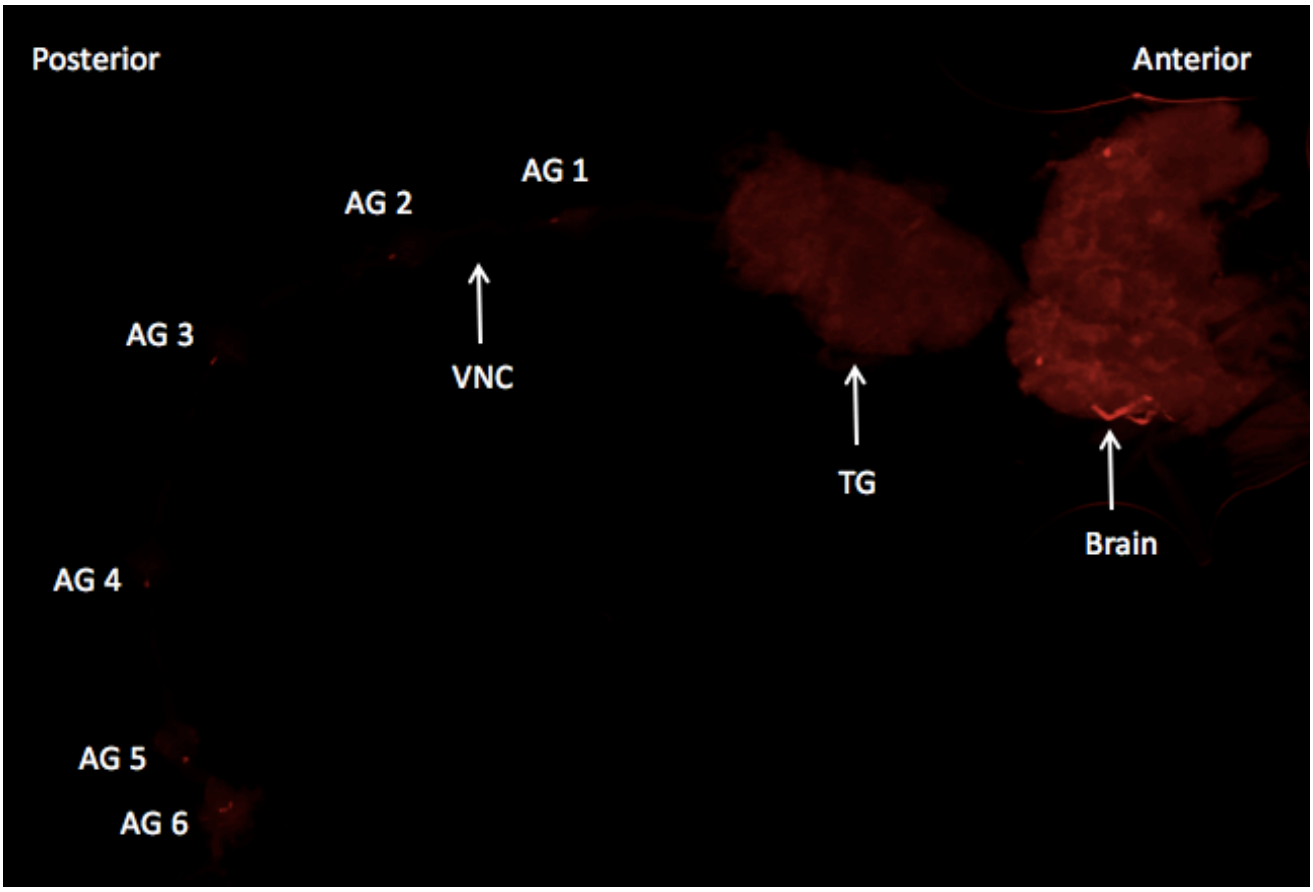

Figure 11: Distribution of ITP-like immunoreactivity (red) in the female central nervous system (CNS) of 4-day-old adult *A. aegypti*. ITP-immunoreactivity is present in the brain, thoracic ganglia (TG) as well as the posterior region of each abdominal ganglia (AG). Stitched image of the CNS was obtained using an EVOS FL Auto live-cell imaging system.

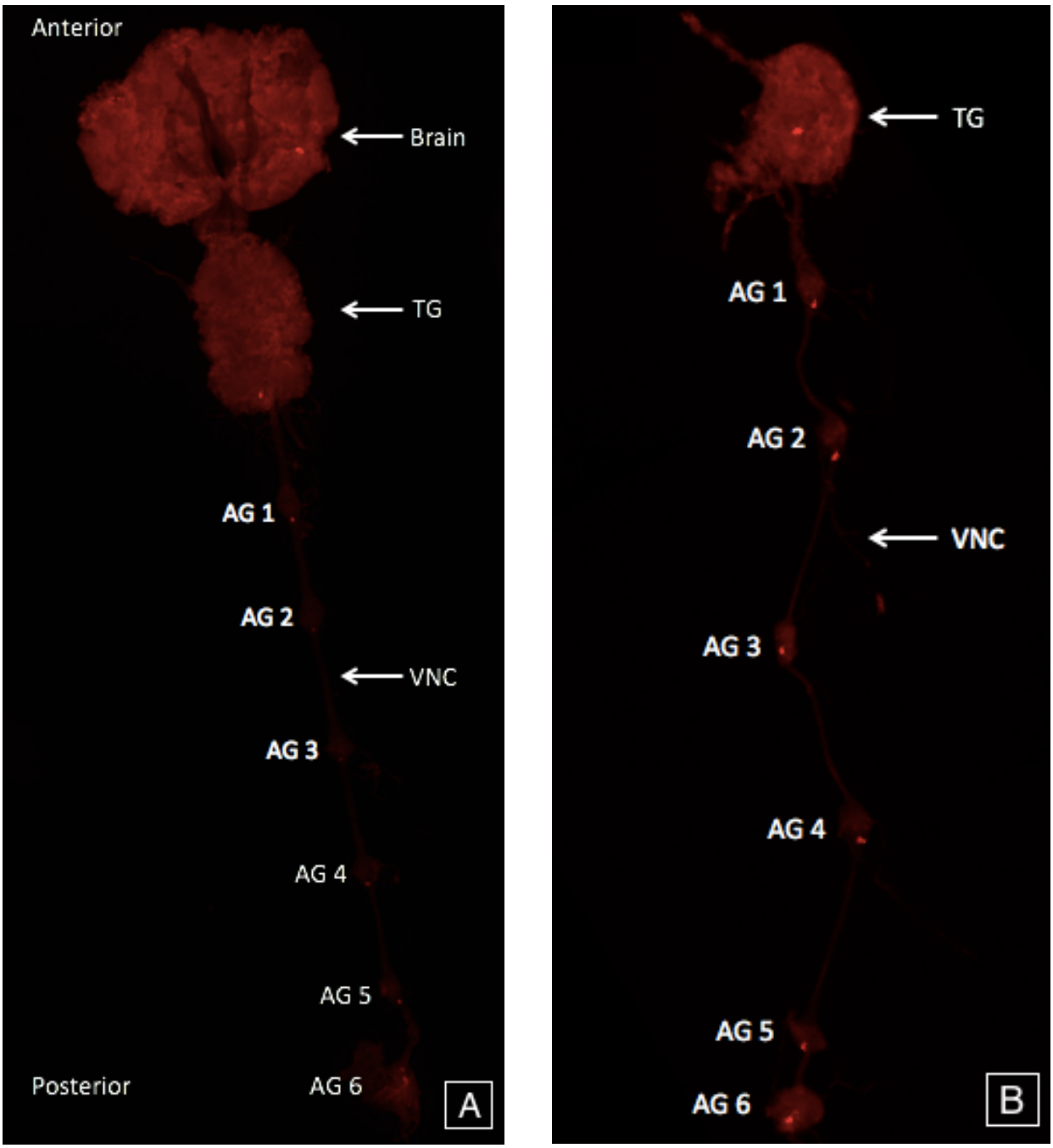

Figure 12: Distribution of ITP-like immunoreactivity (red) in the male (A) and female (B) central nervous system (CNS) of 4-day-old adult *A. aegypti*. ITP-immunoreactivity is present in the brain, thoracic ganglia (TG) as well as the posterior region of each abdominal ganglia (AG). Stitched images of the CNS was obtained using an EVOS FL Auto live-cell imaging system.

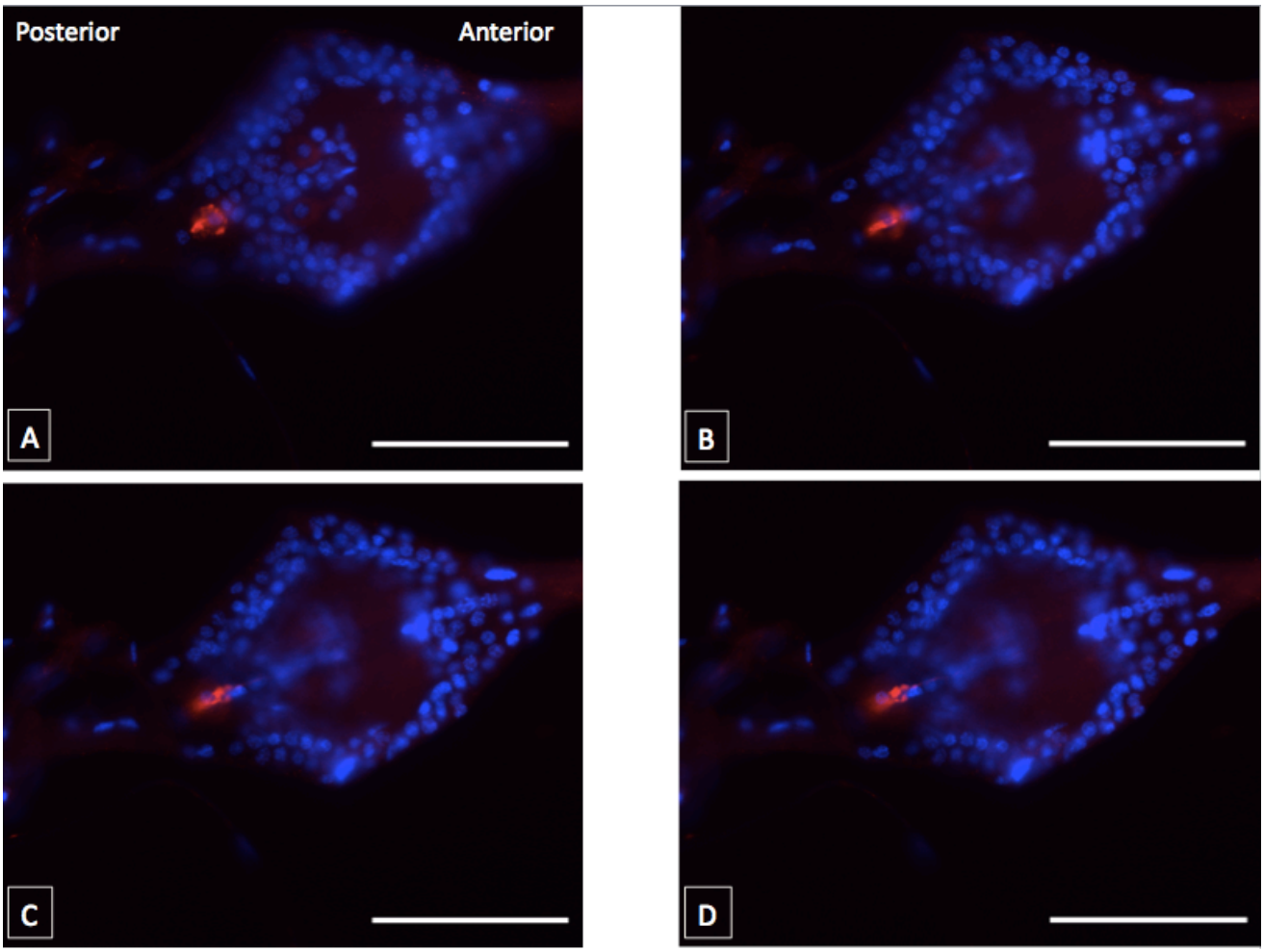

Figure 13: Distribution of ITP-like immunoreactivity (*red*) and DAPI (*blue*) in the female abdominal ganglia of adult 4-day-old *A. aegypti*. ITP-immunoreactivity was shown in the posterior end of the abdominal ganglia. Images (A-D) show the same abdominal ganglia in different planes of focus. This allows for the visualization of ITP-immunoreactivity exiting proposed neurosecretory cells into processes of the abdominal ganglia. Scale bars 100 μm

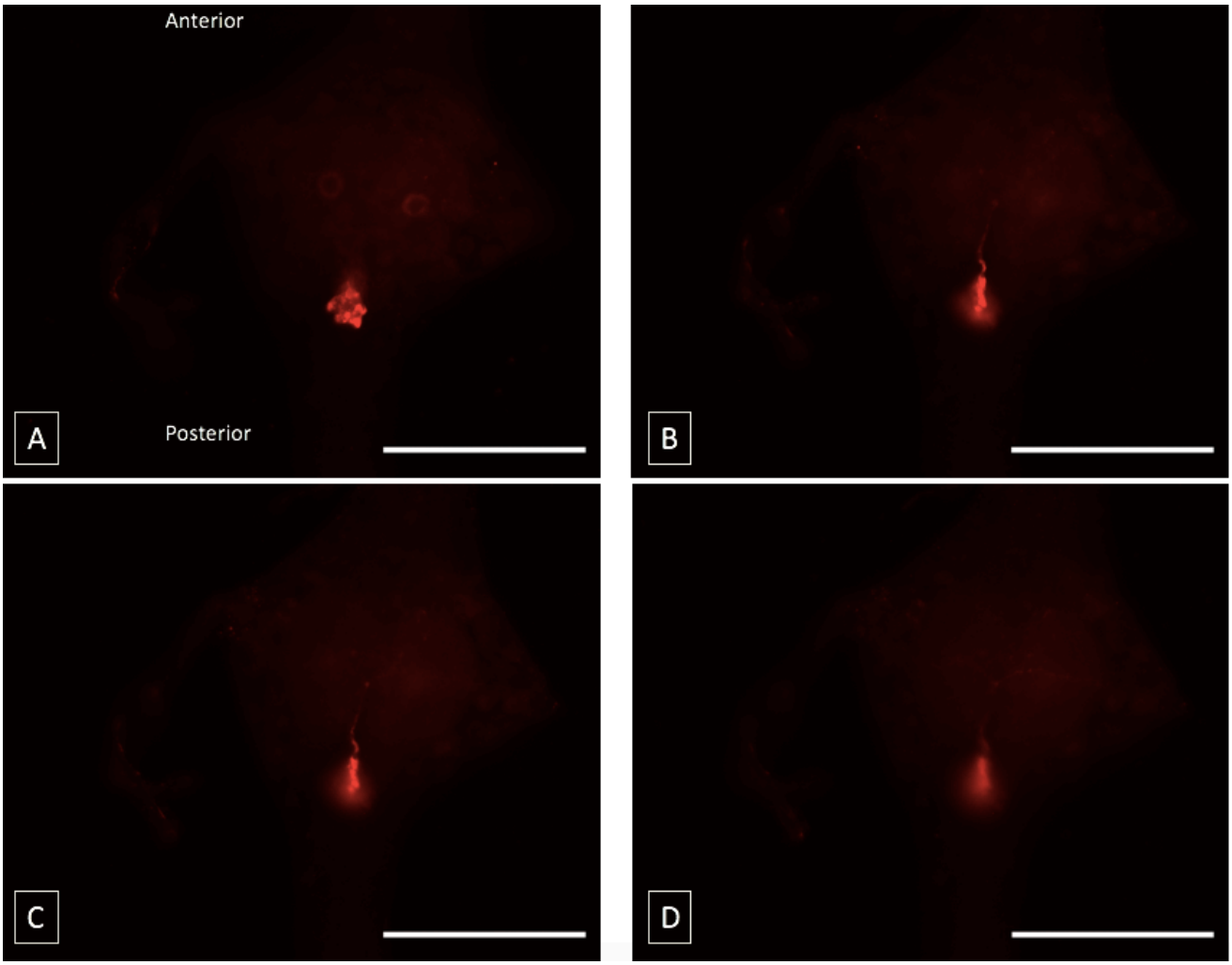

Figure 14: Distribution of ITP-like immunoreactivity (*red*) in the female abdominal ganglia of adult 4-day-old *A. aegypti*. ITP-immunoreactivity was shown in the posterior end of the abdominal ganglia. Images (A-D) show the same abdominal ganglia in different planes of focus. This allows for the visualization of ITP-immunoreactivity exiting proposed neurosecretory cells into processes of the abdominal ganglia. Scale bars 100 μm

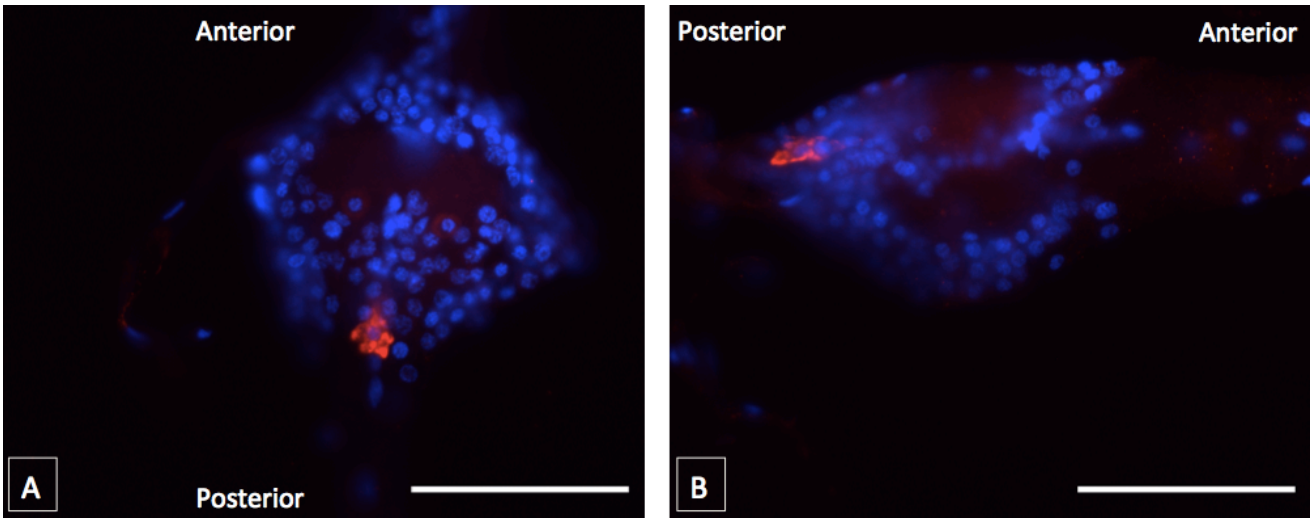

Figure 15: Distribution of ITP-like immunoreactivity (*red*) and DAPI (*blue*) in the female abdominal ganglia of adult 4-day-old *A. aegypti*. ITP-immunoreactivity was shown in the posterior end of the abdominal ganglia in what is suggested to be one cell (A) versus two cells (B). Scale bars 100 μm

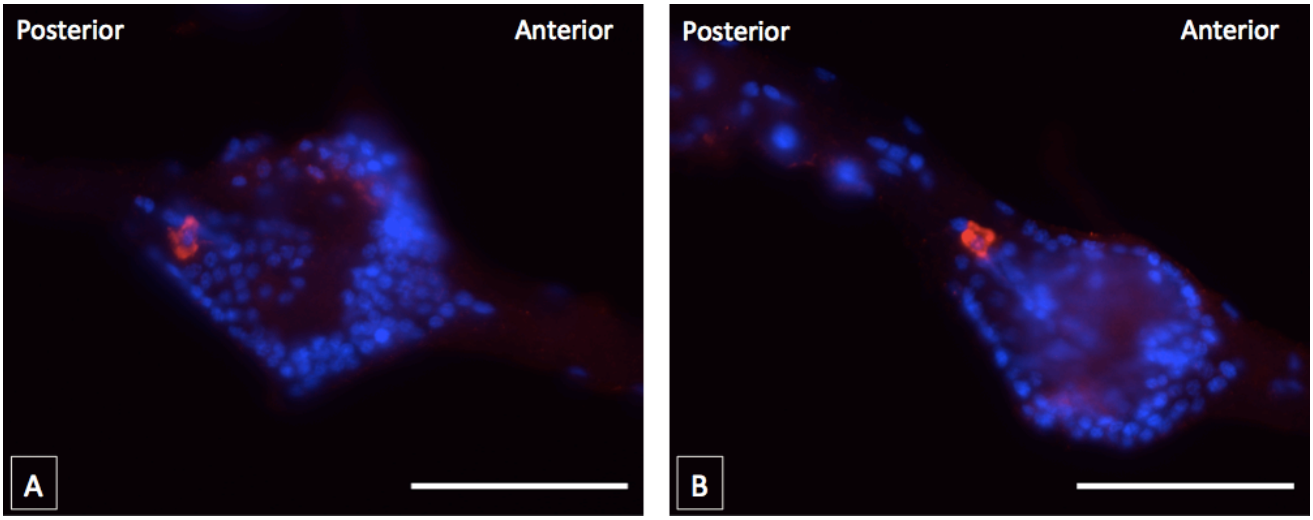

Figure 16: Distribution of ITP-like immunoreactivity (*red*) and DAPI (*blue*) in the male abdominal ganglia of adult 4-day-old *A. aegypti*. ITP-immunoreactivity was shown in the posterior end of the abdominal ganglia in what is suggested to be one cell (A) versus two cells (B). Scale bars 100 μm

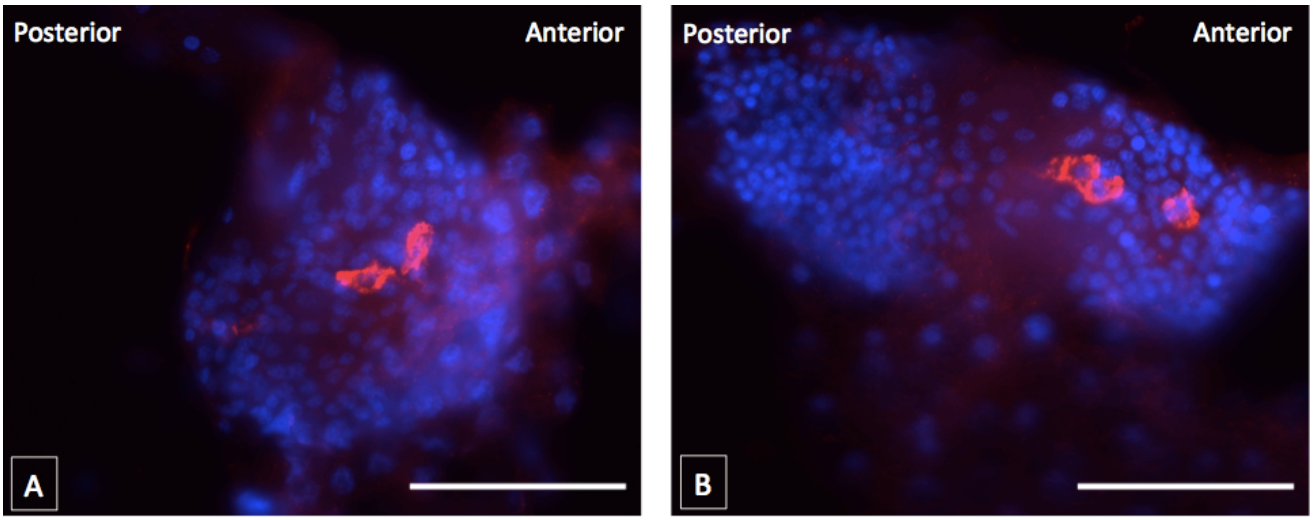

Figure 17: Distribution of ITP-like immunoreactivity (*red*) and DAPI (*blue*) in the female (A) and male (B) terminal abdominal ganglia of adult 4-day-old *A. aegypti*. ITP-immunoreactivity suggests that there are two cells (A) versus three cells (B) in the terminal abdominal ganglia of females and males, respectively. Scale bars 100 μm.

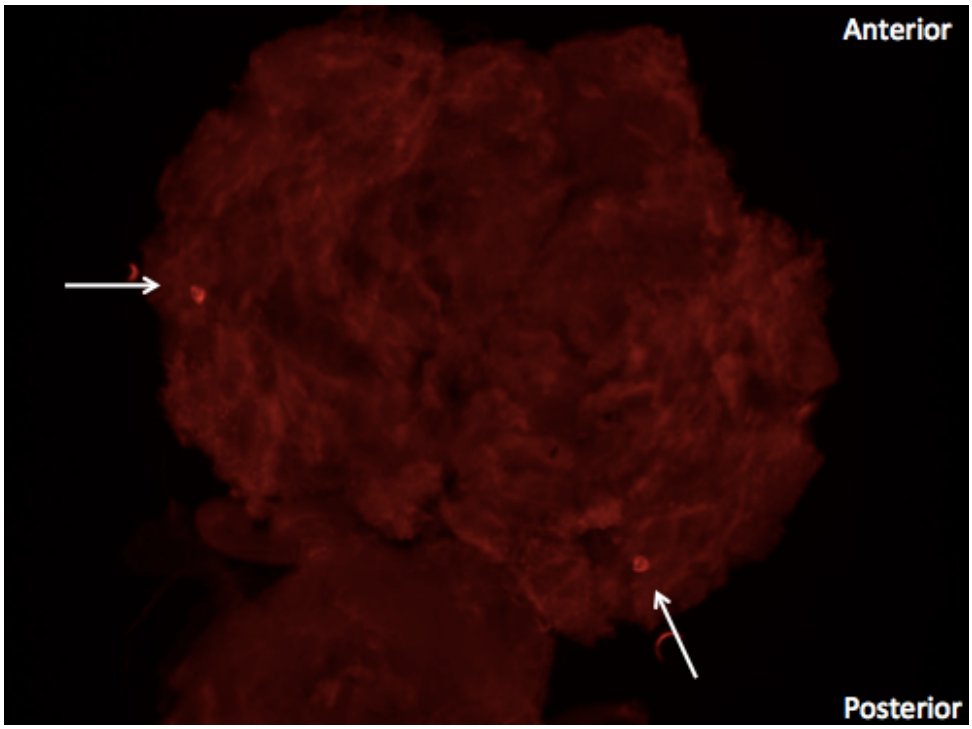

Figure 18: Distribution of ITP-like immunoreactivity *(red)* in the brain of male 4-day-old adult *A. aegypti.* ITP-immunoreactivity was observed in cells localized laterally and posteriorly in both left and right hemispheres of the brain. Similar results were observed for female mosquito brain preparations (not shown). Stitched image of the CNS was obtained using an EVOS FL Auto live-cell imaging system.

Scanning Ion-selective Electrode Technique (SIET): measuring ion transport across the hindgut

Using Scanning Ion-selective Electrode Technique (SIET) to measure ion transport across the adult hindgut epithelia, the influence of recombinant AedaeITP and its suspected second messengers, cAMP and cGMP, were investigated. Notably, average ion flux values greater than zero correspond to haemolymph-directed ion transport (i.e. absorption), and average ion flux values less than zero (i.e. negative values) correspond to lumen-directed ion transport (i.e. secretion). Prior to measuring the effect of test factors on the ion flux across the hindgut of adult mosquitoes, control trials were performed by exposing the hindgut to Ca^{2+}-free *Aedes* saline to record the basal ion flux of untreated hindgut tissue. Experimental trials were performed with the addition of either cAMP or cGMP having a final concentration of 1mM, or alternatively, recombinant AedaeITP was applied with an estimated effective concentration of 1nM bathing the hindgut preparation. Electrical recordings indicative of ion transport were taken beginning at the rectum-ileum junction, which served as an anatomical landmark, and subsequently measurements were taken moving either anteriorly over the ileum, or posteriorly over the rectum.

Results indicate that application of cAMP generally promoted haemolymph directed Na^+ flux (i.e absorption) in the hindgut of adult males, and the rectum of adult females (Figure 19a, b); cAMP inhibited Na^+ absorption in the ileum of adult females (Figure 19a). A general trend whereby the application of cAMP inhibited K^+ absorption in the hindgut of males and the ileum of females was noted (Figure 20a, b). Particularly, K^+ absorption was significantly inhibited in the ileum of males (Figure 20a). This trend was not observed in the rectum of females, where cAMP promoted K^+ absorption (Figure 20b).

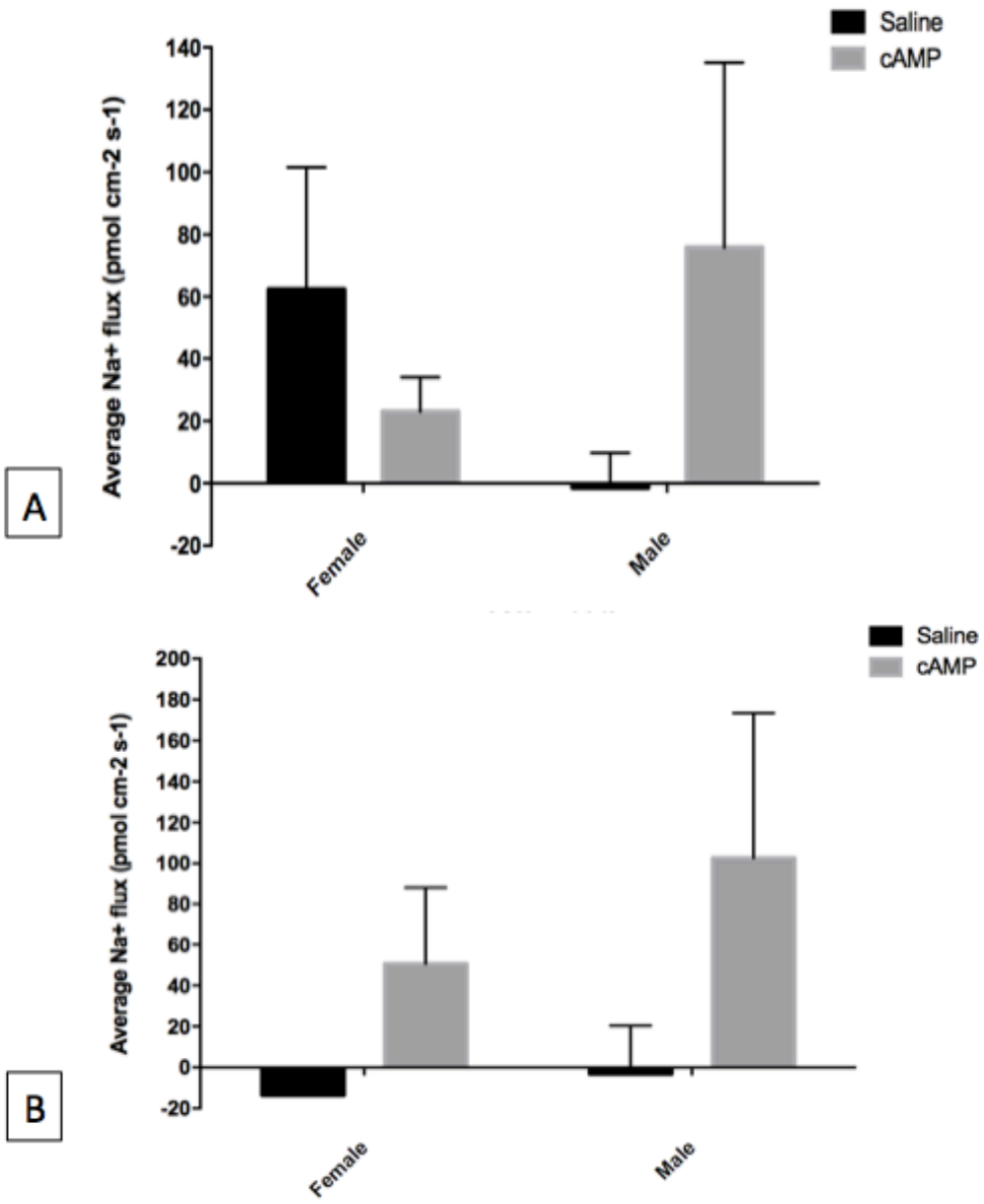

Figure 19: Effect of 1 mM cAMP on Na^+ transport across the adult hindgut of *A. aegypti.* Female and male adult mosquitoes, between 1-4 days old, were dissected and the excised hindgut tested for Na^+ transepithelial transport across the ileum (A) and rectum (B). Control treatments consisted of *Aedes* saline solution alone whereas experimental treatments involved 1 mM cAMP applied to the hindgut. A total of 20 female and 20 male adult mosquitoes were tested for each treatment. The ion flux calculated at each site, and along the entire ileum or rectum, were averaged across all preparations and SEM was calculated, n=20. cAMP inhibited haemolymph-directed Na^+ transport (i.e. absorption) across the ileum of females and promoted haemolymph-directed Na^+ transport across the ileum of males (A). cAMP promoted haemolymph-directed Na^+ transport (i.e. absorption) across the rectum of both female and male adult mosquitoes (B). Ultimately, cAMP reduced natriuresis in males. Unpaired t-tests were used to compare control and experimental treatments, and differences between treatments were considered statistically significant if $p<0.05$.

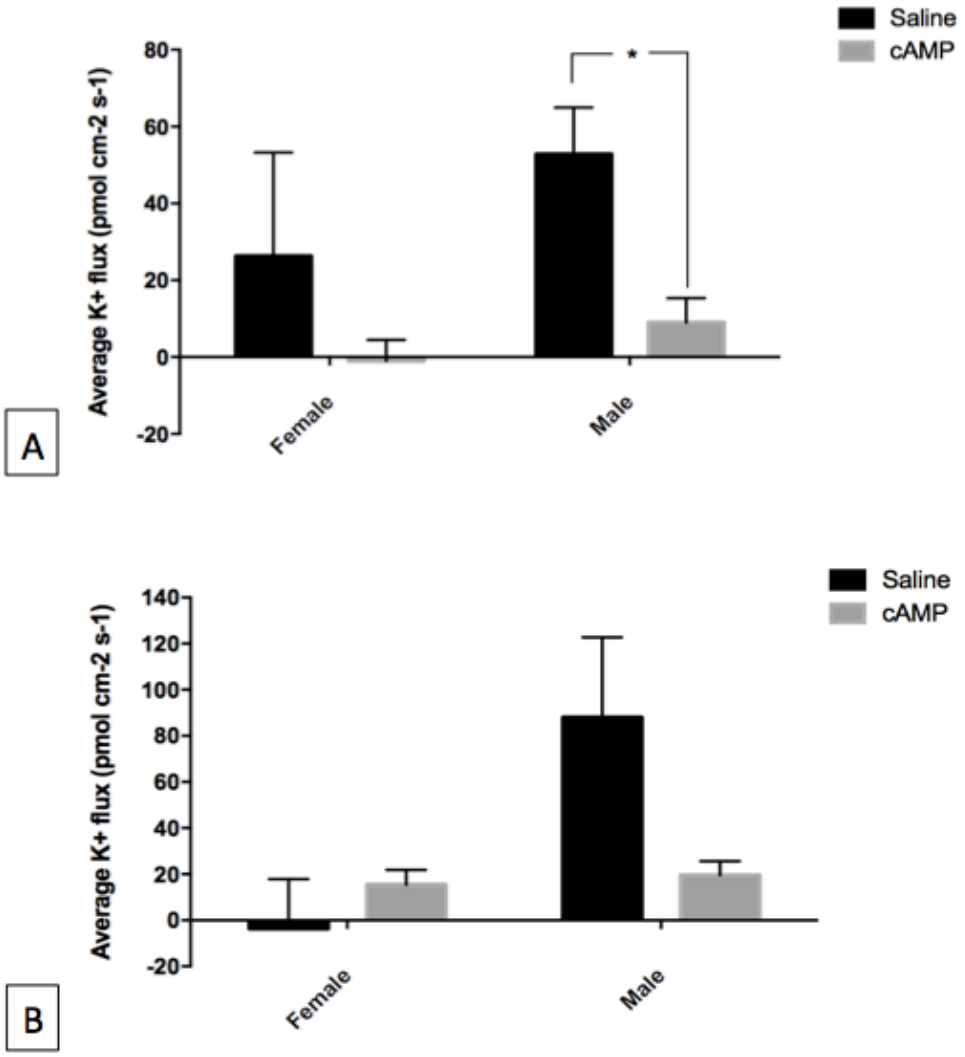

Figure 20: Effect of 1 mM cAMP on K^+ transport across the hindgut of adult *Aedes aegypti.* Female and male adult mosquitoes, between 1-4 days old, were dissected and the excised hindgut tested for K^+ transepithelial transport across the ileum (A) and rectum (B). Control treatments consisted of *Aedes* saline solution alone whereas experimental treatments involved 1 mM cAMP applied to the hindgut. A total of 20 female and 20 male adult mosquitoes were tested for each treatment. The ion flux calculated at each site, and along the entire ileum, were averaged across all preparations and SEM was calculated, n=20. cAMP inhibited haemolymph-directed K^+ transport (i.e. absorption) across the ileum of females and males as well as the rectum of males (A, B). Conversely, cAMP promoted K^+ absorption across the rectum of females (B). cAMP promoted kaliuresis in males. Unpaired t-tests were used to compare control and experimental treatments, and differences between treatments were considered statistically significant if $p<0.05$*.

The application of 1 mM cGMP significantly promoted lumen-directed Na^+ flux (i.e secretion) in both the ileum and rectum of adult females (Figure 21a, b). The same trend, although not significant, was noted in both the ileum and rectum of adult males: 1mM cGMP promoted Na^+ secretion (Figure 21a, b). Opposing trends were observed on the effects of 1 mM cGMP on K^+ transepithelial transport in females vs. males. The addition of 1 mM cGMP inhibited K^+ absorption in both the ileum and rectum of females (Figure 22a, b). Conversely, 1 mM cGMP promoted K^+ absorption in the ileum and rectum of males (Figure 22a, b).

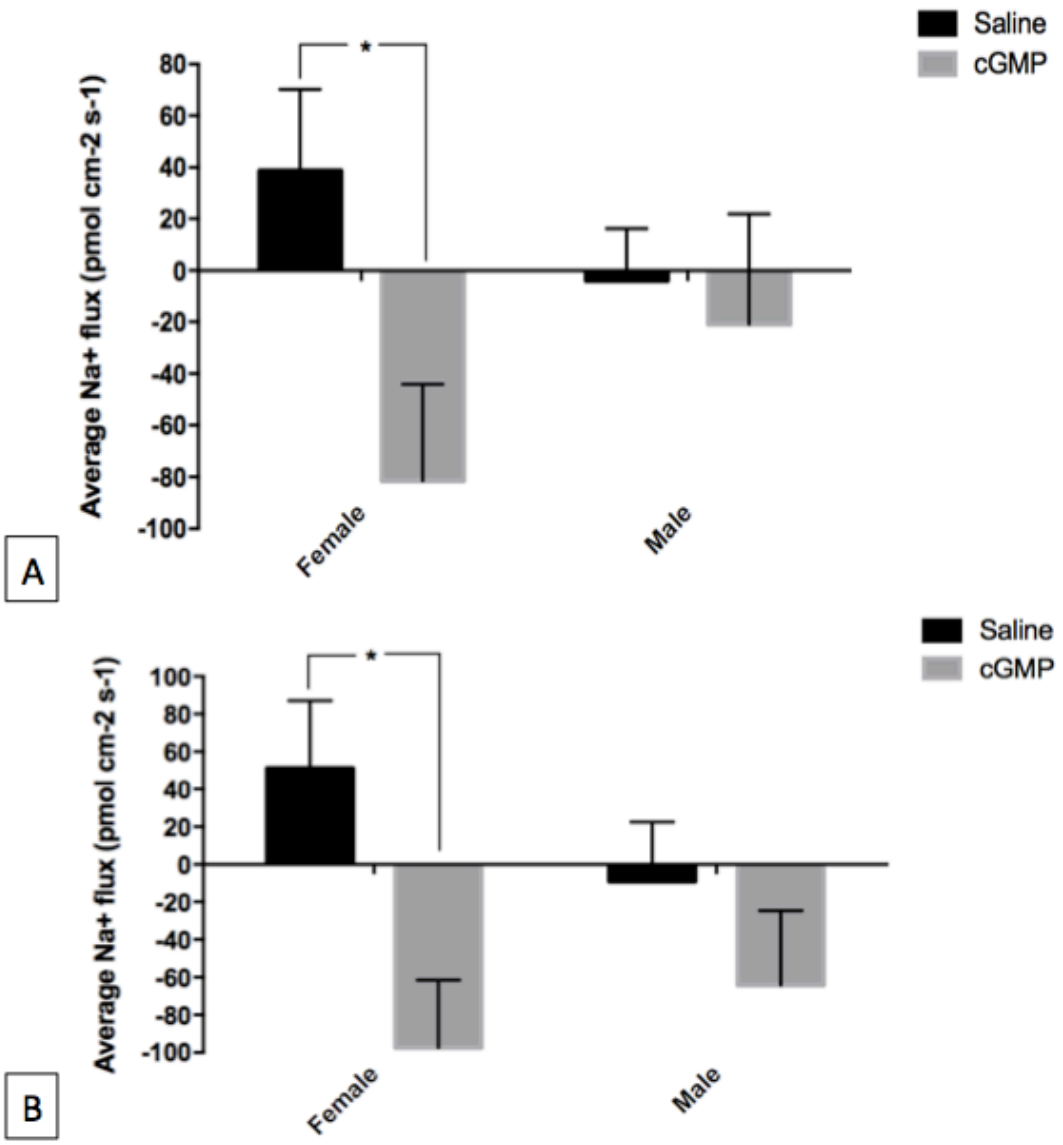

Figure 21: Effect of 1 mM cGMP on Na^+ transport across the hindgut of adult *Aedes aegypti.* Female and male adult mosquitoes, between 1-4 days old, were dissected and the excised hindgut tested for Na^+ transepithelial transport across the ileum (A) and rectum (B). Control treatments consisted of *Aedes* saline solution alone whereas experimental treatments involved 1 mM cGMP applied to the hindgut. A total of 20 female and 20 male adult mosquitoes were tested for each treatment. The ion flux calculated at each site, and along the entire ileum or rectum, were averaged across all preparations and SEM was calculated, n=20. cGMP promoted lumen-directed Na^+ transport (i.e. secretion) across the ileum and rectum of both males and females (A, B). Unpaired t-tests were used to compare control and experimental treatments, and differences between treatments were considered statistically significant if $p<0.05$*.

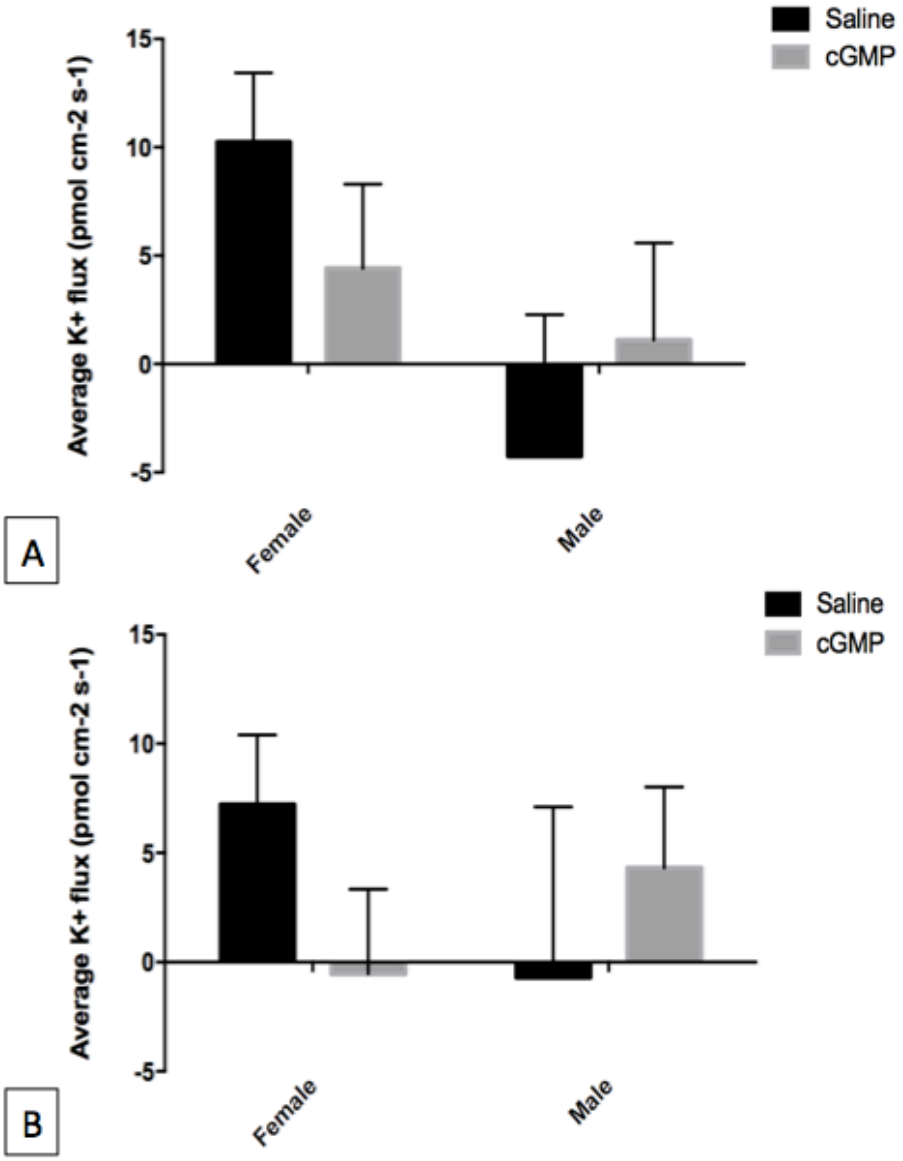

Figure 22: Effect of 1 mM cGMP on K^+ transport across the hindgut of adult *Aedes aegypti.* Female and male adult mosquitoes, between 1-4 days old, were dissected and the excised hindgut tested for K^+ transepithelial transport across the ileum (A) and rectum (B). Control treatments consisted of *Aedes* saline solution alone whereas experimental treatments involved 1 mM cGMP applied to the hindgut. A total of 20 female and 20 male adult mosquitoes were tested for each treatment. The ion flux calculated at each site, and along the entire ileum, were averaged across all preparations and SEM was calculated, n=20. cGMP inhibited haemolymph-directed K^+ transport (i.e. absorption) across the ileum and rectum of females (A, B). Conversely in males, cGMP promoted K^+ absorption in both the ileum and rectum (A, B). Unpaired t-tests were used to compare control and experimental treatments, and differences between treatments were considered statistically significant if $p<0.05$.

SIET analysis of hindgut following treatment with recombinant AedaeITP

Control trials containing an equal volume of concentrated untransfected cell media to the volume used in recombinant AedaeITP trials, promoted the secretion of Na^+ in both the ileum and rectum of males and females (Figure 23a, b). The application of 1 nM recombinant AedaeITP did not cause a change in the secretion of Na^+ in either the ileum or rectum of both sexes (Figure 23a, b).

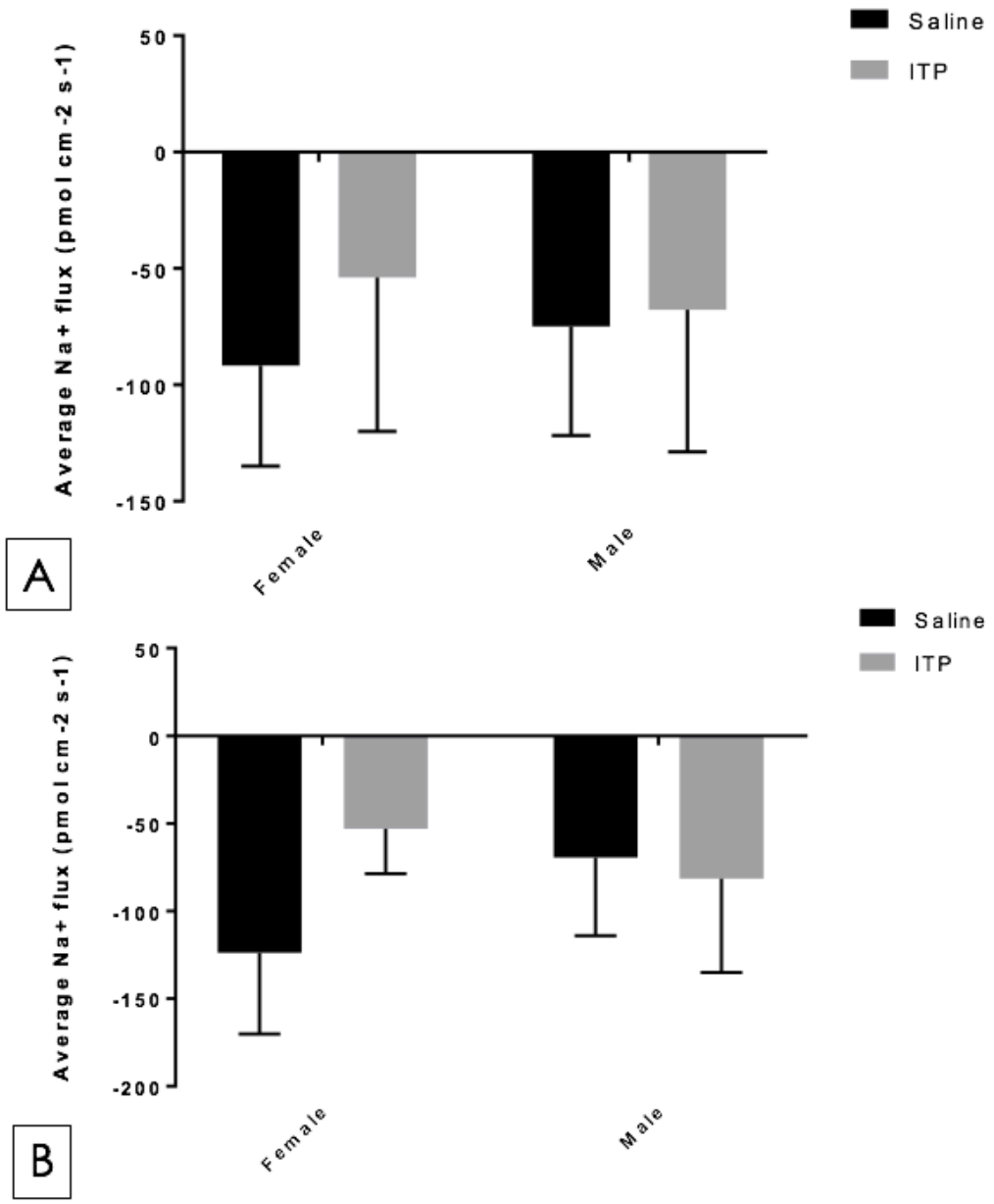

Figure 23: Effect of 1 nM recombinant ITP on Na^+ transport across the hindgut of adult *Aedes aegypti.* Female and male adult mosquitoes, between 1-4 days old, were dissected and the excised hindgut tested for Na^+ transepithelial transport across the ileum (A) and rectum (B). Control treatments consisted of untransfected cell media in *Aedes* saline solution alone whereas experimental treatments involved 1 nM recombinant AedaeITP applied to the hindgut. A total of 12 female and 12 male adult mosquitoes were tested for each treatment. The ion flux calculated at each site, and along the entire ileum, were averaged across all preparations and SEM was calculated, n=12. AedaeITP did not have any significant effect on the lumen-directed Na^+ transport (i.e. secretion) across the ileum and rectum of either sex (A, B). Unpaired t-tests were used to compare control and experimental treatments, and differences between treatments were considered statistically significant if $p<0.05$.

Discussion

The discovery of the first antidiuretic hormone mediating its effects on the hindgut of insects was made in 1992 by Audsley *et al.*, when Ion Transport Peptide was purified from the corpora cardiaca of the locust, *S. gregaria.* Later, a conserved ITP gene was uncovered in the genome of the mosquito, *A. aegypti,* suggesting it might play a similar role in maintaining iono- and osmoregulation (Dai et al., 2007). Up to this point however, the mRNA expression and peptide localization of ITP in *A. aegypti* has not been explored. As such, the physiological role of ITP in the mosquito remains unclear. In an attempt to elucidate the function of ITP in the adult mosquito *A. aegpti*, the nervous tissue-specific localization of ITP was investigated. The Scanning Ion-selective Electrode Technique (SIET) was utilized to investigate whether ITP and its putative second messengers, cAMP and cGMP, influenced ion transport across the adult *A. aegypti* hindgut epithelium.

Production of ITP using a neuroendocrine derived cell line: AtT-20

Mouse pituitary AtT-20 cell lines were used to produce both *A. aegypti* ITP (AedaeITP) and *D. melanogaster* ITP (DromeITP) for the first time. Western blot analysis of protein isolated from the media the cells grew in 24 h post-transfection revealed an immunoreactive band at approximately 9 kDa for both insect ITPs. In the locust, *S. gregaria,* the molecular mass of ITP was shown to be 8.6 kDa (Meredith et al., 1996). In *D. melanogaster*, previous western blot analysis from 3rd instar larvae revealed a ITP-immunoreactive band at 8.9 kDa (Dircksen et al., 2008). Interestingly, protein isolated from DromeITP-transfected cells revealed a second band at approximately 13 kDa, which has not been previously documented and was suspected, based on *in silico* analysis of the prepropeptide, to represent a glycosylated form of DromeITP.

Glycosylation is the covalent attachment of an oligosaccharide chain to a protein backbone and is considered to be a very common protein modification. Glycosylation of proteins modulates various processes such as subcellular localization, protein quality control, cell-cell recognition and cell-matrix binding events (Vandenborre et al., 2011). Treatment with Peptide-N-Glycosidase F (PNGase F), a native glycoaminidase cleaving the link between asparagine and N-acetylglucosamines, allowed for the study of N-linked carbohydrates in ITP. PNGase F treatment caused the loss of the higher molecular weight band (13kDa), while the lower molecular weight band was preserved (9 kDa). These findings provided strong evidence that DromeITP is glycosylated, and that its glycosylation may be imperative for its physiological function. A study by Vandenborre *et al.* (2011), studying the glycoproteomes of various insect species, predicted that there are roughly 118 proteins that undergo N-glycosylation in *D. melanogaster*.

Western blot analysis containing protein isolated from both AedaeITP-transfected and DromeITP-transfected cells did not contain a band in the lanes containing protein isolated from AedaeITP-transfected cells. A probable explanation for this finding lies in the fact that the antibody used for detecting both insect ITPs was generated against the specific antigen sequence from the C-terminal region of DromeITP. The homologous region in AedaeITP possessed only 41.7% sequence identity to the DromeITP antigen sequence (5/12 amino acids were identical). Due to the poor specificity of the antibody for AedaeITP, DromeITP protein isolations on the same blot likely sequestered the antibody due to its 100% sequence identity.

Distribution pattern of ITP in the CNS

Previous limited research done on the presence of ITP in the mosquito, *A. aegypti*, simply confirmed its existence in the genome; however, transcript or protein-level expression profiles of

A. aegypti ITP (AedaeITP) had not been examined previously. Immunohistochemistry has provided evidence suggesting the presence of ITP peptide in all regions of the central nervous system studied: the brain, thoracic ganglia, and ventral nerve cord that houses the six abdominal ganglia. ITP-like immunoreactivity in the brain was localized to two lateral neurosecretory cells. Similar staining was observed for *A. aegypti* adipokinetic hormone (AedaeAKH) where two pairs of lateral neurosecretory cells were localized to the same brain region reported here (Kaufmann et al., 2009). Neuropeptides of the AKH family induce the mobilization of energy stores to fuel flight (Wilps and Gade, 1990). Furthermore, allatotropin, allatostatin-A, and allatostatin-C were all found to localize to cells found in a similar posterior lateral region of the brain in *A. aegypti* (Hernández-Martínez et al., 2005). Allatostatins (AS) and allatotropins (AT) were first described as modulators inhibiting juvenile hormone biosynthesis in the corpora allata (Bellés et al., 1999; Kramer et al., 1991; Woodhead et al., 1989). Subsequently, they have been recognized to play multiple physiological roles such has controlling heart rate, gut motility, nutrient absorption, among other roles (Nässel, 2002). Additionally, in all postembryonic stages of *D. melanogaster*, strongly ITP-immunoreactive and fluorescence *in situ* hybridization (FISH)-positive cells always occurred in the lateral protocerebrum (Dircksen et al., 2008). Our findings herein, along with the localization of other *A. aegypti* neuropeptides noted earlier, suggest that neuropeptide-producing cells are often localized to the lateral posterior region of the brain. We did not observe immunostaining in the nerves extending from the brain to the retrocerebral complex (corpora cardia-corpora allata), or inside this complex, suggesting that ITP is neither produced nor stored in the retrocerebral complex. Another and more likely explanation for this result is due to poor antibody cross-reactivity, since the Drome-ITP antigen sequence that was used to generate the antibody shares only 41.7% identity to the equivalent region on the C-

terminus of Aedes-ITP.

ITP-like immunoreactivity was found in one cell localized to the posterior region of the fused thoracic ganglia. A single AKH-immunoreactive cell was also observed in the thoracic ganglia of *A. aegypti* (Kaufmann et al., 2009). Interestingly, the thoracic ganglia did not possess AS- or AT-immunoreactive cells (Hernández-Martínez et al., 2005). ITP-immunoreactivity in the thoracic ganglia suggests the presence of neurosecretory cells or interneurons. Interneurons can be located entirely within a ganglion or can send axonal processes through the ventral nerve cord to synapse with other neurons. Neurosecretory cells, on the other hand, are generally monopolar; axonal processes often project to peripheral tissues, suggesting that they carry their products to functional sites (Nation, 2002). Limited literature exists on the presence of neurosecretory cells in the thoracic ganglia, as they have been most often characterized within the brain and ventral ganglia (Nation, 2002). If a more specific Aedes-ITP antibody becomes available in the future, it will be interesting to confirm if ITP-immunoreactivity exists in processes emanating from the thoracic ganglia and onto target organs (e.g. gut, reproductive, fat body) as this would help to elucidate possible functions of ITP in *A. aegypti*.

Finally, ITP-like immunoreactivity was revealed in the posterior region of all six abdominal ganglia (AG), particularly these cells lie in a ventral and medioposterior location. Some AG appeared to possess one ITP-immunoreactive cell, while other AG appeared to contain two ITP-immunoreactive cells, as shown by co-localization with either one or a pair of nuclei. Notably, the terminal AG (AG 6) contained two or more ITP-immunoreactive cells. Similar to the current results, the distribution patterns of AS and AT varied in the ventral nerve cord. AS-A immunostaining was observed in one cell located medioposteriorly in each AG except for the terminal AG in which eight cells were stained. AS-C immunostaining was observed in two

lateroposterior cells in each AG, and four posterior cells in the terminal ganglion (Hernández-Martínez et al., 2005). The larval ventral nerve cord possesses 8 AG, whereas in the adult stage *A. aegypti*, the first AG fuses to the posterior region of the thoracic ganglia and AG 7 and AG 8 fuse into a single larger terminal ganglia (Brown and Cao, 2001). The presence of multiple ITP-immunoreactive neurosecretory cells in the terminal abdominal ganglia suggests that when AG 7 and AG 8 become fused, the number of ITP-positive neurosecretory cells in the terminal ganglia of adults increased reflecting this ganglionic amalgamation. This also provides evidence supporting that the ITP-like immunoreactivity observed in the thoracic ganglia may be representative of neurosecretory cells that presumably would be localized to the posterior region of AG 1 in larval stage *A. aegypti*. Taken together, these findings suggest the presence of neurosecretory cells in the posterior region of each abdominal ganglia producing ITP, among other neuropeptides. Weak ITP-immunoreactivity in processes emanating from these suggested neurosecretory cells is observed projecting anteriorly and emerging laterally, where it may exit via the AG lateral nerves. AT, AS-A, and AS-C immunoreactive processes projecting from labelled cells of the AG were shown to emerge laterally and innervate various abdominal tissues (hindgut, heart, and oviducts), reproductive tissue (oviducts, bursa, and spermatheca), and the dorsal vessel (Hernández-Martínez et al., 2005). ITP-like immunoreactive cells in the terminal ganglia of *D. melanogaster* contain immunoreactive projections that innervate the hindgut (Dircksen et al., 2008). It will be interesting to see whether similar ITP-like immunoreactive projections exiting the AG exist in *A. aegypti,* and which tissues they innervate in order to better predict ITP's functional target sites. A representative schematic diagram of ITP-like immunoreactive staining in the central nervous system of adult *A. aegypti* provides a summary of immunohistochemical findings from the current investigation (Figure 24).

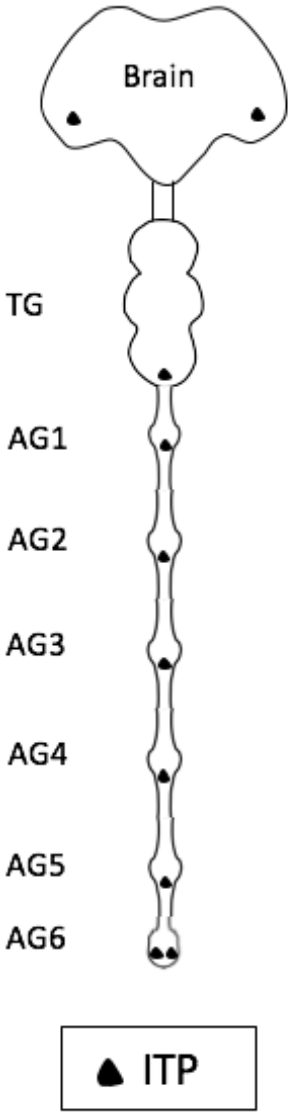

Figure 24: Representative diagram of ITP-like immunoreactive distribution in the central nervous system of *A. aegypti*. The CNS includes the brain, thoracic ganglia (TG), and the six abdominal ganglia (AG) of the adult ventral nerve cord. ITP staining in the abdominal ganglia is shown as one cell in AG 1-5, however some ganglia showed two ITP-immunoreactive cells. Additionally, the terminal AG6 has been shown to contain a minimum of two ITP-immunoreactive cells, and multiple cells in some preparations.

Effect of cAMP on ion transport across the ileum of adult *A. aegypti*

Upon treating adults of both sexes with the membrane permeable analog of cAMP, 8-bromo-cAMP, a general trend of increased ileal haemolymph-directed transport (i.e. absorption) was observed. Application of 8-bromo-cAMP resulted in Na^+ absorption in male ilea, while Na^+ absorption was inhibited in females. Application of 8-bromo-cAMP caused a decrease in K^+ absorption in both male and female ilea. Notably, cAMP significantly inhibited K^+ absorption in male ilea relative to control preparations treated with physiological saline. This suggests the inhibition of haemolymph-directed K^+ transport, and thus the inhibition of K^+ absorption within the ileum of both sexes.

The model of K^+ and Na^+ transepithelial transport in the desert locust, *S. gregaria,* serves as the best model for similar processes in *A. aegypti* mosquitoes (Audsley et al., 2013). In the locust, exogenous cAMP stimulated KCl, NaCl, and fluid absorption several fold across the locust ileum (Audsley et al., 1992b). More specifically, the electrogenic transport of Cl^- can be stimulated 10-fold by the addition of exogenous cAMP, which is the driving force for transepithelial transport of other ions (Phillips & Audsley, 1995). In the locust, the ileum is the predominant site of Na^+ absorption. *S. gregaria* ITP (SchgrITP) acts specifically on the ileum and results in an elevation of intracellular cAMP upon binding to its proposed G-protein coupled receptor (Phillips & Audsley, 1995; Audsley et al., 2013). Audsley et al. (2013) proposed a model for the mechanism of ITP action in the locust ileum, whereby the peptide acts via cAMP to stimulate the ileal absorption of Cl^-, K^+, Na^+, and osmotically obliged water. cAMP increases the uptake of Cl^- across the ileum by stimulating the apical electrogenic Cl^- pump and through the opening of Cl^- ion channels on the basolateral surface. cAMP also stimulates K^+ channel opening on the apical membrane to enhance the passive flow of K^+ ions into the haemolymph through

electrical coupling. Finally, the reabsorption of Na^+ is increased through cAMP as it increases the conductance of Na^+ in the apical membrane (Audsley et al., 2013). In adult *A. aegypti* mosquitoes, the basolateral P-type Na^+/K^+ ATPase was highly expressed in the anterior hindgut (i.e. the ileum); the ATPase enhances K^+ entry into the cell while expelling Na^+ into the haemolymph (Patrick et al., 2006). More recently, Robertson et al. (2014) observed that the membrane-permeable analog of cAMP, 8-bromo-cAMP, stimulated haemolymph-directed K^+ transport at the locust ileum (Robertson et al., 2014). The increase in K^+ and Na^+ absorption caused by cAMP may be explained through a similar mechanism by which hormones bind to their receptors and cause an increase in intracellular cAMP. Given that the locust and adult stage mosquito both face similar challenges to maintaining hydromineral homeostasis during unfed states (Phillips et al., 1998), it is probable that they share similar transcellular transport mechanisms; when both locusts and adult mosquitoes are unfed they must retain water and ions in their haemolymph (Coast 2007; Robertson et al., 2014). Taken together, extensive studies conducted in the locust along with the current report that cAMP stimulated Na^+ absorption in the ileum of male *A. aegypti* mosquitoes supports a reabsorptive role for the ileum.

Our results also presented contrary findings for the role of cAMP in promoting ion reabsorption; cAMP inhibited ileal K^+ absorption in both sexes and Na^+ absorption in females. The inhibition of K^+ and Na^+ haemolymph-directed transport is contrary to previous studies conducted on the effects of cAMP on transcellular transport in the locust. Our data suggests the necessity to expel K^+ ions in particular. As cAMP is the putative second messenger of the ancient glycoprotein hormone, GPA2/GPB5 (Sudo et al., 2005), our findings are congruent with Paluzzi *et al.* (2014) who observed that exposure of the ileum to GPA2/GPB5 (200nM) significantly reduced K^+ absorption below control levels. It is possible that since K^+ levels in the

haemolymph of *A.aegypti* are relatively low in comparison to Na^+, the level of K^+ must be closely controlled to not reach an excessive concentration, which has the potential to disrupt the resting membrane potential of electrically excitable cells such as muscle and neurons (Hoyle, 1953). It is important to note that transepithelial transport in the locust ileum serves only as a model, and a similar model has not yet been proposed for the ileum of adult *A. aegypti.* There is a possibility that alternate ion channels and pumps exist within the hindgut epithelia of the adult mosquito. In addition, it is possible that the addition of exogenous cAMP is mimicking the elevated levels of intracellular cAMP triggered by the activation of receptors that are yet to be elucidated within the ileum of the adult mosquito; these receptors upon activation may signal to inhibit transcelluar transport through intracellular cAMP elevation. Furthermore, there are prominent morphological differences between *A. aegypti* and the locust, primarily, the locust has a larger size and contains many more Malpighian tubules, in comparison to mosquitoes (Hanrahan and Phillips, 1983; Phillips et al., 1988).

It is important to note that the locust does not blood feed while adult female mosquitoes do. In the presence of a blood meal, Na^+ from the plasma content and K^+ released upon lysis of red blood cells poses a challenge to the hydromineral balance of the organism (Clements, 2000; Coast, 2009). These ions must be removed and therefore, it is expected that their absorption would be inhibited while their secretion would be promoted in the ileum. We did not measure the transepithelial ion transport of blood-fed females; however, the potential for adult females to blood feed may lead to sex-specific differences in ion transport mechanisms and/or putative receptor expression, and result in the expulsion of Na^+ upon cAMP treatment; this scenario is supported by the decreased Na^+ absorption observed across the ileum of cAMP-treated females.

Effect of cAMP on ion transport across the rectum of adult *A. aegypti*

Addition of 1 mM 8-bromo-cAMP generally caused an increase in rectal Na^+ haemolymph-directed transport (i.e. absorption) in both male and female mosquitoes, although this was not found to be significant. K^+ absorption was promoted in females and inhibited in males, however variance in transepithelial transport of ions may be influenced sex-specifically due to the presence of six rectal pads in adult females whereas only four occur in adult males (Patrick et al., 2006). Phillips (1964) showed that chloride, sodium, and potassium are actively reabsorbed from the lumen of the rectum *in situ*, in the locust (Phillips, 1964). It was later shown that the neuropeptide Chloride transport-stimulating hormone (CTSH) acts via stimulating intracellular cAMP levels to result in the reabsorption of ions and fluid by the rectum (Phillips et al., 1988). As modeled initially in the desert locust (see Figure 3), CTSH, through elevated levels of intracellular cAMP, stimulates the electrogenic Cl^- pump at the apical membrane, which drives K^+ transport through electrical coupling (Hanrahan & Phillips, 1983). The rate of KCl transport depends on its lumen concentration because K^+ directly stimulates the active entry of Cl^- via the electrogenic pump. Cl^- exits the rectum passively via basolateral cAMP-stimulated ion channels, and K^+ follows passively by electrical coupling through cAMP-stimulated apical and basolateral channels. There is considerable Na^+/K^+ ATPase localized to the basolateral membranes; however, active Na^+ absorption across this epithelium is relatively low because of the low luminal levels of Na^+ that commonly enter this organ (Phillips & Audsley, 1995).

Research done on *A. aegypti* shows that the haemolymph-facing basolateral membrane of adult female rectal pads highly express the P-type Na^+/K^+-ATPase, which has been suggested to serve as the entry step of Na^+ into the haemolymph (Patrick et al., 2006). It was confirmed that the anal papillae of larval *A. aegypti* serve as the major site for Na^+, Cl^- and K^+ uptake with the

use of self-referencing ion-selective microelectrodes (SeRIS) (Donini and O'Donnell, 2005). Using the locust model of transcellular rectal ion transport along with findings specific to *A. aegypti*, the proposed role of the rectum in adult mosquitoes is to absorb K^+ and Na^+ prior to excreting the final urine. The rectal pads are composed of simple columnar cells that function in absorption mechanisms (Hanrahan & Phillips, 1983), suggesting that the rectum only function to absorb, and not secrete, ions within the hindgut.

Recently, the candidate for CTSH, the heterodimeric hormone consisting of a glycoprotein A (GPA) and a glycoprotein B (GPB) was identified first in *D. melanogaster* and then in *A. aegypti* (Sudo et al., 2005; Paluzzi et al., 2014). Its receptor is expressed in the hindgut and couples positively with cAMP (Sellami et al., 2011). Testing the effects of 200 nM GPA2/GPB5, Paluzzi *et al.* (2014) observed an increase in Na^+ absorption in both the anterior and posterior regions of the rectum upon glycoprotein hormone exposure. Similar to these previous studies, the results herein suggest the action of cAMP on the rectum supports the role of GPA2/GPB5 in inhibiting natriuresis in the rectum of adult mosquitoes, thus promoting the retention of Na^+ ions. Additionally, Paluzzi *et al.* (2014) showed that GPA2/GPB5, presumably through increased intracellular cAMP, inhibited the absorption of K^+ in the rectum; this finding is similar to the current study that shows cAMP inhibits K^+ absorption in the rectum of males. Ultimately, the congruence of these findings supports the previous literature that suggests cAMP may act as second messenger for GPA2/GPB5.

Effect of cGMP on ion transport across the hindgut of adult *A. aegypti*

The addition of exogenous cGMP promoted the lumen-directed transport (i.e. secretion) of Na^+ across the ileum and rectum of both sexes. As previously mentioned, the rectal pads are

comprised of epithelia specific for absorptive mechanisms (Piersol, 1897); therefore, our data is incongruent with the currently accepted physiological function of the rectum. The effect of cGMP on K^+ transepithelial transport was negligible as average flux values were close to zero.

In a preliminary locust model proposed by Audsley *et al.,* (2013), if SchgrITP binds to a yet-to-be-identified receptor activating a membrane-bound guanylyl cyclase, then intracellular levels of cGMP are increased. cGMP likely directly stimulates an apical Cl^--electrogenic pump and activates the opening of channels in the basolateral membrane to increase the reabsorption of Cl^-. This is supported by the observation that the addition of cGMP stimulates Cl^--dependent short circuit current across locust ilea (Audsley and Phillips, 1990). By an unknown mechanism, it has been proposed that cGMP stimulates lumen-directed H^+ transport at the apical membrane (Audsley et al., 2013). Unfortunately, this model does not specify whether there is a net absorption or secretion of Na^+ and K^+ ions. No similar study has looked at the role of cGMP on the transepithelial transport of Na^+ and K^+ across the hindgut of adult *A. aegypti*. Therefore, the preliminary findings reported here are the first to suggest cGMP promotes ion secretion in the hindgut of mosquitoes.

Recently, Nagai *et al.* identified three *Bombyx mori* orphan neuropeptide G protein-coupled receptors (BNGRs) (Nagai et al., 2014). In particular, BNGR-A2 and BNGR-A34 were proposed as candidate receptors for *B. mori* ITP as this neuropeptide elicited an increase in intracellular cGMP upon receptor binding. RT-PCR analysis revealed the expression of both BNGR-A2 and BNGR-A34 genes in the hindgut of *B. mori* (Nagai et al., 2014). Future research should investigate whether ITP stimulates an increase in intracellular cGMP in the hindgut of *A. aegypti*, providing insight on whether ITP activates two distinctive receptors as was shown in *B. mori*, which may utilize different second messengers. In the end, this would bring us one step

closer to characterizing the elusive receptors for ITP in *A. aegypti.*

To date, the only neuropeptide receptor identified in the hindgut of the mosquito, *A. aegypti*, is the *Aedes* kinin receptor (*Ae*KR). Three leukokinin-like peptides have been identified in *A. aegypti:* kinins I, II, and III, all of which are released from the abdominal ganglia and interact with *Ae*KR to stimulate hindgut contraction and diuresis in the Malpighian tubules (Pietrantonio et al., 2005). Pietrantonio *et al.* (2011) identified the presence of *Ae*KR in the haemolymph-facing side of the rectal pads, or the basolateral membrane, using immunohistochemistry. Additionally, *Ae*KR dsRNA was used to knockdown ileal and rectal *Ae*KR, after which *in vivo* fluid excretion assays were performed to measure the total urine volume excreted by RNA silenced females. In *Ae*KR silenced females, a significant decrease in fluid excretion rate was observed, suggesting that under normal conditions *Ae*KR plays a role in post-feeding diuresis (Kersch and Pietrantonio, 2011).

Effect of recombinant ITP on ion transport across the hindgut of adult *A. aegypti*

The addition of 1 nM recombinant AedaeITP did not have a significant effect on Na^+ transepithelial transport across the hindgut of males or females. Future research should test higher doses, if possible, of the neuropeptide to see if an effect on ion transport is induced. This will further provide insight as to whether ITP functions as a regulator of the hindgut where it could act as neurohormone or a neurotransmitter. It is important to note that neuropeptides are present in tissues at much lower concentrations than classical neurotransmitters, but are also active at receptors at correspondingly lower concentrations (Mains and Eipper, 1999). For example, the concentration of neurotransmitters in synaptic vesicles is in the 100 mM range, while the concentration of neuropeptide in a large dense core vesicle is 3 to 10 mM at most.

Correspondingly, the affinity of a neurotransmitter for its receptors is in the 100 μm to 1 mM range, while peptides typically bind to their receptors with nanomolar to micromolar affinities (Mains and Eipper, 1999).

The axons of the strongly stained ITP-immunoreactive abdominal ganglia extend, leaving the VNC through the eighth abdominal nerves. Ultimately, these abdominal hindgut-innervating ITP neuronal axons were clearly shown to terminate at the hindgut (Dircksen et al., 2008). This localization of ITP-immunoreactivity found to innervate the hindgut suggests that ITP functions as a neurotransmitter, released at the synapse between axon terminals and the hindgut membrane.

Initial studies on the effects of ITP on ileal short circuit current (I_{SC}) showed that 1.0-5.0 corpus cardiacum (CC) equivalents, corresponding to 0.487-2.44 nM purified ITP, significantly elicited an increase in I_{SC}. At 5 CC equivalents, or 2.44 nM purified ITP, the maximum increase in I_{SC} was observed. The maximum increase in I_{SC} caused by ITP is quantitatively similar to that caused by 5 mM cAMP (Audsley et al., 1992b). A study that sought to characterize the haemolymph concentration of ITP in the locust used an enzyme-linked immunosorbent assay to reveal the presence of 120 fmol of ITP per CC (Audsley et al., 2006). The haemolymph volume of adult locusts has been shown to be 12% of the total body weight, and adult locusts weigh approximately 2 g (Chapman, 1998). Assuming the haemolymph volume is 250 μL, 120 fmol/CC of ITP, if all were to be released into the hemolymph, would equate to a concentration of approximately 0.48 nM ITP, a concentration that was previously shown to increase ileal I_{SC} (Audsley et al., 1992b). A subsequent study showed that 10 nM synthetic *S. gregaria* ITP (SchgrITP) stimulated fluid reabsorption across everted ileal sacs *in vitro*; the rate of fluid absorption across control tissues was 3.98 ± 0.48 nl/h, which significantly increased to 10.89 ± 0.64 nl/h when incubated in the presence of SchgrITP. A 3.3-fold significant increase in fluid

transport was measured over a one hour period after the addition of 5 mM 8-bromo cGMP to the haemolymph side of the locust ileum (Audsley et al., 2013). The dose–response relationship between synthetic SchgrITP and intracellular levels of cGMP and cAMP was such that 100 nM ITP was required to induce an increase in cAMP or cGMP tissue levels in the locust ileum (Audsley et al., 2013). Taken together, the available data on the effectiveness of ITP at eliciting ion transport actions in the hindgut and modulating intracellular second messengers (i.e. cAMP and cGMP) warrants further study on determining physiologically relevant concentrations of ITP in *A. aegypti.*

Concluding remarks and future directions

Ultimately, it is difficult to make any conclusions on the global effects of AedaeITP within the hindgut of *A. aegypti,* as there are many gut region-specific and sex-specific effects on ion transport. Future research on the specific ion transporters within the hindgut epithelia of *A. aegypti* is critical to furthering our knowledge on the role of the hindgut in hydromineral balance, and the neuroendocrine regulation of ion transport mechanisms across this highly unstudied component of the insect excretory system. Additionally, further research on the effects of ITP on the transepithelial transport of other ions such as Cl^- and H^+ will aid in the proposal of a model illustrating the mechanisms responsible for ion transport over the adult *A. aegypti* hindgut epithelia. Furthermore, research should focus on elucidating potential gut region-specific receptors that may modulate hydromineral balance in the hindgut of adult mosquitoes. Notably in the locust, different neuropeptides mediate their effects on different regions of the hindgut; SchgrITP modulates ionoregulation in the ileum, while CTSH functions within the rectum (Audsley et al., 2013). Taking this potentially complex regulatory scheme into consideration, it

suggests that different receptors may also exist within the ileum and rectum of *A. aegypti.* It will be of interest to investigate the potential role of the *Aedes* kinin receptor on post-feeding diuresis in the rectum of *A*. *aegypti* mosquitoes (Kersch and Pietrantonio, 2011).

Furthurmore, SchgrITP itself has been proposed to act upon separate receptors, one resulting in increased intracellular cAMP and the other increasing cGMP (Audsley et al., 2013). As AedaeITP has been postulated to modulate ion balance in the hindgut of mosquitoes, it will be of interest to investigate whether it functions on multiple receptors and whether it activates different intracellular second messenger pathways. On a broader scale, elucidating the effects of neuropeptide hormones has future implications as possible targets for the development of disease vector control agents, as suggested by Van Hiel *et al.* (Van Hiel et al., 2010). Furthermore, Ruiz-Sanchez and O'Donnell (2015) suggest that the insect excretory system is an appropriate target for novel pest control strategies. However, extensive understanding of the mechanisms involved in ion and water transport across the epithelia of the hindgut is necessary to provide the foundation to develop novel pest management strategies (Ruiz-Sanchez and O'Donnell, 2015).

References

Audsley, N. and Phillips, J. E. (1990). Stimulants of ileal salt transport in neuroendocrine system of the desert locust. *Gen. Comp. Endocrinol.* **80**, 127–137.

Audsley, N., McIntosh, C. and Phillips, J. E. (1992b). Actions of Ion-Transport Peptide from Locust Corpus Cardiacum on Several Hindgut Transport Processes. *J. Exp. Biol.* **173**, 275–288.

Audsley, N., McIntosh, C. and Phillips, J. E. (1992a). Isolation of a neuropeptide from locust corpus cardiacum which influences ileal transport. *J. Exp. Biol.* **173**, 261–74.

Audsley, N., Meredith, J. and Phillips, J. E. (2006). Haemolymph levels of Schistocerca gregaria ion transport peptide and ion transport-like peptide. *Physiol. Entomol.* **31**, 154–163.

Audsley, N., Jensen, D. and Schooley, D. A. (2013). Signal transduction for Schistocerca gregaria ion transport peptide is mediated via both cyclic AMP and cyclic GMP. *Peptides* **41**, 74–80.

Bellés, X., Graham, L., Bendena, W., Ding, Q., Edwards, J., Weaver, R. and Tobe, S. (1999). The molecular evolution of the allatostatin precursor in cockroaches. *Peptides* **20**, 11–22.

Beyenbach, K. W. (2003). Review Transport mechanisms of diuresis in Malpighian tubules of insects. *J. Exp. Biol.* **206**, 3845–3856.

Brown, M. R. and Cao, C. (2001). Distribution of ovary ecdysteroidogenic hormone I in the nervous system and gut of mosquitoes. *J. Insect Sci.* **1**, 3.

Clements, A. (2000). *The Biology of Mosquitoes: Development, Nutrition and Reproduction*. London: Chapman & Hall.

Coast, G. et al. (2002). Insect Diuretic and Antidiuretic Hormones. *Handb. Biol. Act. Pept.* **29**, 279–409.

Coast, G. (2007). The endocrine control of salt balance in insects. *Gen. Comp. Endocrinol.* **152**, 332–338.

Coast, G. M. (2009). Neuroendocrine control of ionic homeostasis in blood-sucking insects. *J. Exp. Biol.* **212**, 378–86.

Dai, L., Zitnan, D. and Adams, M. (2007). Strategic expression of Ion Transport Peptide Gene Products in Central and Peripheral Neurons of Insects. *J. Comp. Neurol.* **500**, 353–367.

Dircksen, H. (2009). Insect ion transport peptides are derived from alternatively spliced genes and differentially expressed in the central and peripheral nervous system. *J. Exp. Biol.* **212**, 401–12.

Dircksen, H., Tesfai, L. K., Albus, C. and Nässel, D. R. (2008). Ion transport peptide splice forms in central and peripheral neurons throughout postembryogenesis of Drosophila melanogaster. *J. Comp. Neurol.* **509**, 23–41.

Donini, A. and O'Donnell, M. J. (2005). Analysis of Na+, Cl-, K+, H+ and NH4+ concentration gradients adjacent to the surface of anal papillae of the mosquito Aedes aegypti: application of self-referencing ion-selective microelectrodes. *J. Exp. Biol.* **208**, 603–10.

Hanrahan, J. W. and Phillips, J. E. (1983). Cellular mechanisms and control of KCl absorption in insect hindgut. *J. Exp. Biol.* **106**, 71–89.

Hernández-Martínez, S., Li, Y., Lanz-Mendoza, H., Rodríguez, M. H. and Noriega, F. G. (2005). Immunostaining for allatotropin and allatostatin-A and -C in the mosquitoes Aedes aegypti and Anopheles albimanus. *Cell Tissue Res.* **321**, 105–113.

Hoyle, G. (1953). Potassium ions and insect nerve muscle. *J. Exp. Biol.* **30**, 121–135.
Ionescu, A. and Donini, A. (2012). AedesCAPA-PVK-1 displays diuretic and dose dependent antidiuretic potential in the larval mosquito Aedes aegypti (Liverpool). *J. Insect Physiol.* **58**, 1299–1306.
Kaufmann, C., Merzendorfer, H. and Gäde, G. (2009). The adipokinetic hormone system in Culicinae (Diptera: Culicidae): Molecular identification and characterization of two adipokinetic hormone (AKH) precursors from Aedes aegypti and Culex pipiens and two putative AKH receptor variants from A. aegypti. *Insect Biochem. Mol. Biol.* **39**, 770–781.
Kersch, C. N. and Pietrantonio, P. V (2011). Mosquito Aedes aegypti (L .) leucokinin receptor is critical for in vivo fluid excretion post blood feeding. *FEBS Lett.* **585**, 3507–3512.
King, D. S., Meredith, J., Wang, Y. J. and Phillips, J. E. (1999). Biological actions of synthetic locust ion transport peptide (ITP). *Insect Biochem. Mol. Biol.* **29**, 11–18.
Kramer, S., Toschi, A., Miller, C., Kataoka, H., Quistad, G., Li, J., Carney, R. and Schooley, D. (1991). Identification of an allatostatin from the tobacco hornworm Manduca sexta. *Proc Natl Acad Sci USA* **88**, 9458–9462.
Lide, D. (2002). *Handbook of Chemistry and Physics*. 83rd ed. Boca Raton, FL: CRC Press.
Mains, R. and Eipper, B. (1999). The Neuropeptides. In *Basic Neurochemistry: Molecular, Cellular and Medical Aspects* (ed. Siegel, G.), Agranoff, B.), Albers, R.), and Al., E.), p. Philadelphia: Lippincott-Raven.
Meredith, J., Ring, M., Macins, a, Marschall, J., Cheng, N. N., Theilmann, D., Brock, H. W. and Phillips, J. E. (1996). Locust ion transport peptide (ITP): primary structure, cDNA and expression in a baculovirus system. *J. Exp. Biol.* **199**, 1053–1061.
Nagai, C., Mabashi-Asazuma, H., Nagasawa, H. and Nagata, S. (2014). Identification and characterization of receptors for ion transport peptide (ITP) and ITP-like (ITPL) in the silkworm Bombyx mori. *J. Biol. Chem.* **289**, 32166–32177.
Nässel, D. R. (2002). Neuropeptides in the nervous system of Drosophila and other insects : multiple roles as neuromodulators and neurohormones. **68**, 1–84.
Nation, J. (2002). *Insect Physiology and Biochemsitry*. Boca Raton, FL: CRC Press.
O'Donnell, M. J. (2009). Too much of a good thing: how insects cope with excess ions or toxins in the diet. *J. Exp. Biol.* **212**, 363–372.
O'Donnell, M. J. (2011). Mechanisms of excretion and ion transport in invertebrates. *Compr. Physiol.* 1207–1289.
Orchard, I. and Paluzzi, J. P. (2009). Diuretic and antidiuretic hormones in the blood-gorging bug rhodnius prolixus. *Ann. N. Y. Acad. Sci.* **1163**, 501–503.
Pacey, E. K. and O'Donnell, M. J. (2014). Transport of H+, Na+ and K+ across the postePacey, E. K., & O'Donnell, M. J. (2014). Transport of H+, Na+ and K+ across the posterior midgut of blood-fed mosquitoes (Aedes aegypti). Journal of Insect Physiology, 61(1), 42–50. http://doi.org/10.1016/j.jins. *J. Insect Physiol.* **61**, 42–50.
Paluzzi, J. P. V, Vanderveken, M. and O'Donnell, M. J. (2014). The heterodimeric glycoprotein hormone, GPA2/GPB5, regulates ion transport across the hindgut of the adult mosquito, Aedes aegypti. *PLoS One* **9**, e86386.
Patrick, M. L., Aimanova, K., Sanders, H. R. and Gill, S. S. (2006). P-type Na+/K+-ATPase and V-type H+-ATPase expression patterns in the osmoregulatory organs of larval and adult mosquito Aedes aegypti. *J. Exp. Biol.* **209**, 4638–51.
Phillips, J. (1964). Rectal Absorption in the Desert Locust, Schistocerca Gregaria Forskal. *J. Exp. Biol.* **41**, 15–38.

Phillips, J. E. and Audsley, N. (1995). Neuropeptide control of ion and fluid transport across locust hindgut. *Integr. Comp. Biol.* **35**, 503–514.
Phillips, J., Hanrahan, J., Chamberlin, M. and Thomson, B. (1986). Mechanisms and control of reabsorption in insect hind- gut. *Adv. In Insect Phys.* **19**, 330–422.
Phillips, J. E., Audsley, N., Lechleitner, R., Thomson, B., Meredith, J. and Chamberlin, M. (1988). Some Major Transport Insect Absorptive Mechanisms of. **90**, 643–650.
Phillips, J. E., Wiens, C., Audsley, N., Jeffs, L., Bilgen, T. and Meredith, J. (1996). Nature and control of chloride transport in insect absorptive epithelia. *J. Exp. Zool.* **275**, 292–299.
Phillips, J. E., Meredith, J., Audsley, N., Richardson, N., Macins, A. and Ring, M. (1998). Locust Ion Transport Peptide (ITP): A Putative Hormone Controlling Water and Ionic Balance in Terrestrial Insects. *Integr. Comp. Biol.* **38**, 461–470.
Phillips, J., Meredith, J., Wang, Y., Zhao, Y. and Brock, H. (2001). *Ion transport peptide (ITP): structure, function, evolution*. (ed. Goos, H.), Rastogi, R.), Vaudry, H, P.), and Pierantoni, R.) Bologna, Italy: Medimond.
Piersol, G. (1897). *Normal Histology*. JB Lippincott Company.
Pietrantonio, P., Jagge, C., Taneja-Bageshwar, S., Nachman, R. and Barhoumi, R. (2005). The mosquito Aedes aegypti (L.) leucokinin receptor is a multiligand receptor for the three Aedes kinins. *Insect Mol. Biol.* **12**, 55–67.
Robertson, L., Donini, A. and Lange, A. B. (2014). K+ absorption by locust gut and inhibition of ileal K+ and water transport by FGLamide allatostatins. *J. Exp. Biol.* 3377–3385.
Ruiz-Sanchez, E. and O'Donnell, M. J. (2015). The insect excretory system as a target for novel pest control strategies. *Curr. Opin. Insect Sci.* **11**, 14–20.
Sellami, A., Agricola, H. J. and Veenstra, J. A. (2011). Neuroendocrine cells in Drosophila melanogaster producing GPA2/GPB5, a hormone with homology to LH, FSH and TSH. *Gen. Comp. Endocrinol.* **170**, 582–588.
Sudo, S., Kuwabara, Y., Park, J. Il, Sheau, Y. H. and Hsueh, A. J. W. (2005). Heterodimeric fly glycoprotein hormone-α2 (GPA2) and glycoprotein hormone-β5 (GPB5) activate fly leucine-rich repeat-containing G protein-coupled receptor-1 (DLGR1) and stimulation of human thyrotropin receptors by chimeric fly GPA2 and human GPB5. *Endocrinology* **146**, 3596–3604.
Van Hiel, M. B., Van Loy, T., Poels, J., Vandersmissen, H. P., Verlinden, H., Badisco, L. and Vanden Broeck, J. (2010). Neuropeptide receptors as possible targets for development of insect pest control agents. *Adv. Exp. Med. Biol.* **692**, 211–26.
Vandenborre, G., Menschaert, G., Smagghe, G., Ghesquie, B., Rao, N., Gevaert, K. and Damme, E. J. M. Van (2011). Diversity in Protein Glycosylation among Insect Species. *PLoS One* **6**,.
Vandersmissen, H. P., Van Hiel, M. B., Van Loy, T., Vleugels, R. and Vanden Broeck, J. (2014). Silencing D. melanogaster lgr1 impairs transition from larval to pupal stage. *Gen. Comp. Endocrinol.* **209**, 135–147.
Williams, J. and Beyenbach, K. (1983). Differential effects of secretagogues on Na and K Secretion in the Malpighian tubules of Aedes aegypti. *J. Comp. Physiol.* **149**, 511–517.
Wilps, H. and Gade, G. (1990). Hormonal regulation of carbohydrate metabolism in the blowfly Phormia terraenovae. *J. Insect Physiol.* **36**, 441–450.
Woodhead, A., Stay, B., Seidel, S., Khan, M. and Tobe, S. (1989). Primary structure of four allatostatins: neuropeptide inhibitors of juvenile hormone synthesis. *Proc Natl Acad Sci USA* **86**, 5997–6001.